Volume 14, No. 5

March, 1964

SOVIET ATOMIC ENERGY

АТОМНАЯ ЭНЕРГИЯ
(ATOMNAYA ÉNERGIYA)

TRANSLATED FROM RUSSIAN

CONSULTANTS BUREAU

Declassified and Approved For Release 2013/09/25 : CIA-RDP10-02196R000600100004-4

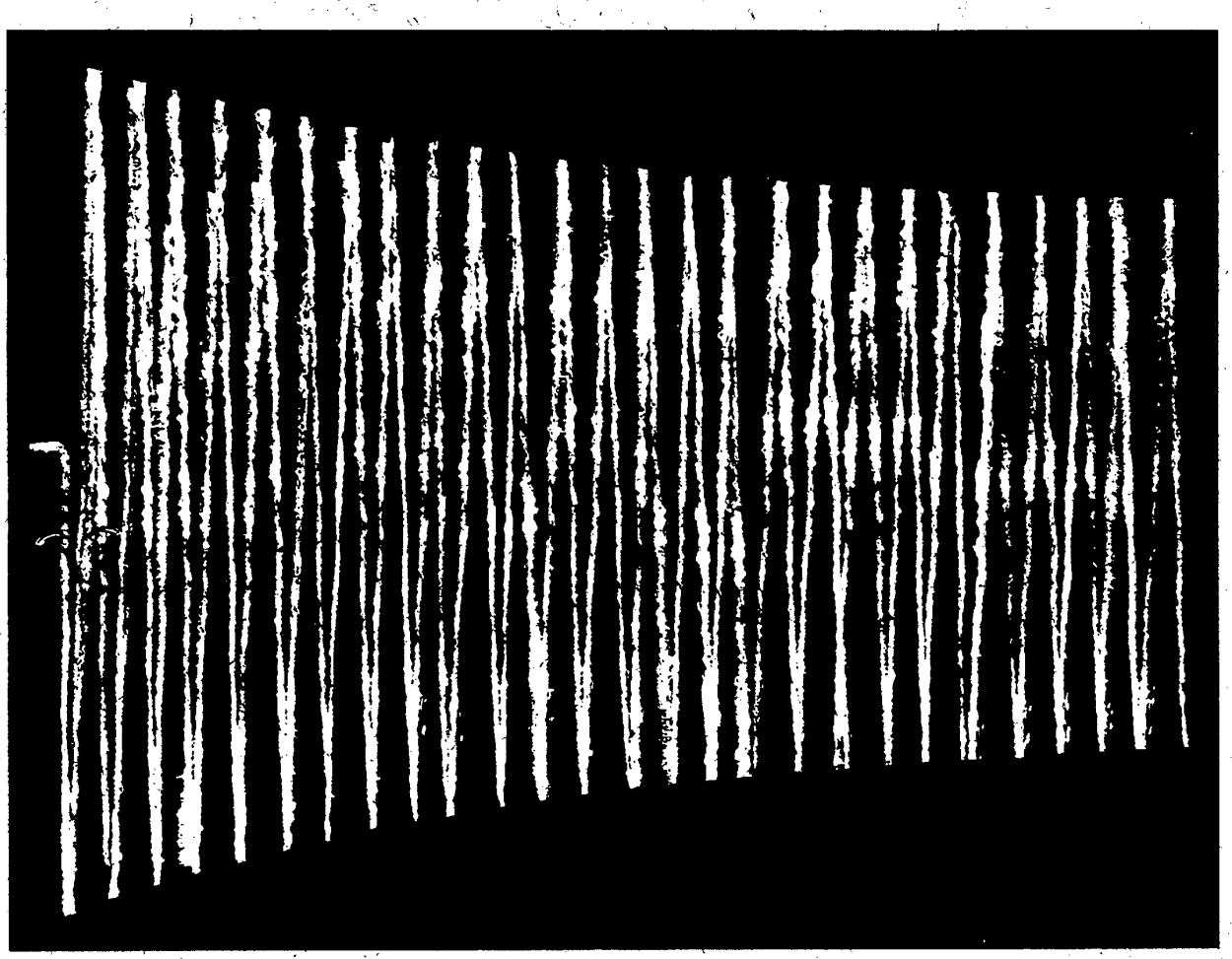

RELAXATION PHENOMENA IN METALS AND ALLOYS

Edited by
B. N. Finkelshtein — Preface by A. S. Nowick

A collection of experimental and theoretical investigations of relaxation phenomena in metals and alloys; the first to be published in English devoted to this field. All the articles in the collection concern themselves with some aspect of internal friction while investigating the phenomenon in a wide variety of metal types. The volume contains several papers of a general and fundamental nature as well as a large fraction dealing with the properties of commercial alloys.

Among some of the effects studied are: The applications of measurements of internal friction to the study of the decomposition of super-saturated solid solutions; defects of crystal lattices; plastic deformation; creep; and the behavior of metals at high temperatures. Also investigated are the relationship between internal friction and brittleness, the possibility of applying the method of internal friction to the study of sintered materials, and the mechanism of impact fatigue. Considerable attention is paid to the effects of cold working and annealing, of alloy transformations, and of grain boundaries on internal friction and anelastic behavior. Of particular interest is evidence of the wide use of the low frequency torsion pendulum for such studies. In addition, the damping characteristics of metals and a new method of defectoscopy are also discussed.

The book includes extensive references taken from a wide range of publications including those of Eastern Europe and China.

252 pages **Translated from Russian** **$40.00**

CONSULTANTS BUREAU 227 West 17 St., New York 11, N. Y.

SOVIET ATOMIC ENERGY

A translation of **ATOMNAYA ÉNERGIYA**
A publication of the Academy of Sciences of the USSR

Vol. 14, No. 5 March, 1964

CONTENTS

(continued)

Annual Subscription: $95 **Single Issue: $30** **Single Article: $15**

CONTENTS (continued)

NOTE

The Table of Contents lists all materials that appear in Atomnaya Énergiya. Those items that originated in the English language are not included in the translation and are shown enclosed in brackets. Whenever possible, the English-language source containing the omitted reports will be given.

Consultants Bureau Enterprises, Inc.

LENIN PRIZE WINNER B. M. PONTECORVO

N. N. Bogolyubov

Translated from Atomnaya Énergiya, Vol. 14, No. 5,
pp. 441-442, May, 1963

The committee on Lenin Prizes in science and technology in the Council of Ministers of the USSR has awarded the Lenin prize for 1963 to Corresponding Member of the Academy of Sciences of the USSR B. M. Pontecorvo.

Pontecorvo has been awarded the Lenin prize for work in one of the most interesting fields of modern science — the problem of weak interactions of elementary particles and neutrino physics. These branches of physics have played an exceptionally important part in the past and they will no doubt be equally important in the future.

The term "weak interaction" is naturally very arbitrary. These interactions are in fact weaker than electromagnetic interactions connected with light radiation, but are much stronger, for example, than gravitational interactions governing the motion of the planets.

The history of the physics of weak interactions involves primarily the investigation of properties of probably the most enigmatic of elementary particles — muons and neutrinos. Bruno Pontecorvo was the first to draw attention to the considerable similarity between the muon and the well-known electron. This idea made it possible to forecast a whole number of properties of elementary particles. Pontecorvo himself established experimentally such fundamental properties as spontaneous decomposition of a muon into three particles, one of which is the ordinary electron, the other two being neutrinos. Pontecorvo found that the mass of the neutrino is very small, at least 500 times less than the mass of the electron which until then had been the lightest particle known.

Experiments also confirmed Pontecorvo's suggestion that the muon and electron have the same values characterizing the natural rotation of these particles. Finally, using an atomic reactor arrangement which he proposed, experiments were conducted in which scientists proved the difference between the neutrino and its antiparticle — the antineutrino.

The extension of the Pontecorvo idea was the initial point in the theory of universal weak interaction. At the Joint Institute of Nuclear Studies he conducted a brilliant experiment on the capture of muons by He^3 nuclei; this experiment not only qualitatively confirmed the analogy between the electron and the muon, forming the basis of the idea of universality of weak interactions, but also gave quantitative agreement with the theoretical forecast.

His experiments on the decay of muons confirmed such detail in the theory of the neutrino as the parallelism of the direction of natural rotation of the neutrino to its direction of motion.

B. M. Pontecorvo's work has made a tremendous contribution in converting a comparatively modest branch of physics — the physics of weak interactions and the neutrino — to one of the most interesting and important fields of science, currently engaging the attention of scientists throughout the world. The rapid development of this field of science has meant that physicists have not only thought about the similarity between the electron and the muon, but also about the difference between these "similar" particles. This has led to an interesting discovery. It has been found that there are two kinds of neutrino: muon and electron neutrinos. Each of them interacts in a pair only with a muon or only with an electron. An extremely bold and clever experiment to check this fact using modern experimental techniques — powerful accelerators of elementary particles — was also suggested by Professor B. M. Pontecorvo.

A study of the role of the neutrino in the evolution of the stars has led B. M. Pontecorvo to the conclusion that the neutrino is very important at certain stages of evolution. His work in this field has considerably helped the development of a new branch of science — neutrino astrophysics.

Ideas on the universality of weak interactions obtained yet another confirmation when physicists discovered a number of new, so-called strange particles. It was found that weak interactions are also characteristic for them.

Using the features of these particles, Pontecorvo forecast and then checked experimentally the law of paired generation of strange particles. These conclusions later became a fundamental part of the systematics of strange particles.

The brilliant experimenter Pontecorvo also has a fine understanding of theoretical matters. These qualities combined with considerable organizational talent have enabled him to develop a fine group of talented physicists.

The outstanding achievements of Bruno Pontecorvo in the physics of weak interactions and neutrino physics have rightly earned him the highest award—the Lenin prize.

AN ADIABATIC TRAP WITH COMBINED MAGNETIC FIELD

Yu. T. Baiborodov, M. S. Ioffe, V. M. Petrov, and R. I. Sobolev

Translated from Atomnaya Énergiya, Vol. 14, No. 5,
pp. 443-445, May, 1963
Original article submitted April 11, 1963

We present the results of the first experiments conducted with the PR-5 apparatus—an adiabatic trap with magnetic field increasing in the longitudinal and radial directions. We have shown that in such a trap magetohydrodynamic instability of the plasma is absent; the lifetime of the plasma is limited by the recharging of the fast ions on the neutral gas. The maximum times of decay of the plasma observed in these experiments reach 10-15 msec.

At the International Conference on Plasma Physics and Controlled Thermonuclear Synthesis (Salzburg, 1961) results were presented of preliminary experiments on the retention of the plasma in an adiabatic trap with plugs in which the magnetic field increases in the radial as well as the longitudinal direction [1].

The idea of such a trap is based on the fact that the increase in field in the radial direction should prevent the development of convective instability in the plasma, causing leakage of the plasma across the magnetic field in an ordinary trap with plugs [2-5]. To set up a field increasing along the radius, the coils of the longitudinal field were supplemented by a stabilizing winding. The latter is a system of linear conductors parallel to the axis of the trap and placed symmetrically over the azimuth near the side wall of the vacuum chamber; the current passes through neighboring conductors in mutually opposite directions.

The main conclusion to be drawn from the above experiments was the fact that at a fairly high field intensity of the stabilizing winding the lifetime of the plasma in the trap increases considerably (approximately fivefold: from 100 to 450-500 μsec). There was also reason to believe that under the stabilized conditions the lifetime is determined mainly by losses of fast ions of the plasma due to charge-exchange and not to any instabilities. However, due to imperfections in the vacuum conditions in the apparatus (the minimum hydrogen pressure in the presence of plasma was $1 \cdot 10^{-6}$ mm Hg) this conclusion could not be drawn with sufficient reliability.

The new PR-5 apparatus was built in 1962—an adiabatic trap with combined magnetic field of the type mentioned above and with better vacuum conditions. We present the results of the first experiments carried out with this apparatus.

A diagram of the apparatus is given in Fig. 1. A longitudinal magnetic field with intensity up to 5000 Oe in the central part of the trap and with a mirror ratio of 1.7 is set up by coils which are fed from a dc generator. The stabilizing winding is placed in the gap between the vacuum chamber and the coils of the longitudinal field; the intensity of the field of the stabilizing winding at the wall of the vacuum chamber is up to 4500 Oe. The winding is fed from a capacitor battery; the half-period of the current is 55 msec. The vacuum chamber, 40 cm in diameter and 400 cm in length, is made of stainless steel; the chamber is first evacuated to a pressure of 10^{-6} mm Hg by two vapor pumps fitted with nitrogen traps. Diaphragms separate the chamber into a number of sections, in each of which there are titanium evaporators; the titanium is sprayed directly onto the inside surface of the chamber. The differential system of evacuation by titanium ensures the maintenance of a pressure in the central part of the chamber of $5 \cdot 10^{-8}$ mm Hg with the stationary admission of hydrogen into the plasma source of 500 cm^3/h.

The trap was filled with plasma by the "magnetotron" injection described in detail in [6]. In the described experiments $n \approx 10^9$ cm^{-3}; $T_i \approx 5$ keV; $T_e \approx 20$ eV. The effect of the field of the stabilizing winding $H_\perp$ on the retaining properties of the trap was determined from the change in decay time of the plasma τ as a function of $H_\perp$. The value of τ was measured by the same method as in [6], based on the recording of the flux of fast neutral charge-exchange atoms.

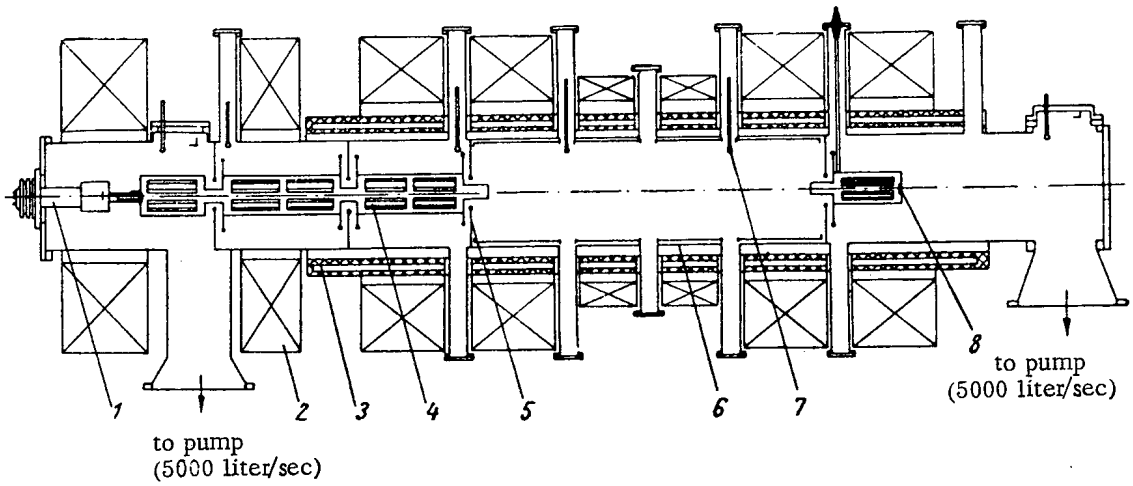

Fig. 1. Diagram of apparatus: 1) plasma source; 2) longitudinal field coils; 3) stabilizing winding; 4) protective cylinders; 5) diaphragms; 6) vacuum chamber; 7) titanium evaporators; 8) pickup electrode.

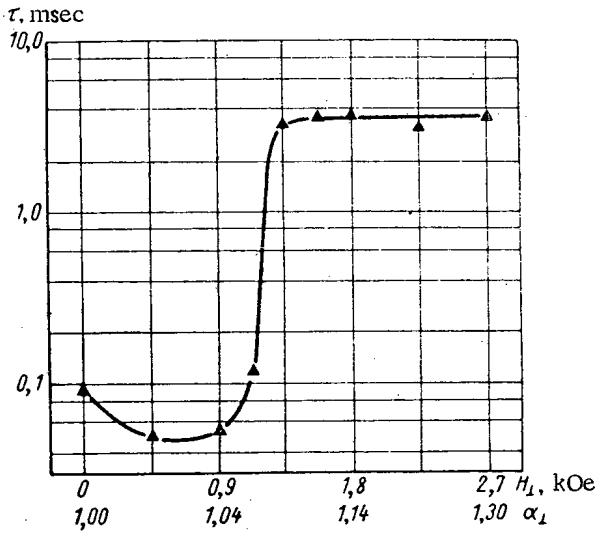

Fig. 2. Dependence of decay time of the plasma τ on the field intensity of the stabilizing winding $H_\perp$ ($H_{0\parallel}$ = 3.3 kOe; p = $1.5 \cdot 10^{-7}$ mm Hg).

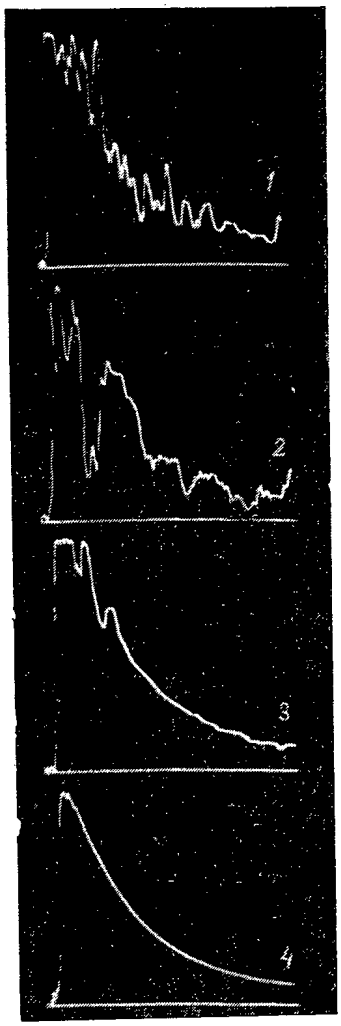

Fig. 3. Current oscillograms on probe for various values of the stabilizing field ($H_{0\parallel}$ = 3300 Oe; p = $1.5 \cdot 10^{-7}$ mm Hg): 1) $H_\perp$ = 0, $\alpha_\perp$ = 1.00; 2) $H_\perp$ = 900 Oe, $\alpha_\perp$ = 1.04; 3) $H_\perp$ = 1400 Oe, $\alpha_\perp$ = 1.09; 4) $H_\perp$ = 2400 Oe, $\alpha_\perp$ = 1.21.

Figure 2 gives the dependence of τ on $H_\perp$, obtained with a longitudinal field at the center of the trap $H_{0\parallel}$ equal to 3300 Oe, and a hydrogen pressure of $1.5 \cdot 10^{-7}$ mm Hg. In addition to $H_\perp$, the quantity $\alpha_\perp$ is also plotted along the abscissa axis; this quantity is equal to $\frac{\sqrt{H_{0\parallel}^2 + H_\perp^2}}{H_{0\parallel}}$ and characterizes the so-called wall-mirror ratio, i.e., the ratio of the intensity of total magnetic field at the wall of the vacuum chamber to the intensity of the field at the center of the trap. The curve of Fig. 2 shows that the field of the stabilizing winding acts very effectively on the plasma: for $H_\perp$ = 1500 Oe ($\alpha_\perp$ = 1.1) the plasma decays 35 times more slowly than for $H_\perp$ = 0. In this experiment the absolute value of the decay time under stabilized conditions ($\alpha_\perp \geq 1.1$) was 3.5 msec, as opposed to 0.5 msec in [1]. This difference is due to the different pressure of the neutral gas in the chamber ($1.5 \cdot 10^{-7}$ mm Hg with the new apparatus and $1.2 \cdot 10^{-6}$ mm Hg previously). This shows that the decay is determined by the charge exchange.

The maximum decay times observed with the new apparatus at still lower pressures reach 10-15 msec.

An illustration of the effectiveness of the stabilizing field in suppressing the plasma instability is provided by the current oscillograms on a Langmuir probe placed inside the trap. Figure 3 shows these oscillograms for a spherical 4-mm dia. probe placed at a distance of 50 mm from the side wall in the central cross section of the chamber. The probe was at a potential of -40 V relative to the walls and measured the ionic saturation current, i.e., the value proportional to the plasma density in the neighborhood of the probe. It can be seen that the deep density pulsations due to the plasma instability in the "barrel-shaped" field of an ordinary trap completely disappear as the stabilizing field is increased. It is an interesting fact that a probe of even such relatively small dimensions considerably reduces the lifetime of the plasma under stabilized conditions. This fact also points to the prolonged existence of plasma in a trap in the presence of a stabilizing field.

The new data obtained with the PR-5 apparatus therefore completely confirm the results of the preliminary experiments described in [1]. They show quite clearly that at least for a low-density plasma ($\beta = \frac{n(T_i + T_e)}{H^2/8\pi} \approx 10^{-5}$) an adiabatic trap with combined magnetic field ensures stable retention of the plasma, undisturbed by magnetohydrodynamic instabilities.

The authors would like to thank L. A. Artsimovich for his constant interest in the work, for helping with it and for very valuable discussions of the results.

LITERATURE CITED

1. Yu. V. Gott, M. S. Ioffe, and V. G. Tel'kovskii, Report CN 10/262 to the International Conference on Plasma Physics and Controlled Thermonuclear Synthesis, Salzburg, IAEA (1961).
2. M. Rosenbluth and C. Longmire, Ann. Phys., 1, 120 (1957).
3. B. B. Kadomtsev, "Zh. éksperim. i teor. fiz.", 40, 328 (1961).
4. M. S. Ioffe, R. I. Sobolev, V. G. Tel'kovskii, and E. E. Yushmanov, "Zh. éksperim. i teor. fiz.", 40, 40 (1961).
5. M. S. Ioffe and E. E. Yushmanov, Nucl. Fusion, Suppl., part 1, 177 (1962).
6. M. S. Ioffe, R. I. Sobolev, V. G. Tel'kovskii, and E. E. Yushmanov, "Zh. éksperim. i teor. fiz.", 39, 1602 (1960).

All abbreviations of periodicals in the above bibliography are letter-by-letter transliterations of the abbreviations as given in the original Russian journal. *Some or all of this periodical litereture may well be available in English translation.* A complete list of the cover-to-cover English translations appears at the back of this issue.

INJECTING THE ION BEAM INTO THE "OGRA" MAGNETIC MIRROR MACHINE

A. L. Bezbatchenko, V. V. Kuznetsov, N. P. Malakhov, and N. N. Semashko

Translated from Atomnaya Énergiya, Vol. 14, No. 5, pp. 446-452, May, 1963
Original article submitted July 5, 1962

This paper gives results of experiments on producing and focusing beams of molecular hydrogen ions with energies up to 180 keV, and injecting them into the magnetic field of the "Ogra". The ion current injected into the machine is ~150 mA. It is shown that in the operating range, the perturbation produced in the "Ogra" magnetic field by the injector channel is not more than a few percent.

The idea that forms the basis of the "Ogra" design is that it is possible to accumulate plasma in a magnetic mirror machine as a result of dissociation by the residual gas of molecular ions injected into the machine. It has been shown in [1-3] that assuming stable plasma containment, the injection current required to get to a high density plasma drops off sharply with increase in the energy and mean free path of the molecular ions in the machine before they are lost at the injector. The ion source developed by P. M. Morozov [4] made it possible, when the "Ogra" was first built, to get a current of H_2^+ molecular ions of about 400 mA with energies up to 50 keV. Further improvement in the source should increase the energy of the ions to 200 keV. With these injected beam parameters, a molecular ion free path length of 10^5 cm before being lost at the channel must be provided in order to pass to a state where a dense plasma is being built up. It is practically impossible to get such a path length during the time the ion is moving from the injector to the mirror and back. In the "Ogra," as a result of the finite angular divergence of the beam, this length is only 30-40 m for a distance between the mirrors of ~10 m.

Accordingly, the point and the method chosen for injection into the machine must provide for ten or twenty or more oscillations of the ions between the mirrors before they are lost in the channel. This means, first, that as a result of azimuthal drift, the ions must get out of contact with the channel as quickly as possible, which is achieved by proper choice of configuration of the magnetic field, and second, that the beam losses must be as small as possible at each contact with the channel. The fraction of the beam incident on the channel at each contact is equal to the ratio of the width of the channel to the pitch of the spiral. Accordingly, in a machine in which particle capture occurs through dissociation of molecular hydrogen by the residual gas, injection in the vicinity of the mirrors (as in the DSKh-II equipment) is not so good, although here it is able to produce an almost perpendicular magnetic field, which greatly simplifies the injector construction.

The center part of the apparatus was chosen for injecting particles into the "Ogra." The magnetic field has an opening in the injector region, produced by a break in the solenoid, as required to introduce the beam. Inside the magnetic channel, the beam is bent and injected into the machine at an angle of 20° to a plane perpendicular to the magnetic field. This gives a large pitch to the spiral in the injector region. After getting out onto the plateau of the magnetic field, the pitch of the spiral decreases, which increases the mean path length of the particles before they are lost in the injector.

Three methods have been discussed for injecting particles into the magnetic field:

1) Giving the ions additional acceleration as they enter the magnetic field, and retarding them to their initial energy as they leave the channel,

2) Balancing out the deflection produced by the magnetic field by means of a transverse electric field,

3) Injection through the magnetic channel, namely, through an iron screen with a compensating current winding to reduce the field inside the channel. Both electrostatic methods lead to complete decompensation of the beam so

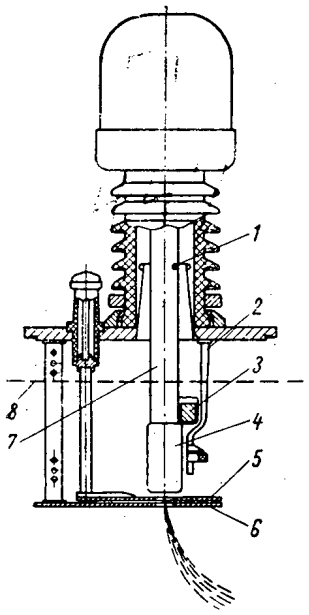

Fig. 1.

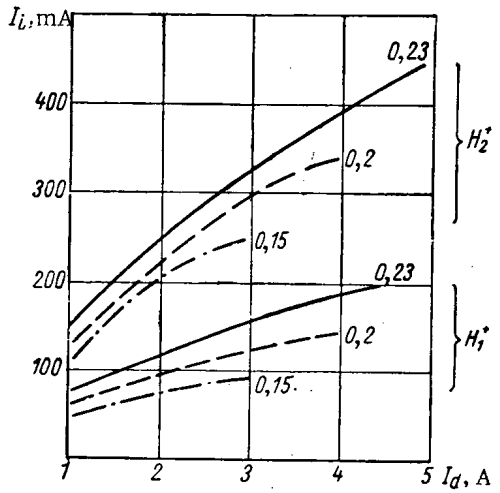

Fig. 2.

Fig. 1. Diagram of ion source with ferromagnetic electron avalanche trap (magnetic field perpendicular to plane of the figure): 1) point where electron avalanches strike without being caught; 2) plate of ferromagnetic trap; 3) trapping electrode with bar of Armco iron (point where electron avalanches strike); 4) gas discharge head at a postive potential of up to 200 kV; 5) intermediate electrode at a negative potential of 15 kV; 6) grounded electrode; 7) supporting post for source; 8) edge of magnet pole.

Fig. 2. Components of the ion current I_i taken from the source as a function of the discharge current I_d for different amounts of gas in the gas discharge chamber of the source.

---

that it is dispersed by its own space charge in a length much less than the length of the channel. The magnetic screen does not produce decompensation of the beam. The authors have used the last method of injecting particles into the magnetic field, namely, through a magnetic channel, the detailed construction of which is described below.

1. Ion Source

The beam of molecular hydrogen ions was produced with the ion source developed by P. M. Morozov, which has an arc discharge taking place along the magnetic field. The hot cathode and the cold anticathode are at the same potential, which is negative with respect to the walls of the gas discharge chamber. The ions are pulled out of the gas discharge chamber across the magnetic field, through a 4×40 mm slit. Between the gas discharge chamber, which is at a high positive potential, and the grounded pull-out electrode, there is an intermediate electrode at a negative potential with respect to ground (Fig. 1).

In a source of this type, it is impossible to raise the voltage above 75 kV (for an accelerating space 8 mm long) without special measures to prevent breakdowns. If a vacuum treatment is used, breakdowns start up again after a while, i.e., the electrode surfaces do not get "treated out." Increasing the length of the accelerating space makes breakdown less frequent, but here the breakdowns tend to develop into avalanches, which melt the parts that are at a positive potential.

Whether or not breakdowns develop with the material used depends essentially on the planeness of the electrodes and the size of the microprojections on the surface. In order to increase the high voltage strength, the parts were given an electrochemical degreasing in an alkali bath and an electrochemical polishing to dissolve off the microprojections. Further, the parts of the source subjected to negative potential were baked in vacuum at a pressure of $5 \cdot 10^{-5}$ mm Hg at temperatures of 600-950°C, depending on the material. These operations greatly increased the high voltage strength of the source. The number of breakdowns was greatly reduced, and when the discharge is going, the voltage on the source may be raised to 200 kV, with a field strength of ~100 kV/cm in the accelerating gap.

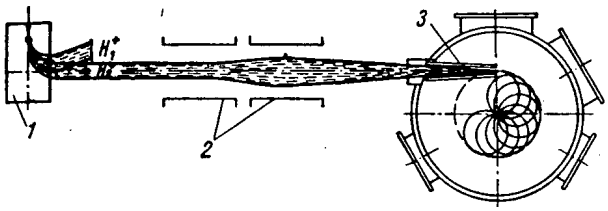

Fig. 3. Schematic diagram of "Ogra" injector: 1) source magnet; 2) quadrupole magnetic lenses; 3) magnetic screening channel.

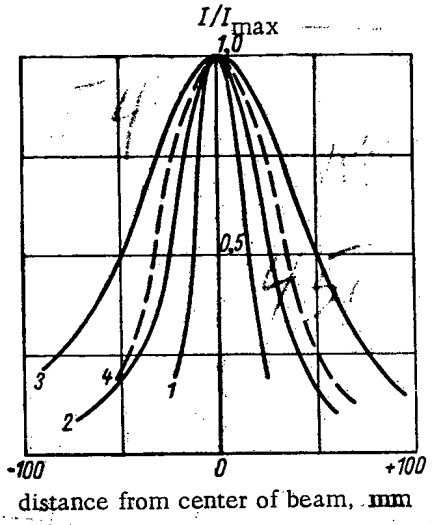

Fig. 4. Relative distribution of current density in the beam, horizontally, in the image plane: 1) curve plotted by adding the current distributions in the separate ion rays for best focusing (the experimental curve for the current distribution in a 0.5 mA ion beam is the same as curve 1); 2, 3) beam currents of 20 and 150 mA respectively (curves taken when the distribution in the separate ion rays was as given in curve 1); 4) distribution for a beam current of 150 mA, with the separate ion rays refocused.

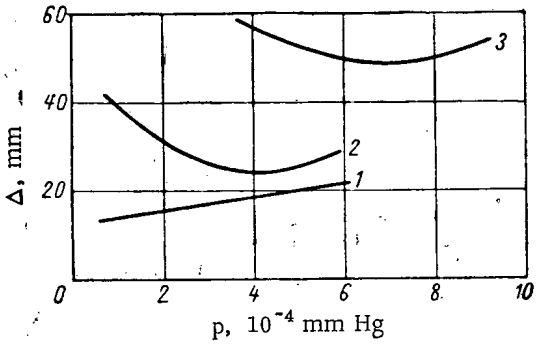

Fig. 5. Beam half width Δ in the image plane, as a function of the pressure p in the ion conductor for different beam currents, mA: 1) 0.5; 2) 20; 3) 150.

However, it is impossible to work with the ion beam with this voltage on the source, since breakdown leads to the development of avalanches which melt the parts in the source. Stable operation of the source is possible with a voltage up to 100 kV and an accelerating gap length of ~8 mm, while at higher voltages measures must be taken to prevent the development of avalanches.

Where the electron avalanches come from and how they develop may be explained in the following way. A breakdown in the accelerating gap develops into an arc between the electrodes which vaporizes the anode and sets free the occluded gases. The electrons formed in the arc are drifting in the crossed electric and magnetic fields in the gap. The height of the electron trochoid is

$$h = 1{,}2 \cdot 10^{-5} \frac{E}{H^2} \text{ cm},$$

where E is in V/cm, and H is in kG. For E ≃ 100 kv/cm, and H ≃ 1.4 kG, the height of the trochoid is 0.6 cm, i.e., for a gap length of 8 mm, the greater part of the electrons formed in the accelerating gap are lost at the anode.

Raising the energy of the ions any further means increasing the length of the accelerating gap, since it is difficult to raise the electric field strength above 100-120 kV/cm because of the electrical strength of the gap. Here, to maintain the angle of rotation of the ion beam, the magnetic field intensity must be increased in proportion to the square root of the energy, i.e., h is inversely proportional to the energy. For an ion energy of 200 keV, and keeping the electric field at 100 kV/cm, the height of the electron trochoid is 3 mm, while the length of the gap is 20 mm. The electrons formed in the accelerating gap are able to get out of the gap and move along the equipotentials in the electric field.

If breakdown develops as a result of evaporating the metal in the electrodes and setting free the occluded gas, there is a sudden increase in pressure with electron multiplication, which ends in an avalanche, increasing exponentially with the distance the avalanche drifts in the crossed fields. The avalanche that has developed, moving along the exponentials, circles around the gas discharge head in the direction in which the ion beam is deflected in the magnetic field, and drops into the region of weak magnetic field.

At the point where the height of the trochoid is equal to the width of the high voltage gap, the electrons are incident on the supporting rod of the source, which is at a positive potential (see Fig. 1). As a rule, the avalanche always strikes at the same place, and it has enough power to melt the supporting rod, in spite of a large amount of cooling from the water flowing through. Breakdowns occurring between the source head and the wall of

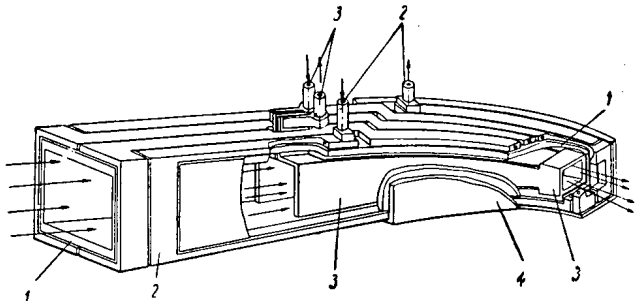

Fig. 6. Diagram of magnetic channel: 1) iron core; 2) compensating winding; 3) deflecting winding; 4) receiving electrode.

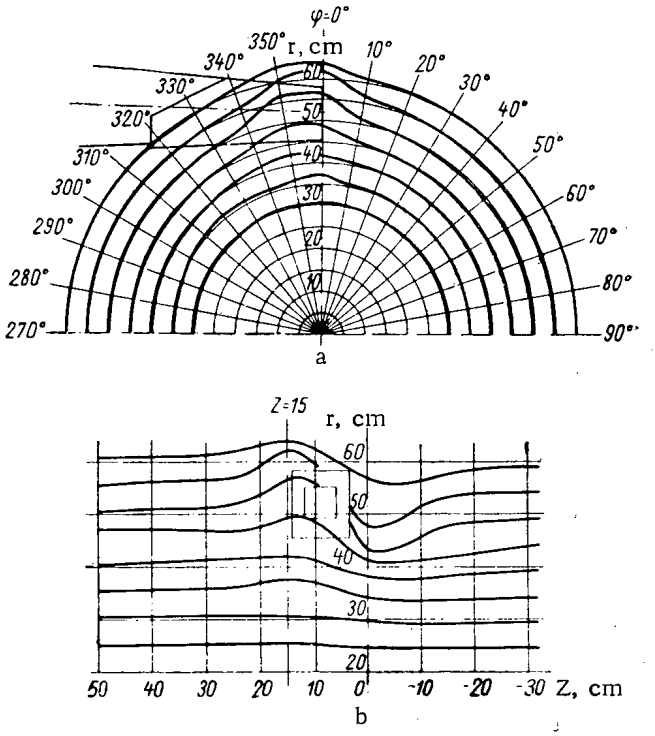

Fig. 7. Perturbation of "Ogra" magnetic field, produced by the magnetic channel, with the optimum current in the compensating winding: a) in the plane Z = 15 cm; b) in the vertical plane, $\varphi = 0°$. (The departure of the curves from the grid lines is proportional to the magnetic field perturbation at the point. A 1 cm displacement of the curve in the r direction means 3% perturbation.)

the vacuum chamber along the magnetic field never produce avalanches, since the electrons are immediately lost at the positive electrode.

The electron flux powers for different ways of operating the source may conveniently be compared from the X-ray intensity given off by the source. A microroentgenometer is set up near the source with an indicating instrument and a recorder. X rays are formed when the high voltage is applied to the source even when the discharge is off. When the source is being given a treatment, it can be seen how the X rays first slowly increase with time, then breakdown occurs, and after restoring the operation of the source, the radiation becomes somewhat less than it was to start with, then increases again, and another breakdown occurs. The mean radiation level drops after a series of breakdowns, while the high voltage strength of the source increases. When the discharge is on, the radiation intensity increases with increase in the ion current taken out. This is apparently due to secondary electron emission from the surface of the intermediate electrode (see Fig. 1, 5) due to a small part of the ion beam being incident on it.

The struggle with avalanches must be conducted along two lines: disconnecting the high voltage from the source when breakdown occurs, and catching the avalanche as close as possible to the place where it starts. The existing maximum current protective relay in the rectifier is too slow to act when an avalanche develops. The voltage is taken off the source in ~2 sec, i.e., long after the avalanche has hit the supporting rod.

Several methods have been tried for catching the avalanches close to the place where they start. One of the methods consists in using a special electrode configuration so that as the electrons move along the magnetic field they will hit an electrode that is at the same potential as the source. So far however this method has not given any positive results. The electrons went between the electrodes and landed on the support rod, which they melted.

A more successful method of catching the avalanches was to produce local weakening of the magnetic field along the path followed by the electrons. In this method the region where the electrons multiply is reduced by putting a grounded plate a distance of 15-20 mm from the gas discharge head (see Fig. 1, 2). A block of Armco iron (see Fig. 1, 3) is placed on the positive electrode to produce local weakening of the magnetic field, so that the height of the trochoid increases, and the avalanche hits principally this electrode. Since the length of the path followed by the avalanche is reduced by a factor of about 3, the power in the avalanche is comparatively small, and so does not melt the ferromagnetic trap. If the ion source operates for a long time with a beam a large amount of heat is generated in both the ferromagnetic trap and the supporting rod. As a result of this, the trap, which is not water cooled, gets heated to ~300°C and the supporting rod to ~100°C. There are some breakdowns in which the electron avalanche starts to melt the ferromagnetic trap. Drops of

molten metal fall onto the grounded plate, thus forming a new flux of electrons which hits the supporting rod and produces extensive evaporation of the metal along with breakdown at the rod.

Breakdown between the gas discharge head and the intermediate electrode at negative potential, for the case of low power in the rectifier supplying voltage to the intermediate electrode, reverses the sign of the potential on the electrode and all the secondary emission electrons help to multiply the avalanche. The magnitude of the negative potential on the intermediate electrode has a substantial effect on avalanche formation. This may be seen from the X-ray intensity present during steady state operation of the source. For example, with a total current of 300 mA from the source, the X-ray intensity is 50 mCu/sec at -5 kV, 20 mCu/sec at -10 kV, and 10 mCu/sec at -20 kV. Putting a negative voltage (~15 kV) on the intermediate electrode from a power supply with small enough internal resistance that the voltage on the electrode remains almost constant when breakdown occurs greatly reduces the power in the avalanche, and prevents melting of the ferromagnetic trap.

Thus, degreasing and electropolishing of the surfaces, baking the various parts in a vacuum furnace, and high voltage treatment of the source, as well as using ferromagnetic traps and a high power rectifier to supply the intermediate electrode provides stable operation of the source at voltages up to 180 kV, and with total ion currents taken out up to 0.7 A.

If the voltage is raised to 200 kV, the source operates stably only if the current is less than 100 mA. Further increase in the total current taken out again caused powerful avalanches to develop on breakdown, together with melting of the source support rod. The relation between the various components of the current from the source and the discharge current for different gas flows into the gas discharge chamber (0.23, 0.2, and 0.15 cc/sec) is shown in Fig. 2. The data in the figure were taken at discharge voltages of 250-300 V, and an ion energy of 180 keV.

2. Ion Optics of the Injector

The ion optics of the injector is to a considerable extent determined by the type of molecular hydrogen ion source used.

The "Ogra" injection system consists of the rectangular magnet in which the source is located, two magnetic quadrupole lenses, and an iron-current screening channel (Fig. 3).

In the uniform field of the rectangular source magnet with 1100×600 mm poles and a 400 mm gap, the ion beam is sorted according to masses, and the molecular component is sorted out and rotated through 90°. The angular divergence of the beam leaving the source is $2\alpha \simeq 25°$ in the plane of symmetry of the magnetic field. After being rotated in the source magnet, the angle of divergence decreases to 1.5°, but aberrations occur in the plane of rotation. The beam width at this point is ~150 mm. The beam height (dimension along the lines of magnetic force) on leaving the source is 40 mm. For the arc running properly, the beam leaving the source is almost parallel to the plane of symmetry of the magnetic field. When it leaves the magnet, the height is not more than 60 mm. In this case, the angular deviation of the ion rays from the plane of symmetry turned out to be approximately proportional to the distance from the plane of symmetry, i.e., the beam is optical in this direction, and there is no need for special correction of the angles. Shimming of the edge of the magnet was used to reduce the aberration in the plane of rotation. Correcting the field reduced the angular divergence to 1° and greatly reduced the aberration. However, this had no effect on the beam focusing.

After leaving the source magnet, the molecular beam goes into a horizontal ion conductor ~8 m long, with two quadrupole lenses around it, each with an aperture of diameter 2d = 600 mm and 1 m long. The lenses consist of quadrupole magnets with cylindrical pole faces having the radius 1.15 d. The lenses are located approximately half way between the source magnet and the magnetic channel, 200 mm from one another. The astigmatism of the system is achieved by adjusting the currents in each of the lenses independently, which focuses the ion beam into the 60×60 mm output aperture of the magnetic channel, with an angular beam convergence of not more than 5°.

An investigation of the optical properties of the injection system without the magnetic channel was made on another injector, just like the "Ogra" injector. At the output from the source magnet, separate 5 mm diameter ion beams may be taken out of the ion flux as a whole, at any point over the cross-section of the beam. In the image plane, i.e., the plane where the output aperture of the magnetic channel is located, two probes were set up which were used to measure the coordinates of the arriving rays, and take the current density distribution over the cross-section of the incident total ion beam.

A focusing calculation made for the sytem of two quadrupole lenses has shown that with the existing input beam angles it is possible to get an image in the plane of the end of the magnetic channel consisting of a 30×20 mm ellipse with the long axis horizontal. Actually, these dimensions are for small beam currents (~0.5 mA), or for combining the currents from separate ion rays. As the current is increased, the dimensions of the image increase rapidly in the horizontal direction, although the distribution of the elementary ion rays remains constant (Fig. 4, curve 1). The beam width may be reduced by refocusing the ion rays (see Fig. 4, curve 4). The beam blow-up apparently comes from an increase in the space charge produced by modulation of the ion current. Oscillographs taken of the ion current have shown that it is always amplitude modulated. If enough gas is put into the gas discharge chamber of the source, the depth of modulation can reach 100%. By regulating the amount of gas, the depth of modulation may be reduced to 15-20%. The modulation spectrum occupies a band from ten or twenty or more cycles per second, without emphasizing any particular frequencies.

The dimensions of the image are only slightly dependent on the energy of the ions, since, although the volume density of particles in the beam drops with increase in energy, there is at the same time a reduction in the ionization cross-section of the residual gas. As a result, the unneutralized charge density changes very little. If the energy of the ions is increased from 100 to 200 keV, the change in width of the beam image is 15%.

The dimensions of the image depend substantially on the pressure in the ion conductor. The compensation of the beam improves with increase in pressure, but the scattering by the residual gas becomes appreciable, with the result that the beam dimensions first decrease, reaching a minimum, and then increase (Fig. 5). As the beam current is increased, compensation is reached at a higher pressure, so that the minimum moves to the right. At a current of 10-200 mA, the minimum beam dimensions occur at a pressure of from 1.5 to $4.5 \cdot 10^{-5}$ mm Hg.

The area of the 60×60 mm output aperture of the magnetic channel accommodates ~70% of the incident beam. Here, the beam losses over the path from dissociation and charge change at optimum pressure are ~30% of the molecular current from the source at an ion energy of 200 keV, or 45% at an ion energy of 100 keV.

3. The Magnetic Channel

The magnetic channel is a continuation of the ion conductor of the injector, and stops at the vertical diameter of the "Ogra" chamber. It is intended to inject the ion beam inside the magnetic field of the machine, and rotate it through an angle of 20° to the plane perpendicular to the magnetic field. In doing this, the channel must produce the minimum amount of perturbation in the axial symmetry of the magnetic field in the machine.

The method used to compensate for the perturbation produced by the iron was proposed by G. I. Budker in 1950 and was investigated experimentally by A. A. Arzumanov et al. [5]. Constructionally, the channel is a curved thin-walled tube of rectangular cross-section made of Armco iron with two windings, a deflecting winding and a compensating winding (Fig. 6).

The deflecting winding consists of a single turn carrying current, placed inside the channel. The shaped winding and internal walls of the channel produce a magnetic field which deflects the beam 20° and compresses it somewhat horizontally. The compensating winding consists of four current-carrying turns, connected in parallel, and placed outside the channel, to produce a horizontal magnetic field bucking the main field of the machine inside the winding. The purpose of this winding is to balance out the perturbation of the "Ogra" magnetic field produced by introducing the iron in the channel, and to weaken the field inside the channel.

Figure 7 shows the measured field perturbations produced by the magnetic channel for optimum current in the compensating winding. The largest field perturbation reaches 20% at $Z = 15$ cm, $r = 50$ cm, and $\varphi = 355°$, i.e., in the region where the molecular and atomic ions are rapidly lost in the magnetic channel. In the region where the atomic ions cannot be lost in the channel, the magnetic field perturbation is several percent.

Getting complete compensation of the perturbation introduced by the iron when using a curved channel requires special shaping of the compensating winding similar to that shown, and in addition a second winding to compensate for the longitudinal magnetization of the iron screen. By adding a second compensating winding we greatly increase the dimensions of the channel, and so it was not done. Further, the perturbation produced by the output end of the channel is not compensated for. Measurements of the magnetic field inside the channel have shown that over the length of the deflecting winding, the case of the channel saturates at the two diagonal corners, at the point where the flux from the external field is in the same direction as the flux from the deflecting field. This leads to the condition where the external field penetrating inside the channel distorts the deflecting field. Studies of the beam motion in-

side the channel show that apparently as a result of this the beam leaving the channel is greatly deformed. The focal spot, consisting of an ellipse with the long axis horizontal, is rotated through an angle of 30°, but the rotation does not produce any appreciable ion losses in the walls of the channel.

The ion current injected into the "Ogra" through the magnetic channel turned out to be somewhat higher than might be expected from the beam dimensions given in Section 2 as found from a study of the ion optics. This may be accounted for by the additional focusing action exerted by the deflecting field of the magnetic channel as well as by the additional neutralization of the beam space charge by secondary emission electrons from the magnetic channel. The secondary emission current from the inside walls of the channel may be quite large, since the ions are incident at glancing angles. For ion energies of 160-180 keV, 155 of 300 mA molecular ions leaving the source were injected into the "Ogra."

LITERATURE CITED

1. I. N. Golovin et al., "Usp. fiz. nauk", 73, No. 4, 685 (1961).
2. A. Simon, ORNL-2802, 96 (1959).
3. F. Gilbert et al., UCRL-5827 (1960).
4. P. M. Morozov and L. N. Pil'gunov, "Zh. tekhn. fiz.", 3, No. 3 (1963).
5. A. A. Arzumanov et al., "Atomnaya énergiya," 10, No. 5, 461 (1961).

All abbreviations of periodicals in the above bibliography are letter-by-letter transliterations of the abbreviations as given in the original Russian journal. *Some or all of this periodical literature may well be available in English translation.* A complete list of the cover-to-cover English translations appears at the back of this issue.

THEORY OF THE PASSAGE OF γ-QUANTA THROUGH MATTER

V. S. Galishev

Translated from Atomnaya Énergiya, Vol. 14, No. 5,
pp. 453-457, May, 1963
Original article submitted July 26, 1962

An analytic treatment is given of the problem of the passage of γ-quanta through a plain parallel slab. The integro-differential equation including boundary conditions for the problem of the scattered γ flux density in the nth approximation reduces to a system of 2nd integro-differential equations of the first order for the coefficients in the Legendre polynomial expansion of the scattered γ flux density. The values of the 2n arbitrary constants are found from the 2n boundary conditions. The final results are given only for the case n = 1, which gives the spectral destribution of the scattered γ flux density at a fixed distance from the source.

INTRODUCTION

A large amount of attention has recently been devoted to the passage of γ-radiation through matter. When they are being propagated in various absorbing media, the γ-rays are absorbed and scattered, where, for a large absorber thickness, the greater part of the intensity goes, not into primary, but into multiply scattered quanta. Because of the multiple scattering, the attenuation of the γ intensity with increase in depth of penetration into the absorber cannot be described by a simple exponential law. The attenuation of the radiation depends in a complicated way on the energy and geometric shape of the source, as well as on the properties and geometry of the absorber. Many methods, rigorous to different degrees, have been proposed to find the relation that applies [1-4].

At the present time, the so-called method of moments [5, 6] must be regarded as one of the most rigorous methods for making calculations on the passage of γ-quanta through matter. The essence of the method is that it reduces the integro-differential kinetic equation for the photon flux density fuction, which depends on three variables, to a system of coupled integral equations for the space-angular moments of the photon flux density function, which are dependent on only one variable. The system of integral equations is solved by numerical methods, after which the moments found are used to get the photon flux density.

The most serious limitation on the method of moments is that it is applicable only to an infinite medium. The method of moments is naturally unsuited to solving the important practical problem of a finite medium.

The purpose of the present paper is to attempt an analytic treatment of the simplest boundary problem in the passage of γ-quanta through matter. The problem reduces to the following. Assume that a beam of monochromatic γ-quanta is incident normally on a plain parallel slab of finite thickness a along the x axis and infinite in extent along the y and z axes. The interest is in the photon flux density leaving the surface (x = a), as well as in the photon flux density coming back from the surface (x = 0).

It may be pointed out in connection with the method used to solve the above problem, that it is in many ways similar to Mertens' [7], used to solve a similar problem, but for charged particles rather than γ-quanta.

Mertens' Method as Applied to the Theory of Multiple γ-Scattering

As the basis of our discussion of the solution of the boundary problem formulated in the introduction on the passage of γ-quanta through a plain parallel slab, we make use of the integro-differential transport equation for a source located in the infinite plane (x = 0) emitting quanta with the wavelength $\lambda = \lambda_0$ (in Compton units) normal to the surface. The equation may be written in the following way [1, 5]:

$$u_x \frac{\partial N(x, u_x, \lambda)}{\partial x} + \mu(\lambda) N(x, u_x, \lambda) = \int_{\lambda_0}^{\lambda} d\lambda' K(\lambda', \lambda) \int_{4\pi} d\mathbf{u}' \frac{1}{2\pi} \delta(1 - \mathbf{u}\mathbf{u}' - \lambda + \lambda') \times N(x, u_x', \lambda') \qquad (1)$$

with the boundary conditions

$$\left.\begin{aligned} N(0,\ u_x,\ \lambda) &= \frac{1}{2\pi}\,\delta(1-u_x)\,\delta(\lambda-\lambda_0) \quad \text{for} \quad u_x > 0; \\ N(a,\ u_x,\ \lambda) &= 0 \quad \text{for} \quad u_x < 0. \end{aligned}\right\} \tag{2}$$

Here $N(x, u_x, \lambda)$ is the flux density of photons with wavelength λ at the distance x from the source, forming the angle $\cos^{-1}u_x$ with the normal to the slab (x axis), $\mu(\lambda)$ is the total attenuation coefficient of the medium for γ-quanta with wavelength λ; $K(\lambda', \lambda)$ is the Klein-Nishina coefficient for Compton scattering with a wavelength change from λ' to λ, and $\delta(x)$ is Dirac's δ-function. Of the two boundary conditions (2), the first reflects the fact that the γ-quanta only enter the slab normal to the surface ($x = 0$), while the second corresponds to the assumption that none of the γ-quanta were turned back from the exit surface ($x = a$).

In considering the possibility of applying Mertens' method to the theory of multiple γ scattering in a finite medium, we shall look for a solution of the original Eq. (1) with the boundary conditions (2) in the form

$$N(x,\ u_x,\ \lambda) = \frac{1}{2\pi}\,\delta(1-u_x)\,\delta(\lambda-\lambda_0)\,e^{-\mu(\lambda_0)x} + N'(x,\ u_x,\ \lambda), \tag{3}$$

where the first term is for unscattered radiation, while the second is for radiation that has undergone scattering. If we further substitute Eq. (3) for the total photon flux density, in Eq. (1), and use the Legendre polynomial representation of the δ-function, it is not difficult to show that the scattered photon flux density satisfies the equation

$$u_x\frac{\partial N'(x,\ u_x,\ \lambda)}{\partial x} + \mu(\lambda)\,N'(x,\ u_x,\ \lambda) = \int_{\lambda_0}^{\lambda} d\lambda' K(\lambda', \lambda)\sum_{l=0}^{\infty}\left(\frac{2l+1}{2}\right)P_l(1-\lambda+\lambda')\,P_l(u_x)$$

$$\times\int_{-1}^{1} du_x' P_l(u_x')\,N'(x,\ u_x',\ \lambda) + e^{-\mu(\lambda_0)x}K(\lambda_0,\lambda)\times\sum_{l=0}^{\infty}\left(\frac{2l+1}{4\pi}\right)P_l(1-\lambda+\lambda')\,P_l(u_x) \tag{4}$$

with the boundary conditions

$$\left.\begin{aligned} N'(0,\ u_x,\ \lambda) &= 0 \quad \text{for} \quad u_x > 0; \\ N'(a,\ u_x,\ \lambda) &= 0 \quad \text{for} \quad u_x < 0. \end{aligned}\right\} \tag{5}$$

Let $N_+(x, u_x, \lambda)$ and $N_-(x, u_x, \lambda)$ be the scattered photon flux densities of wavelength λ at distance x from the source for $u_x > 0$ and $u_x < 0$ respectively, and expand these functions in Legendre polynomial series in the ranges 0 to 1 and -1 to 0. This gives

$$N_{\pm}(x,\ u_x,\ \lambda) = \sum_{l=0}^{\infty}(2i+1)\,N_i^{\pm}(x,\lambda)\,P_i(2u_x \mp 1), \tag{6}$$

where $P_i(x)$ is a Legendre polynomial of the ith degree. Then, the system of integro-differential equations for the expansion coefficients $N_I^{\pm}(x, \lambda)$ takes the form

$$i\frac{\partial N_{i-1}^{\pm}(x,\lambda)}{\partial x} \pm (2i+1)\frac{\partial N_i^{\pm}(x,\lambda)}{\partial x} + (i+1)\frac{\partial N_{i+1}^{\pm}(x,\lambda)}{\partial x} + 2(2i+1)\,\mu(\lambda)\,N_i^{\pm}(x,\lambda)$$

$$= (2i+1)\int_{\lambda_0}^{\lambda} d\lambda' K(\lambda',\ \lambda)\ \times\sum_{l=i}^{\infty}(2l+1)\,P_l(1-\lambda+\lambda')\,P_{li}^{\pm}\times\left\{\sum_{r=0}^{l}(2r+1)\,P_{lr}^{-}N_r^{-}(x,\ \lambda')\right.$$

$$\left.+\sum_{r=0}^{l}(2r+1)\,P_{lr}^{+}N_r^{+}(x,\ \lambda')\right\} + (2i+1)\,e^{-\mu(\lambda_0)x}K(\lambda_0,\ \lambda)\times\sum_{l=i}^{\infty}\left(\frac{2l+1}{2\pi_j}\right)P_l(1-\lambda+\lambda_0)\,P_{li}^{\pm} \tag{7}$$

with the boundary conditions

$$N_i^{+}(0,\ \lambda) = 0, \qquad N_i^{-}(a,\ \lambda) = 0 \tag{8}$$

and

$$P_{li}^{+} = (-1)^{l+i}P_{li}^{-} = \int_0^1 P_l(x)\,P_i(2x-1)\,dx. \tag{9}$$

In order to get a solution in the nth approximation, we retain the system formed by the first n equations of (7): in the nth equation we take $N_n^+(x, \lambda) = N_n^-(x, \lambda) = 0$, and, in addition, we shall everywhere assume $P_n(1-\lambda+\lambda') = P_{n+1}(1-\lambda+\lambda') = \ldots = 0$ (this actually corresponds with replacing the δ-function in Eq. (1) by a finite segment of its Fourier series in Legendre polynomials). Thus, we get a system of 2n linear integro-differential equations in partial derivatives of the first order, which makes it possible to calculate the two unknown functions, $N_i^{\pm}(x,\lambda)$ [i = 0, 1, 2, . . . , (n-1)]. The values of the 2n arbitrary constants are completely determined by the condition (8).

In the first approximation (n = 1), we have, to find the two unknown functions $N_0^{\pm}(x, \lambda)$, the system of two integro-differential equations

$$\pm \frac{\partial N_0^{\pm}(x, \lambda)}{\partial x} + 2\mu(\lambda) N_0^{\pm}(x, \lambda) = \frac{1}{2\pi} K(\lambda_0, \lambda) e^{-\mu(\lambda_0)x} + \int_{\lambda_0}^{\lambda} K(\lambda', \lambda) [N_0^+(x, \lambda') + N_0^-(x, \lambda')] d\lambda' \quad (10)$$

with the boundary conditions

$$N_0^+(0, \lambda) = 0, \quad N_0^-(a, \lambda) = 0. \quad (11)$$

The approximate analytic expressions for the solution of the system of equations (10) may be found by the method of successive approximations.

As a "zero" roughest approximation for the desired solution, we take the functions $N_{00}^{\pm}(x, \lambda)$ found from the two equations

$$\pm \frac{\partial N_{00}^{\pm}(x, \lambda)}{\partial x} + 2\mu(\lambda) N_{00}^{\pm}(x, \lambda) = \frac{1}{2\pi} K(\lambda_0, \lambda) e^{-\mu(\lambda_0)x} \quad (12)$$

with the boundary conditions

$$N_{00}^+(0, \lambda) = 0, \qquad N_{00}^-(a, \lambda) = 0. \quad (13)$$

Then to find the functions $N_{01}^{\pm}(x, \lambda)$ for the first approximation, we will have the following two equations

$$\pm \frac{\partial N_{01}^{\pm}(x, \lambda)}{\partial x} + 2\mu(\lambda) N_{01}^{\pm}(x, \lambda) = \frac{1}{2\pi} K(\lambda_0, \lambda) e^{-\mu(\lambda_0)x} + \int_{\lambda_0}^{\lambda} K(\lambda', \lambda) [N_{00}^+(x, \lambda') + N_{00}^-(x, \lambda')] d\lambda' \quad (14)$$

with

$$N_{01}^+(0, \lambda) = 0, \qquad N_{01}^-(a, \lambda) = 0. \quad (15)$$

Continuing the solution in this way, we obtain the two infinite sequences of functions

$$N_{00}^{\pm}(x, \lambda), N_{01}^{\pm}(x, \lambda), N_{02}^{\pm}(x, \lambda), \ldots, N_{0n}^{\pm}(x, \lambda), \ldots, \quad (16)$$

satisfying the recursion formulas

$$\pm \frac{\partial N_{0n}^{\pm}(x, \lambda)}{\partial x} + 2\mu(\lambda) N_{0n}^{\pm}(x, \lambda) = \frac{1}{2\pi} K(\lambda_0, \lambda) e^{-\mu(\lambda_0)x} + \int_{\lambda_0}^{\lambda} K(\lambda', \lambda) [N_{0, n-1}^+(x, \lambda') + N_{0, n-1}^-(x, \lambda')] d\lambda' \quad (17)$$

with

$$N_{0n}^+(0, \lambda) = 0, \qquad N_{0n}^-(a, \lambda) = 0 \quad (n = 1, 2, 3, \ldots). \quad (18)$$

If we assume

$$N_{0n}^{\pm}(x, \lambda) - N_{0, n-1}^{\pm}(x, \lambda) = \overline{N}_{0n}^{\pm}(x, \lambda), \quad (19)$$

we have

$$N_{0n}^{\pm}(x, \lambda) = \sum_{\nu=0}^{n} \overline{N}_{0\nu}^{\pm}(x, \lambda), \quad (20)$$

where

$$\overline{N}^{\pm}_{\bar{0}}(x,\ \lambda) = N^{\pm}_{00}(x,\ \lambda)$$

and

$$\pm \frac{\partial \overline{N}^{\pm}_{0n}(x,\lambda)}{\partial x} + 2\mu(\lambda)\overline{N}_{0n}(x,\ \lambda) = \int_{\lambda_0}^{\lambda} K(\lambda',\ \lambda)\,[\overline{N}^{+}_{\bar{0},n-1}(x,\ \lambda') + \overline{N}^{-}_{\bar{0},n-1}(x,\ \lambda')]\,d\lambda' \tag{21}$$

for

$$\overline{N}^{+}_{\bar{0}n}(0,\ \lambda) = 0,\quad \overline{N}^{-}_{\bar{0}n}(a,\ \lambda) = 0$$
$$(n = 1,\ 2,\ 3,\ \ldots,). \tag{22}$$

The solutions of Eqs. (21) satisfying the boundary conditions (22) are of the form

$$\overline{N}^{+}_{\bar{0}n}(x,\ \lambda) = \int_{\lambda_0}^{\lambda} d\lambda' K(\lambda',\ \lambda) \int_{0}^{x} dx' e^{-2\mu(\lambda)(x-x')} \times [\overline{N}^{+}_{\bar{0},n-1}(x',\ \lambda') + \overline{N}^{-}_{\bar{0},n-1}(x',\ \lambda')], \tag{23}$$

$$\overline{N}^{-}_{\bar{0}n}(x,\ \lambda) = \int_{\lambda_0}^{\lambda} d\lambda' K(\lambda',\ \lambda) \int_{x}^{a} dx' e^{-2\mu(\lambda)(x'-x)} \times [\overline{N}^{+}_{\bar{0},n-1}(x',\ \lambda') + \overline{N}^{-}_{\bar{0},n-1}(x',\ \lambda')]. \tag{24}$$

The difference between Eqs. (23) and (24) is that in the first case, $\int_0^x dx' \ldots$ is replaced by $\int_x^a dx' \ldots$, and, in addition, x and x' exchange places in the exponent. Accordingly, it is entirely sufficient to make the subsequent transformations, for example, $\overline{N}^{+}_{\bar{0}}(x, \lambda)$. We express the integral in terms of $N^{+}_{00}(x, \lambda)$. For n = 1, we obtain

$$\overline{N}^{+}_{01}(x,\ \lambda) = \int_{\lambda_0}^{\lambda} d\lambda_1 K(\lambda_1,\ \lambda) \int_{0}^{x} dx_1 e^{-2\mu(\lambda)(x-x_1)} \times [N^{+}_{00}(x_1,\ \lambda_1) + N^{-}_{00}(x_1,\ \lambda_1)]. \tag{25}$$

If, however, n > 1, the appropriate expressions take on more complex form:

$$\overline{N}^{+}_{\bar{0}n}(x,\ \lambda) = \int_{\lambda_0}^{\lambda} d\lambda_1 K(\lambda_1,\ \lambda) \int_{0}^{x} dx_1 e^{-2\mu(\lambda)(x-x_1)} \times \prod_{i=2}^{n} \int_{\lambda_0}^{\lambda_{i-1}} d\lambda_i K(\lambda_i,\ \lambda_{i-1})$$

$$\times \left[\int_{0}^{x_{i-1}} dx_i e^{-2\mu(\lambda_{i-1})(x_{i-1}-x_i)} + \int_{x_{i-1}}^{a} dx_i e^{-2\mu(\lambda_{i-1})(x_i-x_{i-1})} \right] \times [N^{+}_{00}(x_n,\ \lambda_n) + N^{-}_{00}(x_n,\ \lambda_n)]. \tag{26}$$

It is natural to expect further that the solution of the system of two integro-differential equations (10) with the boundary conditions (11) will be in the form of a sum of infinite series

$$N^{\pm}_{\bar{0}}(x,\ \lambda) = \sum_{n=0}^{\infty} \overline{N}^{\pm}_{\bar{0}n}(x,\ \lambda), \tag{27}$$

where the expressions for $\overline{N}^{+}_{\bar{0}n}$ are given by Eqs. (25) and (26), while the corresponding expressions for $\overline{N}^{-}_{\bar{0}n}$ are obtained formally from these equations in a way similar to that in which (24) is obtained from (23).

Thus, the method of successive approximations actually enables one to make a more general study of the first approximation to the problem of the passage of γ-quanta through a plain parallel slab.

CONCLUSION

The spectral distribution of the scattered photon flux density at a distance x from the source is given by the integral of $N'(x, u_x, \lambda)$ over all possible values of u_x. From Eq. (6), this integral is

$$\int_{-1}^{1} N'(x,\ u_x,\ \lambda)\,du_x = N^{+}_{\bar{0}}(x,\ \lambda) + N^{-}_{\bar{0}}(x,\ \lambda). \tag{28}$$

The values of $N_0^{\pm}(x, \lambda)$ are given approximately by the first approximation discussed in the preceding section.

Accordingly, the calculations given above point to a method for making an approximate calculation of the spectral distribution of the scattered photon flux density in the problem of the passage of γ-quanta through a plain parallel slab. At the exit surface, because of the boundary conditions (8), $N_0^-(a, \lambda) = 0$, and the spectral distribution of the scattered photon flux density is given by means of

$$N_0^+(a, \lambda) = \overline{N}_{00}^+(a, \lambda) + \overline{N}_{01}^+(a, \lambda) + \overline{N}_{02}^+(a, \lambda) + \ldots . \tag{29}$$

For $\overline{N}_{00}^+(a, \lambda)$, we find, from Eq. (12) and the boundary condition (13)

$$N_{00}^+(a, \lambda) = \frac{K(\lambda_0, \lambda)}{2\pi[2\mu(\lambda) - \mu(\lambda_0)]} e^{-\mu(\lambda_0)a} \times [1 - e^{-[2\mu(\lambda) - \mu(\lambda_0)]a}]. \tag{30}$$

The expressions for the other terms in (29) are also easily found by using Eqs. (25) and (26). At the input surface of the slab, the spectral distribution of the scattered photon flux density is found by means of

$$N_0^-(o, \lambda) = \overline{N}_{00}^-(o, \lambda) + \overline{N}_{01}^-(o, \lambda) + \overline{N}_{02}^-(o, \lambda) + \ldots , \tag{31}$$

where

$$\overline{N}_{00}^-(o, \lambda) = \frac{K(\lambda_0, \lambda)}{2\pi[2\mu(\lambda) + \mu(\lambda_0)]} (1 - e^{-[2\mu(\lambda) + \mu(\lambda_0)]a}), \tag{32}$$

while the expressions for all the other terms are also easily found from equations similar to (25) and (26).

The application to concrete cases of the above method of calculating the passage of γ-quanta through matter will be discussed in a special paper.

LITERATURE CITED

1. V. S. Galishev, V. I. Ogievetskii, and A. N. Orlov, Usp. fiz. Nauk, 61, 161 (1957).
2. N. F. Nelipa, Introduction to the Theory of Multiple Particle Scattering [in Russian], Atomizdat, Moscow (1960).
3. O. I. Leipunskii, B. V. Novozhilov, and V. N. Sakharov, Propagation of γ-Quanta in Matter [in Russian], Fizmatgiz, Moscow (1960).
4. U. Faho, L. Spencer, and M. Berger, Penetration and Diffusion of X Rays, Handbuch der Physik, 38/2, 660 ed., Springer, Berlin (1959).
5. L. Spencer and U. Fano, J. Res. Nat. Bur. Standards, 46, 446 (1951).
6. H. Goldstein and J. Wilkins, Calculations of the Penetration of Gamma Rays, NYO-3075 (1954).
7. R. Mertens, Compt. rend., 236, 1753 (1953); 237, 1644 (1953); 238, 53 (1954).

THE DIFFERENTIAL EQUATION FOR THE THERMALIZATION OF NEUTRONS IN INFINITE HOMOGENEOUS MEDIA

N. I. Laletin

Translated from Atomnaya Énergiya, Vol. 14, No. 5,
pp. 458-464, May, 1963
Original article submitted July 18, 1962

We consider the problem of the calculation of the spectrum of slow neutrons in an infinite, homogeneous medium with constant sources. From the investigation of solutions for cases when absorption is absent and the medium is a gas of heavy atoms ($m \gg 1$) and atoms of hydrogen ($m = 1$), a differential equation of the second order is obtained for the asymptotic solution of the problem for a monatomic gas with arbitrary atomic weight m; this solution is then generalized to apply to a medium with absorption. For $m \gg 1$ and $m = 1$, this equation is converted into known differential equations, and can thus be applied in the case of a monatomic gas with nuclei of arbitrary mass.

INTRODUCTION

The neutron density in an infinite, homogeneous medium with constant temperature T and constant sources satisfies the differential equation

$$[G_a(z) + G_s(z)]\,N(z) = \int G_s(z' \to z)\,N(z')\,dz' + S(z), \tag{1}$$

where z is the energy E of a neutron in kT units, i.e., $z = E/kT$ (k is the Boltzmann constant); N(z) the density of neutrons with energy in the interval (z, z+dz); S(z) the density of sources of neutrons with energy z; $G_s(z)$ the probability that a neutron with energy z' experiences scattering in unit time; $G_s(z' \to z)$ the probability that a neutron with energy z' is scattered and that its resulting energy is in the interval (z, z+dz); $G_a(z)$ the probability that a neutron with energy z is absorbed. It is obvious that, in Eq. (1), $G_s(z)$ and $G_s(z' \to z)$ can cease to be probabilities only in the case of scattering that is connected with the measurement of neutron energy in a laboratory coordinate system.

For neutrons with energies $z \leqslant 1$, the probabilities $G_a(z)$, $G_s(z)$, and $G_s(z' \to z)$ must be calculated taking into account the thermal motion of the nuclei and the interrelations between these motions. This problem is rather complicated, and is of independent interest. But even when the relevant probabilities are known, the solution of Eq. (1) is very difficult. We note that the method of solving the equation for the determination of the energy distribution of the neutrons by dividing up the neutron spectrum into groups relative to their energy (the group method), which is valid in a region of moderation ($z \gg 1$), is exceedingly laborious in problems concerning thermalization ($z \leqslant 1$). To understand the reason for this, we write Eq. (1) in the form

$$\left.\begin{aligned} \frac{dQ}{dz} &= \psi_a(z) - S'(z), \\ Q(z) &= \int_0^z dz'' \int_z^\infty G_s(z' \to z'')\,N(z')\,dz' \\ &\quad - \int_z^\infty dz'' \int_0^z G_s(z' \to z'')\,N(z')\,dz'. \end{aligned}\right\} \tag{1a}$$

where

Here $\psi_a(z) = G_a(z)\,N(z)$ is the absorption density. The meaning of Q(z) is clear from the equation: it is the so-called current along the energy axis. For $z \gg 1$, when neutrons are scattered they can only lose energy, and Q coincides with the moderation density. In the moderation region, $\psi_a(z)$ and S(z) are usually small, and so Q(z) varies only slightly. Even when the neutrons are divided according to energy into relatively large groups, this fact permits a

reasonably accurate description of the behavior of the neutrons inside a group, and a resulting good accuracy in the determination of the group constants.

In a thermalization region, there is not such a small variation in the parameters. The quantities Q(z) and N(z) vary weakly, and so, to obtain a sufficiently accurate solution of Eq. (1), it is necessary to use a large number of groups. [The quantity N(z)/M(z), where M(z) is the equilibrium Maxwellian distribution, varies weakly on the average in the region of thermal neutron energy when the absorption is small, but it increases rapidly with increasing energy in a region of transition from thermal energy to epithermal energy.]

Moreover, in contrast to the problem of moderation, the neutrons in the thermalization problem can pass from one group to another as a result of scattering, and they do not necessarily pass into a group with lower energy. These facts complicate the calculations. It is thus not surprising that a great amount of attention has been paid to the investigation of the simple cases where the integral equation for N(z) can be reduced to a differential equation. A differential equation for N(z), equivalent to the integral equation (1), can be obtained when the medium is a monatomic gas consisting of nuclei with mass m = 1 (the neutron mass is taken as the unit) and the scattering cross section is independent of the relative velocity of motion of neutrons and nuclei. (This latter condition is reasonably well-satisfied when the temperature is not too high, because of the behavior of neutron cross-sections at free, quiescent nuclei for low neutron energy, which is known from the results of quantum mechanics.) In this case, the differential probability of scattering $G_s(z' \to z)$ is given in the ranges $z' \leq z$ and $z' \geq z$ in the form of a product of functions, one of which depends only on z and the other only on z'.

As a result, Eq. (1) for N(z) can be reduced to the following differential equation, known in the literature as the Wigner-Wilkins equation (see, for example, [1])•:

$$\frac{d}{dz}\left\{\mathcal{P}(z)\frac{d}{dz}\left[N(z)\left(G_a(z)+G_s(z)\right)\right]\right\}+\left[R(z)\left(G_a(z)+G_s(z)\right)+\frac{e^z}{\sqrt{z}}\right]N(z)=0, \tag{2}$$

where

$$\mathcal{P}(z)=\frac{\sqrt{\pi z}\,e^z}{e^z+\sqrt{\pi z}\,\operatorname{erf}\sqrt{z}}; \qquad R(z)=\frac{[\mathcal{P}(z)]^2 e^{-2z}}{2z^{3/2}\sqrt{\pi}}.$$

If the medium is a monatomic gas with mass $m \gg 1$, then for N(z) we can obtain an approximate differential equation of the second order, that is to say that this equation is correct to the zeroth and first approximation in the expansion of the probabilities in powers of 1/m

In the zeroth approximation, the equation is

$$z\Phi''+z\Phi'+\Phi\left(1-\frac{\Delta}{4\sqrt{z}}\right)=0, \tag{3}$$

where

$$\Phi=\sqrt{z}N(z); \quad \Delta=\frac{2m\sigma_a(kT)}{\sigma_s(\infty)}; \quad \sigma_i(z)=\frac{G_i(z)}{\sqrt{z}}.$$

This equation was first obtained by V. I. Davydov in [2] in the course of an investigation of the motion of electrons in gases. It was introduced into neutron physics by Wilkins in [3], and is known in this type of work as the Wilkins equation.

The equation of the second order for N(z) in the second approximation was obtained by Corngold in [4], and is

$$z\Phi''+z\Phi'\left[1-\frac{1}{m}\left(\frac{\Delta}{3z^{3/2}}+\frac{1}{z^2}\right)\right]+\Phi\left\{1-\frac{\Delta}{4\sqrt{z}}+\frac{1}{m}\left[\frac{1}{z^2}+\frac{\Delta}{2z^{3/2}}+\frac{1}{z}\left(\frac{\Delta^2}{12}-1\right)-\frac{\Delta}{3\sqrt{z}}\right]\right\}=0. \tag{4}$$

In the present problem it is equivalent to an equation of the fourth order obtained for this case by Wilkins [3].

The fact is that the neutron density N(z) satisfies a differential equation of the second order in two limiting cases; when the mass of the nucleus is m = 1 and the change in the neutron energy due to one collision is large, and

• In [1], Eq. (2) is given in the variables $x = \sqrt{z}$ and for $v(x)=\frac{N(x)}{\sqrt{M(x)}}$.

when $m \gg 1$ and the energy variation is small. This points to the conjecture that there is a differential equation for the asymptotic part of N(z) for a gas of nuclei of arbitrary mass. (Such an equation can evidently not describe the nonasymptotic part of the solution, such as the irregularities in the solution investigated by Placzek [5] in the theory of neutron moderation.)

We recall that, in the problem of the space distribution of neutrons in a breeding medium, the asymptotic part of the solution Φ_{as} satisfies the differential equation of the second order (see [6] for example)

$$\nabla^2\Phi_{as}(\bar{r}) - \frac{1}{L^2}\Phi_{as}(\bar{r}) = 0, \tag{5}$$

where L^2 is the solution of a certain transcendental equation [for a medium with isotropic scattering it is the solution of the equation $(l/L) = \tanh(l_s/L)$, where l is the total free-path length and l_s is the path length relative to the scattering].

The desired differential equation for the energy distribution of neutrons in a homogeneous medium must evidently be sought as having the same relation to Eq. (1) as Eq. (5) has relative to the kinetic equation for $\Phi(\bar{r})$.

If we succeeded in finding the differential equation for N(z) in the case when the medium is a monatomic gas, then by ascribing a definite physical sense to the coefficients of this equation we could try to extend it to be applicable to other media. An advantage of such an equation, in addition to the fact that it can be much more easily solved numerically than the integral equation, would be that, instead of a complete knowledge of the scattering indicatrix $G_s(z' \to z)$ which is a function of two variables and a knowledge of which is consequently equivalent to a knowledge of an infinite number of functions of one variable, a knowledge of a bounded number of functions of a single variable (in our case not more than three) is all that would be needed. In the present article, an attempt will be made to find the differential equation for the asymptotic part of the solution of Eq. (1). In view of the fact that the equation proposed in this work was obtained from the integral equation in a not completely rigorous way, and that our results are based on an investigation of known limiting cases (a monatomic gas with $m = 1$ and $m \gg 1$), its range of applicability is not completely clear. However, using the fact that even calculations using a rough model of a heavy, monatomic gas yield satisfactory results in many interesting cases and need only small correction, we can hope that our differential equation will be useful.

A Homogeneous Medium without Absorption

In order to obtain the differential equation for the asymptotic solution of Eq. (1), we turn at once to the investigation of the homogeneous integral equation

$$[G_a(z) + G_s(z)]\,N(z) = \int_0^\infty G_s(z' \to z)\,N(z')\,dz'. \tag{6}$$

We start by considering a medium without absorption, i.e., with $G_a(z) = 0$. In this case, the solution is the Maxwell distribution: $M(z) = \sqrt{z}\,e^{-z}$. This is however not the only solution of Eq. (6). In fact this equation can be written in the form $dQ/dz = 0$, where Q is obtained from (1a). The solution is obviously $Q = \text{const}$. But the Maxwell distribution corresponds to a zero current along the energy axis $Q = 0$. There must therefore be one or several solutions for a constant current along the energy axis. The objection might be raised that, in an infinite medium without sources or absorption, there can be no current along the energy axis, and because of the existence of such a current our solution has no physical meaning. This, of course, is true, but the consideration of this case is nevertheless of value.

To clarify the position, we again turn to the problem of the propagation of monoenergetic neutrons in an infinite medium. In such a medium with no absorption, the general solution of the kinetic equation for $\Phi(\bar{r})$ is a linear function. If the medium is infinite, then only the constant component of the solution has any physical sense. The variable component due to the constant propagation of the current must be discarded. But if the medium is finite but large, i.e., its dimensions are much greater than the length of the mean free path of a neutron in matter and at its boundary there are neutron sources on one side and neutron sinks at the other, then in the whole region, except for small neighborhoods of the sources and sinks (of the order of the free-path length), the solution will coincide with the general solution of the equation for an infinite medium, i.e., it will be a linear function.

In our case we can similarly assume that there is a source emitting neutrons with a finite but very large energy $z_1 \gg 1$, and that neutrons are being absorbed in regions of very low energy $z \leq z_2$, where $z_2 \ll 1$. Then for the en-

ergy range $z_2 < z < z_1$ we should expect that N(z) would give a good description of the general solution of Eq. (6) everywhere except in the immediate neighborhood of the energy boundaries z_1 and z_2.

We rewrite (6) for $G_a = 0$ in the form

$$\int_0^\infty G_s(z \to z') \left[\frac{N(z')}{M(z')} - \frac{N(z)}{M(z)} \right] dz' = 0. \tag{7}$$

Here the detailed-balance principle

$$G_s(z' \to z) M(z') = G_s(z \to z') M(z).$$

is used. We will assume that, in addition to the obvious solution N(z)/M(z) = const, there is a further solution N(z)/M(z) = f(z).

The function f(z) cannot have a largest or smallest value for any z in the range $0 < z < \infty$. In fact if the inequality $f(z) \gtrless f(z_0)$ were satisfied for all $z \neq z_0$, then the integrand in (7) would have a constant sign at the point z_0 because of the definiteness of $G_s(z \to z')$, and the integral could not be zero. Since Eq. (7) must also hold at the ends of the z range, then f(z) can increase indefinitely at only one end of the interval and must decrease indefinitely at the other.

We thus assume that the asymptotic solution of (7) has the form

$$\frac{N}{M}(f) = C_1 + C_2 f,$$

where C_1 and C_2 are arbitrary constants. Since there are only two constants, the function N/M, and thus N, can satisfy a differential equation of only the second order.

We write this equation as two linear equations of the first order:

$$\left.\begin{aligned} \frac{dQ}{dz} &= 0; \\ Q &= \frac{dz}{df} \cdot \frac{d}{dz}\left(\frac{N}{M}\right). \end{aligned}\right\} \tag{8}$$

Up to this stage, our investigation has proceeded without the use of any concrete model of the medium. To obtain a definite form for the function f(z) we must now consider known, simple cases: monatomic gases with m = 1 and $m \gg 1$.

The solutions of the Wigner-Wilkins, Corngold, and Wilkins equations for $G_a = 0$ can be obtained simply. We write them in succession, and also the expression for the probability of neutron scattering in a gas with mass m:

for m = 1,

$$\frac{N(z)}{M(z)} = C_1 + C_2 \times \left[\int_0^z \frac{e^{z'}\, dz'}{\left(z' + \frac{1}{2}\right) \operatorname{erf} \sqrt{z'} + \sqrt{\frac{z'}{\pi}} e^{-z'}} - \frac{e^z}{\left(z + \frac{1}{2}\right) \operatorname{erf} \sqrt{z} + \sqrt{\frac{z}{\pi}} e^{-z}} \right];$$

for $m \gg 1$,

$$\frac{N(z)}{M(z)} = C_1 + C_2 \left[\int_0^z \frac{e^{z'}\, dz'}{\left(z' + \frac{1}{2m}\right)} - \frac{e^z}{z + \frac{1}{2m}} \right]; \quad \frac{N(z)}{M(z)} = C_1 + C_2 \left[\int_{-\infty}^z \frac{e^{z'} dz'}{z'} - \frac{e^z}{z} \right]^*; \tag{9}$$

* The integral in the Wilkins solution must be taken from $-\infty$, since the integral from 0 to z diverges. A comparison of the expressions in (9) clearly shows that the equations obtained by expanding the probabilities in powers of 1/m is not applicable for $z \ll 1/m$.

$$G_s(z)=\left(\sqrt{z}+\frac{1}{2m\sqrt{z}}\right)\operatorname{erf}\sqrt{mz}+\frac{e^{-mz}}{\sqrt{\pi m}}. \tag{10}$$

It is obvious from a comparison fo the formulas in (9) and (10) that, for a gas with arbitrary mass m, the solution for N(z)/M(z) can naturally be expressed in the form

$$\frac{N(z)}{M(z)}=C_1+C_2\left(\int_0^z\frac{dz}{\psi_s^0}-\frac{1}{\psi_s^0}\right),$$

where $\psi_s^0 = G_s(z)\,M(z)$ is the equilibrium scattering density. It is not hard to see that all the formulas in (9) can be obtained from this expression.

Thus the second equation of the sytem (8) can be written as

$$Q=\text{const}\ \frac{(\psi_s^0)^2}{\psi_s^0+\frac{d}{dz}\psi_s^0}\cdot\frac{d}{dz}\left(\frac{\psi_s}{\psi_s^0}\right),$$

where $\psi_s = G_s(z)\,N(z)$ is the scattering density. The constant is easily obtained by using the fact that, for $z \gg 1$, we must obtaine the known solution of the neutron-moderation problem at motionless nuclei

$$\psi_s(z\gg 1)\simeq\frac{Q}{\xi z}.$$

Noting that $\dfrac{-\frac{d}{dz}\psi_s^0}{\varphi_s^0+\frac{d}{dz}\psi_s^0}\simeq z$ for $z \gg 1$, we obtain $\text{const}=\xi=1+\dfrac{\alpha}{1-\alpha}\ln\alpha$ as the mean logarithmic loss of energy when a neutron is scattered at a motionless nucleus $\left(\alpha=\left(\dfrac{m-1}{m+1}\right)^2\right)$.

We finally wirte the equations for a monatomic-gas medium without absorption

$$\left.\begin{aligned}&\frac{dQ}{dz}=0;\\ &Q=\frac{(\xi\psi_s^0)^2}{\xi\psi_s^0+\frac{d}{dz}(\xi\psi_s^0)}\cdot\frac{d}{dz}\left(\frac{\psi_s}{\psi_s^0}\right).\end{aligned}\right\} \tag{11}$$

Two functions $G_s(z)$ and ξ characterize the scattering properties of the medium in Eq. (11). The second of these functions is constant in the case of a monatomic gas. For an arbitrary medium, it is natural to assume that the form of the equations remains unaltered, and that the functions $G_s(z)$ and $\xi(z)$ occur in them. In the general case, the quantity $\xi(z)$ naturally does not have to be constant. Only for $z \gg 1$ will it tend to a constant value, which will be characteristic of scattering at motionless, free nuclei.

A Homogeneous Medium with Absorption

We will try to extend the differential equations to be applicable to media with absorption. The first of the Eqs. (11) will now be

$$\frac{dQ}{dz}=\psi_a(z),$$

where $\psi_a(z) = G_a(z)\,N(z)$ is the neutron-absorption density. To find out how to change the second equation, we argue as follows. In a medium without absorption, the current along the energy axis depends only on the scattering density. When there is absorption, the current must also depend on the absorption density. It is natural to expect that the absorption and scattering densities will occur in the expression for the current along the energy axis in the same way. We again turn to the consideration of the relation between the current in the direction of the energy axis and the neutron density for high energies. For neutron moderation, we have the following relation at free, motionless nuclei:

$$Q = \xi z \left[\psi_s + \frac{\gamma}{\xi} \psi_a \right]^*; \quad \frac{\gamma}{\xi} = \frac{1}{2} \frac{\left(\ln \frac{E'}{E} \right)^2}{\left(\ln \frac{E'}{E} \right)^2} = \frac{\left[1 - \alpha + \alpha \ln \alpha - \frac{1}{2} \alpha (\ln \alpha)^2 \right] (1-\alpha)}{(1 - \alpha + \alpha \ln \alpha)^2}.$$

Thus, in a medium with absorption, the scattering and absorption densities occur in the combination $\psi_s + \frac{\gamma}{\xi} \psi_a$. in the expression for the current along the energy axis for $z \gg 1$.

Assuming that these densities occur for other energies in the same combination, we obtain

$$\left.\begin{aligned} \frac{dQ}{dz} &= \psi_a(z); \\ Q &= \frac{(\xi \psi_s^0)^2}{\xi \psi_s^0 + \frac{d}{dz} \xi \psi_s^0} \cdot \frac{d}{dz} \left(\frac{\psi_s + \frac{\gamma}{\xi} \psi_a}{\psi_s^0} \right). \end{aligned}\right\} \tag{12}$$

For $\xi = \gamma = 1$ and values of $G_s(z)$ given by the formula (10), Eq. (12) for N(z) with m = 1 yields the Wigner-Wilkins equation (2). On the other hand, taking $m \gg 1$ and $mz \gg 1$ and expanding in (12) in powers of 1/m and 1/mz, we obtain the Wilkins equation (3) for a zeroth approximation, i.e., when we have discarded all terms of the order of 1/m and 1/mz (here we must assume that $\frac{m\sigma_a(kT)}{\sigma_s(\infty)} \leqslant 1$). In the next approximation we obtain the Corngold equation (4). (In the latter case the expansions $\xi \simeq \frac{2}{m}\left(1 - \frac{2}{3m}\right)$ and $\gamma \simeq \frac{4}{3m}$ are used.)

Thus Eqs. (12) give us the desired differential equation of the second order for a monatomic-gas medium.

Equation (12) can be written in the integral form

$$\left.\begin{aligned} Q &= \int_0^z \psi_a(z)\, dz; \\ N(z) &= \frac{M(z)}{1 + \frac{\gamma}{\xi} \frac{G_a(z)}{G_s(z)}} \times \left[\int_0^z \frac{\psi_s^0 + \frac{d}{dz} \psi_s^0}{\xi (\psi_s^0)^2} Q(z)\, dz + C \right]. \end{aligned}\right\} \tag{13}$$

Here we have taken into account the fact that Q(0) = 0. The constant C can be found by various methods, for example by normalizing the asymptotic solution in a definite way.

Equation (13) is useful for obtaining the solution by the method of successive approximations. Thus for $\frac{\sigma_a(kT)}{\xi \sigma_s(\infty)} \ll 1$, and using the zeroth approximation Q(z) = 0 and N(z) = M(z), we obtain the first approximation

$$Q^{(1)}(z) = \int_0^z G_a(z)\, M(z)\, dz;$$

$$N^{(1)}(z) = \frac{M(z)}{1 + \frac{\gamma}{\xi} \frac{G_a(z)}{G_s(z)}} \times \left[\int_0^z \frac{\psi_s^0(z') + \frac{d}{dz'} \psi_s^0(z')}{\xi (\psi_s^0(z')^2} \int_0^z G_a(z')\, M(z')\, dz' + 1 \right].$$

For G_a = const with m = 1 and $m \gg 1$, the last formula gives the expressions in [6].

• This is the exact expression for hydrogen moderation. For moderation at other nuclei, the validity of the expression requires that the scattering and absorption cross sections have only a small variation in a lethargy region of order ξ (see [7] for example).

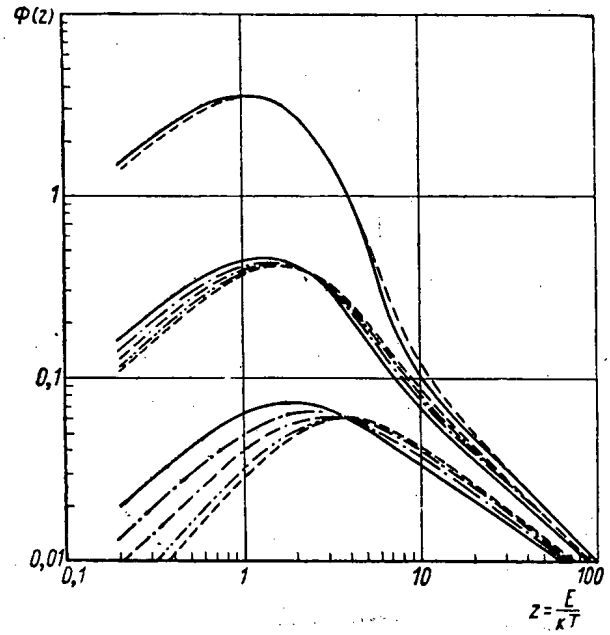

Fig. 1. The relation between the neutron flux and the energy: the upper group of curves are for $\delta = 0.1$; the middle group for $\delta = 0.5$; the lower group for $\delta = 1.5$;

$\delta = \frac{\sigma_a(kT)}{\xi\sigma_s(\infty)}$; —— $m=1$; —·—·— $m=2$; —·—·—·— $m=4$; —··—··— $m=12$; – – – – $m=\infty$.

Integral Characteristics of Neutron Spectra

m	Values of δ								
	0,1			0,5			1,5		
	R_{Cd}	α	β	R_{Cd}	α	β	R_{Cd}	α	β
1	19,3	1,620	1,93	4,63	2,48	3,80	2,10	3,80	6,23
2	18,9	1,650	1,96	4,49	2,62	3,92	1,99	4,21	6,40
4	18,8	1,653	1,97	4,41	2,69	3,98	1,92	4,54	6,57
12	18,7	1,665	1,98	4,34	2,79	4,04	1,88	4,81	6,68
$+\infty$	18,6	1,670	1,98	4,31	2,72	4,07	1,84	4,96	6,77

Notes.

1. $R_{Cd} = \dfrac{\int_0^\infty N(E)dE}{\int_{0,4\,ev}^\infty N(E)dE}$;

2. $\alpha = \dfrac{\int_0^{0,4\,ev} \sigma_a^{Pu}(E)\Phi(E)dE}{\int_0^{0,4\,ev} \sigma_a^{U}(E)\Phi(E)dE}$;

3. $\beta = \dfrac{\int_0^{0,4\,ev} \sigma_a^{Pu}(E)\Phi(E)dE + I^{Pu}}{\int_0^{0,4\,ev} \sigma_a^{U}(E)\Phi(E)dE + I^{U}}$;

4. $I^{Pu} = \int_{0,4\,ev}^\infty \sigma_a^{Pu}(E)\frac{dE}{E}$;

5. $I^{U} = \int_{0,4\,ev}^\infty \sigma_a^{U}(E)\frac{dE}{E}$.

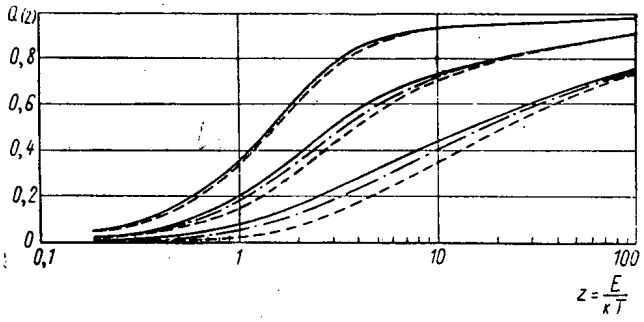

Fig. 2. The relation between the neutron flux for the energy axis and the energy: the upper group of curves is for $\delta = 0.1$; the middle group for $\delta = 0.5$; the lower for $\delta = 1.5$; —— $m=1$; —·—·— $m=2$ – – – – $m=\infty$.

The relation (13) is also useful for numerical calculations. Figure 1 shows curves for the neutron flux $\Phi(z) = \sqrt{z}\,N(z)$ as a function of the energy z for three values of the parameter $\frac{\sigma_a(kT)}{\xi\sigma_s(\infty)}$ and for various values of the nuclear mass m. The curves are normalized to the same behavior for $z \to \infty$*.

It can be seen from the graphs that, for fixed values of $\frac{\sigma_a(kT)}{\xi\sigma_s(\infty)}$, the curves for different values of m are not greatly different. The difference is apparent only for the curves corresponding to a sufficiently strong absorption $\frac{\sigma_a(kT)}{\xi\sigma_s(\infty)} = 1.5$. (Here approximately one-half the neutrons are absorbed above the "cadmium limit" of 0.4 eV.) Figure 2 shows the corresponding curves for the relation between the energy of the flux along the energy axis (the curves are normalized to a unit neutron source of infinite energy).

* Here the asymptotic representation for the functions N(z) and Q(z) have been used:

$$N(z) \sim \frac{1}{z^{3/2}} \sum_{n=0}^{4} a_n z^{-n/2}; \quad Q(z) \sim \frac{2}{z^{1/2}} \sum_{n=0}^{4} \frac{a_n z^{-n/2}}{n+1},$$

where

$$a_1 = -\frac{G_a}{\xi}(2+\gamma)\,a_0; \quad a_2 = \left[2 - \frac{1}{m} + \frac{G_a^2}{\xi^2}(2+3\gamma+\gamma^2)\right] a_0;$$

$$a_3 = \left[-\frac{G_a^3}{\xi^3}\left(\frac{4}{3}+4\gamma+\frac{11}{3}\gamma^2+\gamma^3\right) - \frac{G_a}{\xi}\left(\frac{19}{3}-\frac{8}{3m}+2\gamma-\frac{3\gamma}{2m}\right)\right] a_0;$$

$$a_4 = \left[\frac{G_a^4}{\xi^4}\left(\frac{2}{3}+\frac{10}{3}\gamma+\frac{35}{6}\gamma^2+\gamma^4\right) + \frac{G_a^2}{\xi^2}\left(\frac{55}{6}+\frac{31}{3\gamma}+2\gamma^2-\frac{10}{3m}-\frac{65\gamma}{12m}-2\frac{\gamma^2}{m}\right) + 6 - \frac{3}{m}+\frac{3}{4m^2}\right] a_0.$$

The accompanying table gives some integral characteristics of neutron spectra for various values of $\frac{\sigma_a(kT)}{\xi\sigma_s(\infty)}$ and $\underline{m}$. For the integral characteristics we have taken quantities that can be relatively easily obtained experimentally. Here R_{Cd} is the cadmium ratio for an absorber with absorption cross-section $\sigma_a \sim \frac{1}{v}$, and also the ratio of the integral absorption cross sections for U^{235} and Pu^{239} averaged over the relevant spectra. The characteristic β is defined as follows: to the calculated values of the integrals are added the corresponding, experimentally determined resonance integrals. Their values are taken from the results in [8]. It is assumed here that the dependence of the form of the spectrum in the energy range above 0.4 eV on $\underline{m}$ and the parameter $\frac{\sigma_a(kT)}{\xi\sigma_s(\infty)}$ is weak, and that the variation in the resonance integrals due to this dependence can be neglected. The temperature of the medium is assumed to be 300°K, and the absorption cross sections for U^{235} and Pu^{239} are taken from [9].

We stated above that Eqs. (12) could be tested for applicability to an arbitrary medium. For this we must understand the physical meaning of the functions $\xi(z)$ and $\gamma(z)$ that characterize the scattering. It is clear that, in contrast to the quantity $G_s(z)$ which gives information only on the probability of scattering, the functions $\xi(z)$ and $\gamma(z)$ must characterize, so to speak, the quality of the scattering. For a monatomic gas, these functions are constants, i.e., the "quality" of the scattering is the same for all neutron energies. When it is necessary to take into account the relations between the nuclei, the functions $\xi(z)$ and $\gamma(z)$ must obviously depend on the energy.

In conclusion I must thank P. E. Stepanov, Ya. V. Shevelev, and L. V. Maiorov for many valuable discussions of the work.

LITERATURE CITED

1. E. Kogen, in the book: "Experimental Reactors and the Physics of Reactors" [in Russian], Reports of Foreign Scientists at the International Conference on the Peaceful Uses of Atomic Energy (Geneva, 1955), Gostekhteorizdat, Moscow (1956), p. 257.
2. V. I. Davydov, "Zh. eksperim. i teor. fiz.", 7, 9-10, 1069 (1937).
3. J. Wilkins, Ann. Math., 49, 189 (1948).
4. N. Corngold, Ann. Phys., 6, 368 (1959).
5. G. Placzek, Phys. Rev., 69, 423 (1946).
6. A. D. Galanin, The Theory of Nuclear Reactors with Thermal Neutrons [in Russian], Atomizdat, Moscow (1957).
7. S. Gléston and M. Édlund, The Elements of Nuclear-Reactor Theory [in Russian], Izd-vo inost. lit., Moscow (1954).
8. R. Stoughton and J. Halperin, Nucl. Sci. Engng, 6, No. 2, 100 (1959).
9. D. Huges and R. Schwartz, BNL-325, Neutron Cross Section, II ed. US AEC, New York (1958).

STUDY OF SPENT FUEL ELEMENTS FROM THE FIRST ATOMIC ELECTRIC STATION

Sh. Sh. Ibragimov, L. A. Syshchikov, I. M. Voronin, and V. G. Kudryashov

Translated from Atomnaya Énergiya, Vol. 14, No. 5, pp. 465-468, May, 1963
Original article submitted June 21, 1962

Data are given from a metallurgical study of three fuel elements from the First Atomic Electric Station, which had operated in the reactor for 111, 324.5, and 557 effective days. The results may be of use in designing reactors of the same type as the First Atomic Electric Station.

The length of operation of nuclear power plants is determined principally by the behavior of the fuel elements in use. During use, the fuel elements operate under very complex conditions (compound stressed state, neutron field, elevated temperature, contact with a different medium, etc.). Investigating the changes in properties of the fuel elements after a definite period of service makes it possible to judge whether or not the design is reliable, and whether or not it should be used in further operation.

The present paper gives the results of a study made on fuel elements that had operated in the reactor of the Atomic Electric Station for 111, 324.5, and 557 effective days to mean burnouts (of U^{235} atoms) of 11.8%, 28%, and 59% respectively.

The total length of the ring type fuel elements in the Atomic Electric Station is 1700 mm, and they consist of two steel tubes, the inner of which is the main element, while the outer is principally a cladding to catch fission fragments. The angular space (between the tubes) is filled with fuel (grains of a uranium-molybdenum alloy containing 9% molybdenum, held together by metallic magnesium). The U^{235} enrichment for two of the fuel elements (the ones that had operated 111 and 557 days) is 5%, while that of the third is 6%. During operation, coolant flows through the inner tube, consisting of water at an input temperature of 175-190°C and an output temperature of 260-280°C for nominal reactor power. Here, the maximum temperature of the outer surface of the fuel element is not greater than 360-370°C. The outer surface is in contact with a gas mixture of the following composition [1]: O_2 (0.2%); H_2 (0.2%); CO_2 (0.5%); and the rest N_2.

After the fuel elements had operated for the above lengths of time, they were discharged until the shortlived fission products had decayed, and then taken to the "hot" laboratory for tests, where they were subjected to the following operations:

1) external inspection and diameter measurement,
2) mechanical disassembly and cutting of samples,
3) metallographic tests, and
4) mechanical tests of the tube material.

External Examination and Diameter Measurement of Fuel Elements

The external observation of the fuel elements, made visually through the viewing window of the "hot" chamber using binoculars with a magnification of 10, did not show any defects on the outer surface, except for a thin (about 1 μ) oxide film of various colors (from light brown to dark gray).

The diameter measurement, made with a remote-controlled micrometer in two perpendicular directions along the length, indicated swelling, the amount of which varies along the fuel element, and is determined by the degree of burnout (Fig. 1). The maximum increase in diameter was observed approximately in the center of the fuel element, and was 0.10, 0.15, and 0.20 mm for fuel elements that had operated 111, 324.5, and 557 effective days respectively.

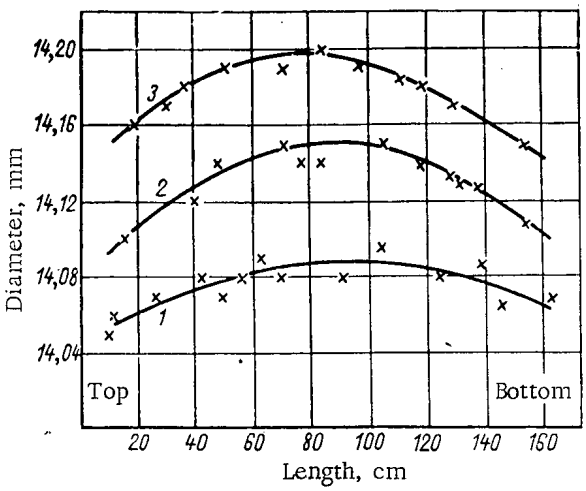

Fig. 1. Diameter change of fuel elements along the length (1, 2, 3--fuel elements that have operated 111, 324.5, and 557 effective days respectively).

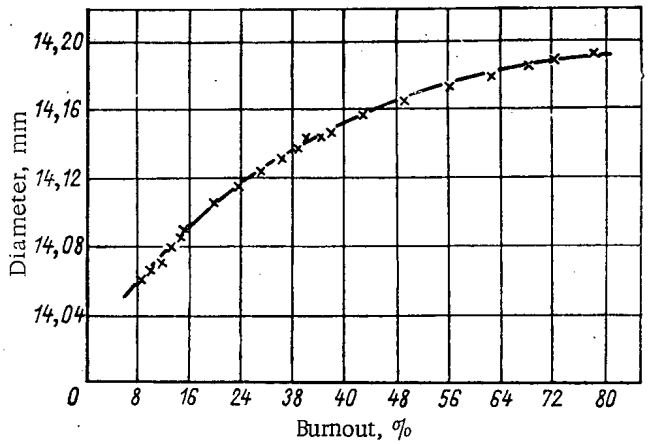

Fig. 2. Fuel element diameter change as a function of U^{235} burnout.

Fig. 2 gives the curves showing the change in fuel element diameter as a function of U^{235} burnout* (in terms of atoms of the U^{235} isotope). It may be seen that the diameter change has a tendency to saturation, which is apparently reached at burnouts of about 80%. The diameter change in the fuel elements is probably due to swelling of the uranium-molybdenum fuel at the operating temperature. A simple calculation shows that the change in volume of a fuel element for 1% U^{235} burnout (of all the atoms in the uranium-molybdenum alloy) is about 1%, while for 1% U^{235} burnout, the swelling will be approximately 3% from the formation of solid fragments alone. Accordingly, swelling of the uranium-molybdenum alloy during irradiation is to a considerable degree held down by the magnesium filling and the material in the cladding.

Mechanical Disassembly of Fuel Elements and Cutting of Samples

Mechanical disassembly of the fuel elements and cutting of samples was done on a special remote-controlled milling machine and lathe. Samples for mechanical tests and microstructure study were cut out at 4 places on the length of the tube in the form of toroids (rings) 4 mm high. The uranium-molybdenum alloy held together with magnesium was got out of the rings by dissolving the magnesium chemically in aqueous NH_4NO_3 solution at a temperature 70-80°C.

Metallographic Study

The samples were polished and examined by remote control in two hot chambers. The microstructure of the samples was observed under a remote-controlled MIM-14 optical microscope at magnifications of from 100 to 1000. The microhardness of the material in the tubes was also determined by remote control on a PMT-4 apparatus at loads of 50 and 100 g. Before measurement, the samples were subjected to electropolishing. Not less than 10 impressions were made in each sample to determine the mean value of the microhardness.

TABLE 1. Mechanical Properties of Tube Material

Place cut out	Fuel element operating time, effective days												
	111				324,5				557				
	Position of tube												
	inner		outer		inner		outer		inner			outer	
	σ_w, kg/mm²	δ, %	σ_w, kg/mm²	δ, %	σ_w, kg/mm²	δ, %	σ_w, kg/mm²	δ, %	σ_w, kg/mm²	δ, %	H_μ, kg/mm²	σ_w, kg/mm²	δ, %
Top	64,0	21,5	—	—	66,0	28,0	77,5	11,5	72,0	14,5	310	81,0	8,5
375 mm from top. . . .	69,0	21,0	75,5	21,5	70,0	23,5	82,0	15,5	77,0	11,5	315	89,5	5,5
850 mm from top (center)	72,0	18,5	76,0	20,5	75,0	20,0	80,5	—	79,0	16,0	300	86,5	3,0
1375 mm from top . . .	68,0	19,0	78,0	15,0	—	18,0	83,0	6,5	72,0	17,0	290	80,0	11,0

*The values for U^{235} burnout are calculated, and, as is shown in [2, 3], are in satisfactory agreement with the experimental data.

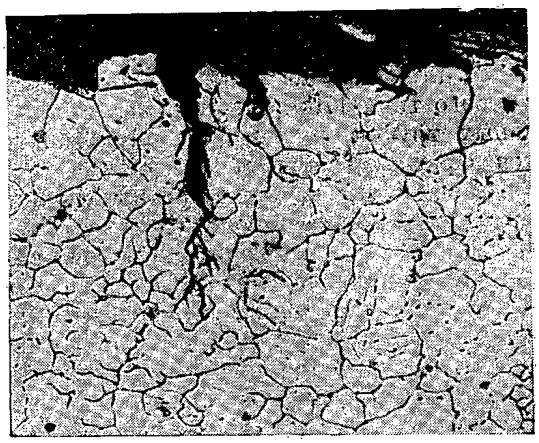

Fig. 3. Microstructure of the material in the outside fuel element cladding (middle part), after operating 557 effective days.

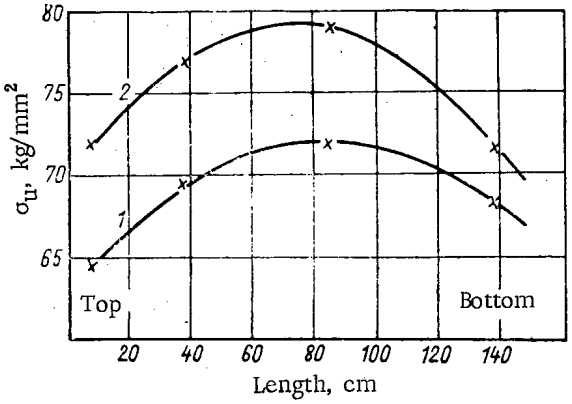

Fig. 4. Variation of the ultimate strength of the material in the inner tube of the fuel element along the length (1, 2—fuel elements that had operated 111 and 557 effective days respectively).

A study of the microstructure of the samples cut from four different parts of the fuel elements shows no appreciable changes in the microstructure of the material in the tubes and the samples from fuel elements that had operated 111 and 324.5 effective days, nor is there any interaction between the steel and the magnesium or between the fuel and the surrounding medium. There is practically no deposit from the cooling medium on the outer tube surface, but visual observation shows a uniform light brown film, 1-2 μ thick.

The outer cladding of the samples cut from the fuel element that had operated 557 effective days shows microscopic cracks (Fig. 3) running axially, which start on the outside of the cladding, and, propagating from grain boundary to grain boundary, reach depths of 100 μ. Further, there is an increase in etching of the outer surface of the steel samples of thickness up to 30 μ. The formation of microscopic cracks is probably due to the constantly acting radial stresses (from flowing of the uranium-molybdenum alloy, and to radiation brittleness of the 1Kh18N9T steel.

Determination of Mechanical Properties of Tube Material

The ring samples were tensile tested at room temperature on a remote-controlled UMD-5 machine. All the measurements of the ultimate strength σ_u and the relative elongation δ were made on no less than five samples. Although the tests on the rings are nonstandard, and do not show the true mechanical characteristics of the material, they nevertheless give quite satisfactory results in comparative studies of the properties of the material before and after irradiation.

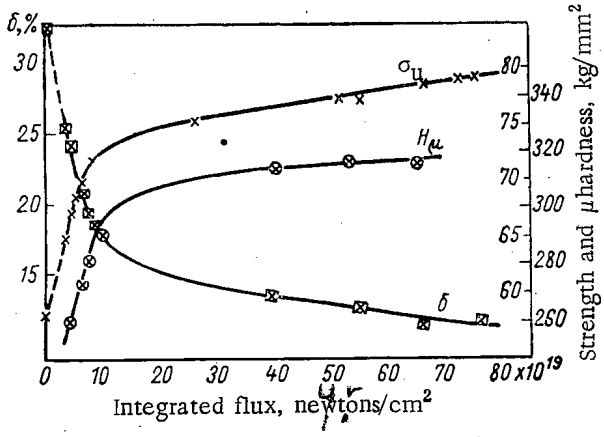

Fig. 5. Mechanical properties of the material in the inner tube of a fuel element as a function of integral radiation dose.

TABLE 2. Mechanical Properties of Tube Material after Annealing at 650°C*

Fuel element operating time, effective days	Position of tube				
	inner			outer	
	σ_w kg/mm^2	δ, %	H_μ, kg/mm^2	σ_w kg/mm^2	δ, %
111	58,5	27,5	190,0	63,5	33,0
324,5	59,0	40,5	205,0	67,5	36.0
557	55,0	32,0	200,0	64,0	30,0

* Samples from middle of fuel elements.

Mechanical properties of the samples cut from different parts of fuel elements before and after heat treatment (annealing* at 650°C for 0.5 h), are given in Tables 1 and 2. It may be seen from the Tables that as a result of operating the fuel elements in the reactor, σ_u and the microhardness of the material in the tubes (cladding) increase, while δ decreases, i.e., hardening and brittleness of the steel is observed with the properties in the material of the outer cladding changing considerably more than the inner, and depending on the place the samples were cut out. A curve showing the change in σ_u of the tube material as a function of length, as well as the curve of fuel element diameter change, is similar to the burnout distribtuion curve (Fig. 4). With increase in burnout, and hence in integrated neutron flux, the degree of hardening and brittleness of the material in the tubes becomes greater.

The greatest change in mechanical properties is observed in the material of the tubes in the fuel elements that had operated 557 effective days†. Figure 5 gives curves of σ_u, the microhardness, and δ of the material in the inner tube as a function of the integrated fast neutron flux ($\geq$ 1 MeV). It may be seen that for fluxes of about $5 \cdot 10^{20}$ neutrons/cm^2, the curves for these properties reach saturation. Note that for practical purposes, saturation from neutron irradiation of small size samples at 220-255°C occurs at doses of about $3 \cdot 10^{20}$ neutrons/cm^2 (mean neutron energy 36 keV, neutrons with energies > 1 MeV amount to 10%). Here, the maximum changes in σ_u and δ are 10 kg/mm^2 and 40% respectively [5]. When using ring samples cut from fuel elements, the increase in σ_u at saturation doses is 20-22 kg/mm^2. The relative elongation reduces by a factor of almost 2.5. This probably comes from the compound stressed state of the material in the tube during irradiation.

The effect of heat treating the samples at temperatures of 650°C for 30 min is to remove the hardening and brittleness of the material almost completely, i.e., the radiation defects which produce the change in the mechanical properties of the material are annealed. After such an annealing, the properties of the material in the fuel element tubes are very nearly the same as the properties of nonirradiated 1Kh18N9T steel (see Table 2).

LITERATURE CITED

1. N. A. Dollezhal' et al. in the book: "Transactions of the Second International Conference on the Peaceful Uses of Atomic Energy"(Geneva, 1958), Papers by Soviet Scientists, Vol. 2 [in Russian], Atomizdat, Moscow (1959), page 15.
2. A. P. Smirnov-Averin et al., "Atomnaya Énergiya," 8, No. 5, 446 (1960).
3. A. P. Smirnov-Averin et al., "Atomnaya Énergiya," 11, No. 2, 122 (1961).
4. Sh. Sh. Ibragimov, V. S. Lyashenko, and A. I. Zav'yalov, "Atomnaya Énergiya," 8, No. 5, 413 (1960).
5. Sh. Sh. Ibragimov, I. M. Voronin, and A. S. Kruglov, "Atomnaya Énergiya" (in press).

* It is known from [4] that in austenite steels irradiated at temperatures below 400°C, the radiation hardening defects anneal out almost completely at 650°C.

† Note that part of the samples—the rings cut from the outer cladding of the fuel element that had operated 557 effective days—showed zero elongation in tests, and failed at low stresses, which is due to the presence of the microscopic cracks observed in the metallographic study.

NOTE ON DETERMINING IRRADIATION COSTS IN A RESEARCH REACTOR

V. A. Tsykanov

Translated from Atomnaya Énergiya, Vol. 14, No. 5,
pp. 469-473, May, 1963
Original article submitted October 11, 1962

A method is presented for determining expenses in operating a research reactor and calculating experimental research costs, with allowance for the effectiveness of channels used, and such factors as reactor contamination, effect of research specimen on reactivity, compatibility of experiments, and specimen cooling time.

From a costs standpoint, the research reactor may be approached as a plant designed to produce neutrons. As in the case of any other operating plant, materials and means are consumed in operating a research reactor, and its output—neutrons—has a certain cost.

Since most of the neutrons produced in a reactor are used to sustain reactor operation, and a fraction of the remaining neutrons is unavailable for use because of leakage and useless absorption, it is only natural that reactor operation losses must be scaled to those neutrons actually used in experiments.

Neutrons are consumed when a particular experiment is carried out, and the cost of a given experiment may be determined, therefore, if the relative fraction of neutrons used is known. The problem lies in correctly assessing this relative fraction.

The availability of data from which to estimate the costs of an experiment or pile irradiation program aids not only in correctly distributing expenses between simultaneous experiments, but also in analyzing the cost factors of different types of research reactors. The latter point takes on added importance as applications of research reactors continue to expand.

At the present stage, capital investment and running costs in research reactors vary over quite a wide range, depending on the reactor type and the basic design function. Some experiments can be carried out in principle with equal chances of success on many different reactor types, although the costs incurred in performing the experiment will not be the same in every case. A proper costs analysis must therefore take appropriate stock of the particular experiment geared to a concrete reactor. This in turn will free certain special experimental reactors from experiments which could just as well be performed on other, cheaper reactors.

In the present article, we shall make an attempt to elaborate a useful procedure for assessing irradiation costs in research reactors.

Running Reactor Costs

The total expenditures in materials in the course of reactor operation may be broken down into amortizable costs, operating costs, and fuel costs (the fuel component). Capital installation costs* are known so that, if the useful reactor operating life is properly determined, amortizable items may be readily spread over the entire period. At the present time, however, there is no basis for any firm assertions on the useful life of a research reactor, since the performance characteristics and the design of each particular research reactor vary considerably depending on the function seen for the reactor. Even in standardized research reactors, their individual components are constantly being

* In very-low-power reactors, the fuel load may remain unchanged for several years. In that case, fuel costs should obviously be accounted as part of the total capital investment and, on that basis we may proceed to determine the amortizable portion of the expenses. However, in practice, reactors developing appreciable power and in which fuel reloading is frequent are of greater interest. On that account, fuel costs are accounted for separately in the form of the fuel contribution to the total costs.

replaced and improved, and operating experience has yet to be accumulated. Under these conditions, an individual approach to determining the useful lifetime of each particular reactor is out of the question, and we have to be content with averages derived from experience. In most cases, it is a reasonable assumption that the lifetime of a research reactor will span 15-odd years.

Operating costs may be broken down into labor costs for the servicing personnel, costs for materials used (including electricity, steam, water, etc.), and maintenance costs. All of these entries may be determined with reasonable accuracy.

We shall deal in somewhat greater detail with the fuel component in the total costs.

The labor costs do not depend on reactor power level, and materials costs, with a certain allowance, may also be viewed as not dependent on reactor power and on variations in reactor experiment load with time. The fuel component, on the other hand, is directly affected by these factors. It is therefore determined as the integrated energy output of the reactor over a certain time span. If the thermal reactor power is Q(t), in MW, and the reactor has been in operation for t_0 h, then the integrated energy output during that time will be

$$Q^* = \int_0^{t_0} Q(t)\,dt \text{ MWh.} \tag{1}$$

For each reactor, the amount of nuclear fuel burned up is known (in grams), as the amount required to produce one MWh energy*. If we denote this quantity as g (in g/MWh), then $G' = gQ^*$ grams of nuclear fuel will be burned up in the reactor over a time t_0.

We know that nuclear fuel is not completely burned up in a pile. If the relative and average burnup is denoted as φ, then the total expenditure of nuclear fuel will come to

$$G = \frac{G'}{\varphi} = \frac{gQ^*}{\varphi}. \tag{2}$$

The nuclear fuel is loaded into the reactor core in the form of fuel elements costing a known amount ($C_{f.el}$) with a known fuel content (G_1). Dividing the cost per fuel element by the fuel content in an element, then, we may determine the fuel cost per item

$$C_f = \frac{C_{f.el}}{G_1} \text{ rubles/gram.} \tag{3}$$

Next, we determine with ease the nuclear fuel costs spread over a time t_0:

$$C_{fuel} = GC_f = \frac{gQ^*}{\varphi} C_f \text{ rubles.} \tag{4}$$

An assumption was made, in performing these calculations, to the effect that the fuel left over in spent fuel elements is not recovered. When fuel is reprocessed for recovery, the purchase costs of the fuel elements, which depend on the difference in the cost of residual-enrichment uranium and recovery costs, may be partially offset.

We may now proceed to calculate the total reactor operating costs over the time t_0. In fact, designating the total sum of annual amortization writeoffs as A, and the annual salary and wage fund for servicing personnel as C_p, and the annual running materials costs as C_M, we find that the round-the-clock operating total costs over the time interval t_0 will be

$$C_t = \frac{A + C_p + C_M}{8760} t_0 + C_{fuel} = \frac{A + C_p + C_M}{8760} t_0 + \frac{gQ^*}{\varphi} C_f. \tag{5}$$

---

* This amount depends on the pile neutron spectrum and on the type of nuclear fuel used (because of variations in the σ_f/σ_a ratio).

If, in the course of a certain time, the pile thermal power is kept constant at Q (MW), then the costs for 1 h of reactor performance will be

$$C = \frac{A + C_p + C_M}{8760} + \frac{gQ}{\varphi} C_f \quad \text{rubles/hour.} \tag{6}$$

Distributing Costs Between Experiments and Determining Irradiation Costs

The distribution of costs is proportional to channel effectiveness. An experimental reactor is usually provided with several irradiation channels. These channels differ in size and neutron flux. The larger the volume of the experimental channel and the greater the neutron flux in the channel, the greater will be the amount of material that can be placed in the channel for irradiation and the more efficient will be the irradiation process. In simultaneous exposures involving all the channels, then, costs could not possibly be distributed evenly over all the experiments. The effectiveness of each particular channel must be taken into proper account.

A measure of channel effectiveness is the product of the effective channel volume V_{eff} (in cm^3) by the (volume) average neutron flux in the channel, $\bar{\Phi}_K$ (in neutrons cm/sec). The effectiveness of a particular channel is

$$E_K = V_{eff} \bar{\Phi}_K \text{ neutrons·cm/sec.} \tag{7}$$

If there are n channels in the reactor and the effectiveness of each of the channels is known, then the irradiation cost in the i-th channel (with full utilization of all the channels) will be

$$C_i = \frac{C}{\sum_{j=1}^{n} E_K^j} E_i = \frac{C}{\sum_{j=1}^{n} V^j_{eff} \bar{\Phi}^j_K} V^i_{eff} \bar{\Phi}^i_K. \tag{8}$$

The formula so obtained is valid for the ideal case when the degree of reactor contamination does not vary with time during the irradiation process, the reactor suffers no shutdown for miscellaneous reasons, and so forth. Proper corrections must be introduced for all such factors which will affect the result.

Taking into account the effective utilization of the reactor. We come across cases where not all the experimental potentialities of the reactor are being exploited, even though the experiments being performed in the occupied channels require operation of the reactor and of all the associated equipment at the rated conditions. In that case, the reactor operates solely to provide the exposure in some of the experimental channels, and all the costs fall on the experiments being conducted in those channels.

If, in carrying out a given series of experiments, K channels (K < n) are occupied, then the irradiation costs in the i-th channel may be found from formula (8) by replacing the summation limit by K in that formula. The more K differs from n, the more the experiments will cost.

It is very important, in this context, to plan the reactor operating schedule so that peak loading will be assured. It is also worthy of note that, if the reactor is being operated not with the rated number of experimental channels (e.g. when the experimental channels are put into use successively with the reactor already in operation), there will necessarily result an overexpenditure of means on experiments.

Compatibility of in-pile experiments. In the preceding section, we considered the case of incomplete reactor loading due to incorrect planning or a limited demand on the experimental channels. We shall now take up the case of incomplete loading of the reactor due to incompatibility of the experiments. Incompatibility of the experiments is always possible eventually, since it frequently occurs that some experiments will either require different reactor power levels, or else the program of reactor work required for one particular experiment will render the simultaneous conducting of other experiments unfeasible or impossible.

If among K experiments being conducted in a pile, there are K_1 ($K_1 < K$) such that experiments cannot be conducted at a particular moment in $K_2 = n - K$ channels, then the irradiation costs in the K_2 channels over the time in question (the cost of the "nonexistent" experiments) must be added to the cost of just the K_1 experiments, with the supplements proportional to the effectiveness of the channels occupied during these experiments. In that case, the cost of the compatible $(K - K_1)$ experiments will be determined from Eq. (8), and the cost of the incompatible experiments (K_1) from the formula

$$C_i = \frac{C E_K^i}{\sum_{j=1}^{n} E_K^j} + \frac{\sum_{q=1}^{K_2=n-K} C_q}{\sum_{m=1}^{K_1} E_K^m} E_K^i. \qquad (9)$$

The sense of this formula is quite understandable: the first term is the irradiation cost in the i-th channel (i of the number K_1) when the reactor is fully loaded, the second term is the supplement to the cost owing to the fact that experiments were not carried out in K_2 channels. The sum in the numerator of the second term is equal to the cost of the nonexistent experiments in K_2 channels, with C_q determined from Eq. (8). Summing over q is carried out with respect to the channels not occupied during the experiments (K_2 channels). The ratio $E_K^i / \sum_{m=1}^{K_1} E_K^m$ is the portion of the additional cost falling on the experiment in the i-th channel. Summing over m is carried out with respect to the number of channels occupied by the incompatible experiments.

By way of elucidation, consider the following example. The reactor has six experimental channels. Their effectiveness is reported below (in relative units).

Channel number	1	2	3	4	5	6
E_K	2	1	5	3	10	4

Over a certain time span, the reactor was operating at constant power, with experiments in progress in channels 2, 3, 4, and 5. Channels 1 and 6 remained free, since the experiments in channels 2 and 5 required conditions under which experiments in channels 1 and 6 would have been impossible.

It is required to determine the costs for experiments when the total reactor operating costs during that time amounted to C. [The value of C is determined here from Eqs. (5) or (6).] In our notation, K = 4 (channels 2, 3, 4, 5); K_1 = 2 (channels 2 and 5); K_2 = 2 (channels 1 and 6).

The costs of the compatible experiments are: $C_3 = \frac{C}{25} 5 = 0{,}2C$; $C_4 = \frac{C}{25} 3 = 0{,}12C$. The costs of the incompatible experiments are: $C_2 = \frac{C}{25} 1 + \frac{\frac{C}{25} 2 + \frac{C}{25} 4}{1+10} 1 = 0{,}04C + \frac{0{,}08C + 0{,}16C}{11} = 0{,}04C + 0{,}0218C = 0{,}062C$;

$C_5 = \frac{C}{25} 10 + \frac{\frac{C}{25} 2 + \frac{C}{25} 4}{1+10} 10 = 0{,}4C + 0{,}218C = 0{,}618C$. Now check the total costs:

$$C_2 + C_3 + C_4 + C_5 = 0{,}062\,C + 0{,}2C + 0{,}12\,C + 0{,}618\,C = C.$$

Taking into account the effect of specimens on reactivity. Specimens loaded into experimental channels for irradiation always exert some effect on the pile reactivity, but the extent of this effect varies and is dependent on the properties of the specimen and on where the channel is located in the pile. The effect of specimens placed in channels remote from the core on reactivity may be ignored in actual practice. On the other hand, specimens in core channels may exert a significant effect on reactivity.

In a research reactor, the output parameter is the amount of neutron flux, which depends, for a given reactor design and set of reactor properties, on the power generated per unit core volume. Consequently, at different pile thermal power levels, if the core varies in volume, a neutron flux of uniform magnitude may be achieved in any channel. The volume of the core (or the effective loading of the reactor) is related to the change in reactivity, and therefore depends on the specimens loaded in. A specimen introducing positive reactivity makes it possible to reduce the effective core volume, and this leads to a diminished pile thermal power level and, as a consequence, to fuel savings. On the other hand, a specimen introducing negative reactivity is responsible for fuel penalties. Consequently, both the savings achieved in the first instance and the additional costs incurred in the second instance must be ascribed to those experiments which affect the pile reactivity.

Since the reactivity varies as a rule more during the time the reactor is in operation than during loading and unloading of specimens, corrections for reactivity in the irradiation costs must be introduced only in the case of specimen irradiations which drastically affect the reactivity. A yardstick for the amount of reactivity starting with which

it becomes necessary to introduce this correction can be arrived at only concretely for each reactor, with the change in reactivity during operation due to the properties of the reactor itself given due attention. In any case, this correction would hardly necessitate being introduced in most modern reactors when the specimens bring about a reactivity change less than 0.5%.

In order to determine the required corrections for irradiation costs necessitated by reactivity changes, we must have information on the relationship between the amount of fuel loaded into the core and the reactivity, on the one hand, and on the mean thermal power per unit weight of fuel or per unit core volume, on the other.

Suppose that among n experiments being carried on, there is one which severely affects the reactivity. We then proceed as follows in order to calculate irradiation costs. The loading and the reactor power are known, and the change in reactivity brought out by each given specimen is taken into account. We term this power level the actual power, and designate it by the symbol Q_a. In addition we know (or are in a position to determine) the reactor loading, and this means that we also know the reactor power (without taking the reactivity introduced by the specimen into account). We call this power level the computed power, and designate it by the symbol Q_c. Using Eq. (6), we can determine the following costs in operating the reactor:

$$C_a = \frac{A+C_p+C_M}{8760} + \frac{gQ_a}{\varphi} C_f \tag{10}$$

$$C_c = \frac{A+C_p+C_M}{8760} + \frac{gQ_c}{\varphi} C_f \tag{11}$$

The difference in the cost categories

$$\Delta C = C_a - C_c = \frac{gC_f}{\varphi}(Q_a - Q_c) \tag{12}$$

($\Delta C < 0$ when the reactivity $\rho > 0$, $\Delta C > 0$ at reactivity $\rho < 0$).

Calculations for n-1 experiments are carried out with respect to the computed costs, since the specimens used in this case do not affect the reactivity, and the difference in costs must be laid at the door of an experiment responsible for the change in reactivity. Accordingly, for n-1 experiments, irradiation costs may be determined, depending on the case involved, from either Eq. (8) or Eq. (9). The cost of an experiment in which reactivity is affected is also computed using these same formulas (depending again on the case involved), but the quantity ΔC determined from Eq. (12) is then added to the result so obtained.

If among n simultaneous experiments, there are K such that the reactivity is affected, then similar calculations may be carried out for each such experiment.

Taking the specimen cooling time into account. During the time it takes any given specimen to cool down before it is withdrawn from the channel, there will be a forced reactor outage, if no measures are taken to provide for the cooling-down process during reactor operation (e.g. remotely controlled withdrawal of specimens and automatic displacement of the specimens to a cooling-down zone).

Whenever the reactor is shut down, the total costs will be reduced only by the amount of the fuel contribution to the costs. If the shutdown is not due to cooling (preventive maintenance, fuel reloading, etc.) and the shutdown time is automatically taken into account in determining costs by Eq. (5), with these costs distributed over all the experiments, then the costs accompanying a cooling shutdown will have to be determined separately, and these costs will have to be accounted to the experiment which called for the cooling time in the first place. There would be no point in charging up this downtime to the other experiments.

This points up the striking importance of instrumentation designed to achieve this cooling while the reactor is in operation, as well as adequate and correct planning ahead of experiments which call for simultaneous cooling-down of several specimens. Let a specimen be cooled down over a time t in one channel and, simultaneously, let cooling of a second specimen begin in another channel, where the latter specimen requires a cooling-down time t/2. The total reactor operating costs during that time will be

$$C_t' = \frac{A+C_p+C_M}{8760} t.$$

During the first half of this time, the costs will be spread over the two experiments, and later the first experiment will carry the entire cost. Any additional costs for cooling the second specimen down will therefore come to

$$\Delta C_2 = \frac{C_t}{4} = \frac{A+C_p+C_M}{8760} \cdot \frac{t}{4},$$

and costs for cooling down the first specimen will be

$$\Delta C_1 = \frac{C_t}{4} + \frac{C_t}{2} = \frac{3}{4} C_t = \frac{A+C_p+C_M}{8760} \cdot \frac{3t}{4}.$$

Neutron beam experiments. Experiments on neutron beams brought outside the reactor are of a very unique nature. In the interests of a uniform approach to the problem, the cost of conducting this type of experiment will be handled in the same way, by reference to effectiveness. In determining the effectiveness of the neutron beam, we must take the channel volume into account only inside the core and inside the reflector (but not inside the shielding), as well as the neutron flux in that volume. It should be noted that the channel effectiveness arrived at in this fashion may not always correctly characterize the value of the channel for beam experiments. However, introduction of further refinements in this application would hardly find justification at the present state of knowledge.

SOME LAWS OF THE FORMATION OF EPIGENETIC URANIUM ORES IN SANDSTONES, DERIVED FROM EXPERIMENTAL AND RADIOCHEMICAL DATA

L. S. Evseeva, K. E. Ivanov, and V. I. Kochetkov

Translated from Atomnaya Énergiya, Vol. 14, No. 5,
pp. 474-481, May, 1963
Original article submitted June 21, 1962

The paper gives the results of experiments on the simulation of precipitation of uranium from aqueous solutions in a sandstone bed enriched with freshly precipitated iron sulfides. An oxidation zone and a cementation zone enriched with uranium precipitated from aqueous solutions were obtained in the bed model. Neogeneses of iron sulfides in the form of "rolls," analogous to natural ore beds, were observed in the cementation zone. It is shown that the formation of ore concentrations of uranium takes place during the continuous movement of the oxidation zone in the direction of movement of the solutions and the redistribution of uranium near the boundary between the oxidized and unmodified rocks. The experimental results are confirmed by the results of an investigation of radioactive equilibrium between ionium and uranium under natural conditions.

INTRODUCTION

As a result of the increased importance of epigenetic sedimentary deposits in the over-all balance of uranium reserves there has recently been increasing interest in study of the formation of these deposits.

Deposits in permeable arenaceous-argillaceous rocks with oval and crescentiform ore bodies, known as "rolls," are of particular interest. These ore bodies have been described in detail by D. Shaw [1], who indicates that an investigation and explanation of their structure may help to determine the genesis of a deposit.

A. I. Germanov [2] suggested that bodies of the roll type originated by infiltration and are formed under conditions of descensional pressurized movement of underground waters where the strata are of relatively uniform composition and permeability.

The rate of movement of water in a uniform permeable bed with impermeable strata above and below decreases from the center of the bed to the periphery. As a result, the oxidized zones formed in the sandstone beds are in the form of tongues extending in the direction of movement of the water, while the ore bodies, localized near the contact of the oxidized and unmodified rocks and following the outline of this contact, are crescentiform or roll-shaped. Deposition of uranium from the waters takes place when oxidizing conditions are replaced by reducing ones, in which the migration capacity of uranium is markedly reduced. It is evident that the greater the content of matter in the reduced state in the rocks and the more uniform the rate of its oxidation, the greater will be the contrast in the boundary between the different conditions and the more favorable will be the environment for uranium concentration near this boundary. Substances which are intensively oxidized by the oxygen of waters in sandstone rocks include sulfides, coalified plant debris, bituminous substances, ferrous compounds, etc.

These theories of the conditions of formation of roll-like ore bodies formed the basis of experiments by L. S. Evseeva and V. I. Kochetkov on the simulation of uranium precipitation from aqueous solutions in a bed of sand enriched with iron sulfides. K. E. Ivanov's radiochemical investigations on a natural ore occurrence confirmed the infiltration genesis of such bodies and made it possible to establish the date of their formation.

EXPERIMENTAL PROCEDURE

The bed model (Fig. 1) was a glass-like transparent plastic box (2.0 × 0.15 × 0.20 m) filled with fine-grained homogeneous ferruginous quartz sand. Clay was deposited in the floor and roof of the bed. To isolate the bed from

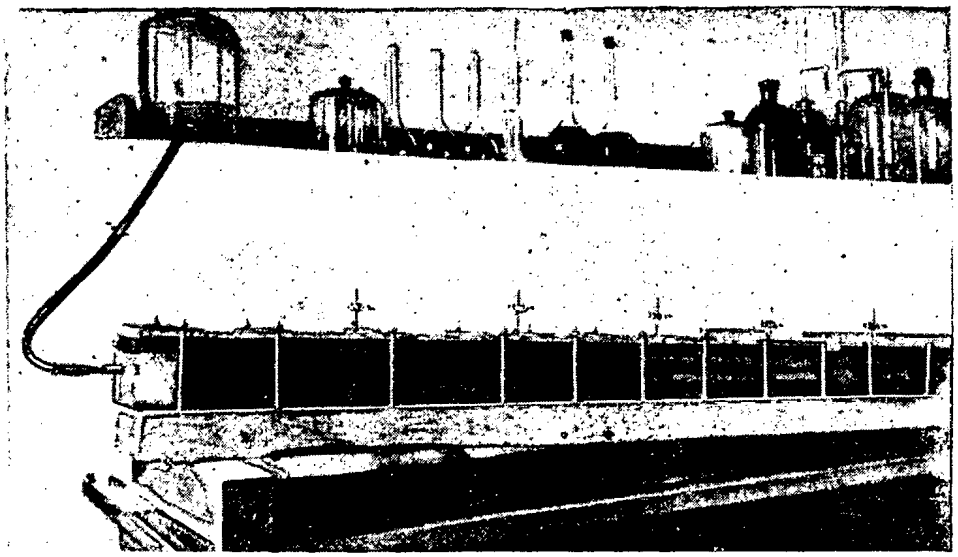

Fig. 1. Model of a bed of sand.

atmospheric oxygen, it was covered by a close fitting lid with a rubber lining. The model was fixed at a moderate angle, the rate of movement of solutions through the bed being 5 liters/day, corresponding to a linear filtration velocity of 12.5 m/day. To convert iron oxide in the sand to sulfides, distilled water saturated with hydrogen sulfide was passed through the sand before commencing the experiment. When all the sand had turned black, the bed was washed with distilled water until there was no odor of hydrogen sulfide. Uranium-containing water was then passed through the bed for a considerable time. In the first experiment, uranium was added to the solutions in the form of sodium uranyltricarbonate, and in the subsequent experiments, as uranyl nitrate. Solutions with uranium concentrations of $n \cdot 10^{-6}$-$n \cdot 10^{-5}$ g/liter and $n \cdot 10^{-3}$-$n \cdot 10^{-2}$ g/liter were passed through the bed. At the bed outlet the uranium content of the solutions was $(1\text{-}4) \cdot 10^{-7}$ g/liter and $(1\text{-}4) \cdot 10^{-6}$ g/liter in the first and second cases respectively.

Solutions with a uranium concentration of $2 \cdot 10^{-3}$ g/liter were used as the working solutions in the experiments; their pH was 6-7. The uranium content of the solutions at the bed outlet was checked once per day. The analyses were carried out by the luminescence method.

The Fe_2O_3 content of the initial sand was 0.5 and 1.3% in the first and second experiments respectively. The volume of uranium-containing solution passed through was 75 and 245 liters respectively. The first experiment lasted 20 days and the second about two months. It should be mentioned that during the feed of the solution the hydrostatic head in the bed varied slightly as the water level in the feed bottle fell (see Fig. 1).

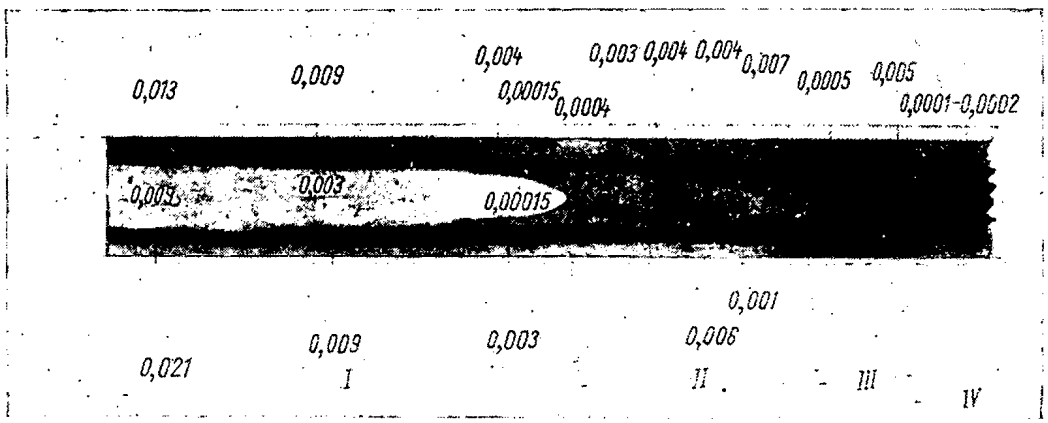

Fig. 2. Zonality and distribution of uranium in a sandstone bed (second experiment). Zones: I) oxidation; II) clarification (transitional); III) roll-like neogeneses; IV) unchanged rocks.

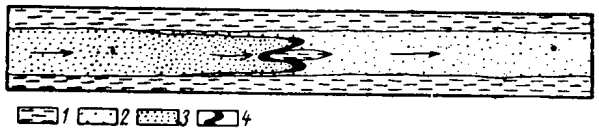

Fig. 3. Diagram of the formation of "inverted" rolls: 1) clay; 2) unchanged sand; 3) oxidation zone; 4) ore roll; the arrow indicates the direction of movement of water.

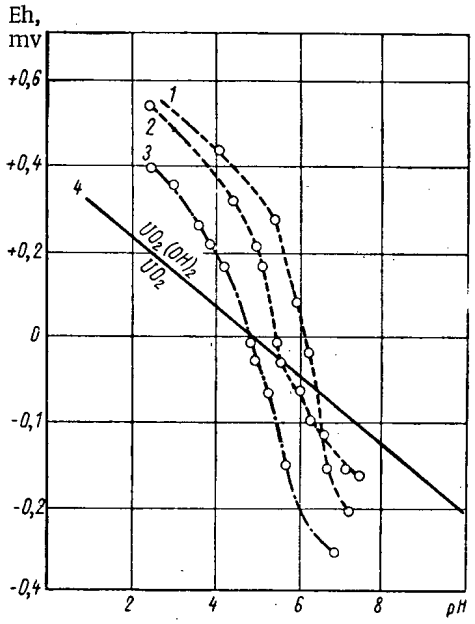

Fig. 4. Relation between the redox potential (Eh) and pH in solutions obtained by oxidation of sulfides: 1, 2) pyrite; 3) pyrite with a chalcopyrite admixture; 4) boundary between the UO_2 and $UO_2(OH)_2$ stability fields.

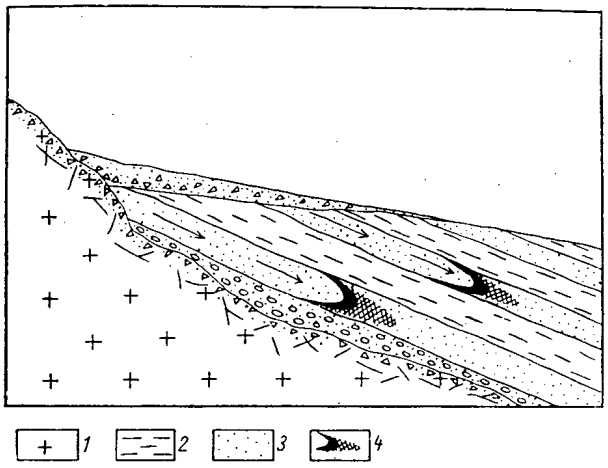

Fig. 5. Diagram of the location of ore rolls in an arenaceous-argillaceous formation: 1) crystalline rocks; 2) clays; 3) sandstones; 4) ore rolls.

After the experiments had been completed, the uranium distribution in the bed was investigated. Sand samples were taken with a stainless steel tube at 20 cm intervals over the bed cross section. Nine samples were taken from each cross section. Where the uranium content was at least 0.003% it was determined chemically, the luminescence method being employed for lower uranium contents.

RESULTS OF THE EXPERIMENTS

First experiment. As filtration of solutions containing uranium and atmospheric oxygen proceeded, a distinct oxidation zone in the form of a tongue, extended in the direction of movement of the water and advancing continuously through the bed at a rate of 1-2 cm/day, was formed in the latter. This rapid advance was due to the fact that freshly formed iron sulfides are oxidized very readily. During the advance of the oxidation zone, unoxidized areas in the form of disconnected lenses enclosing clay interlayers, remained in the roof and floor of the bed. The uranium content of these lenses was 0.009%. A uranium content of 0.008% was observed in the unoxidized sand near the contact with the oxidized part of the bed. Further away from the contact, both the oxidized and unoxidized sand contained 0.002-0.003% uranium.

Second experiment. As a result of filtration of uranium-containing solutions, four distinct zones were formed in the sand bed: I) oxidation; II) clarification (transitional); III) roll-like neogeneses; IV) unchanged (unoxidized) rocks (Fig. 2). The formation of a more complex zonality in the second experiment than in the first one may be due to the higher sulfide content of the sand and the greater duration of the experiment. The transitional, clarified zone was evidently formed as a result of the non-uniform rate of oxidation of iron sulfides, due partially to their crystallization in the form of minerals oxidized less rapidly than amorphous sulfide. Under natural conditions, the spotted ore (incomplete oxidation) zone, formed as a result of the different rates of oxidation of individual sulfides and the non-uniform permeability of the strata, may correspond to this zone.

The third zone consists of roll-like accumulations of black sand alternating with interlayers of light-gray sand. This is a cementation zone enriched with redeposited iron sulfides. According to analytical data, the iron content of the rolls, calculated as Fe_2O_3, is 1.80-1.85%, whereas in the oxidation zone and unchanged sand it is < 0.44% and 1.20% respectively.

The oxidation and clarification zones were clearly outlined soon after the commencement of the experiment, but the third zone was formed only towards the end. All three zones were mobile, moving slowly in the direction

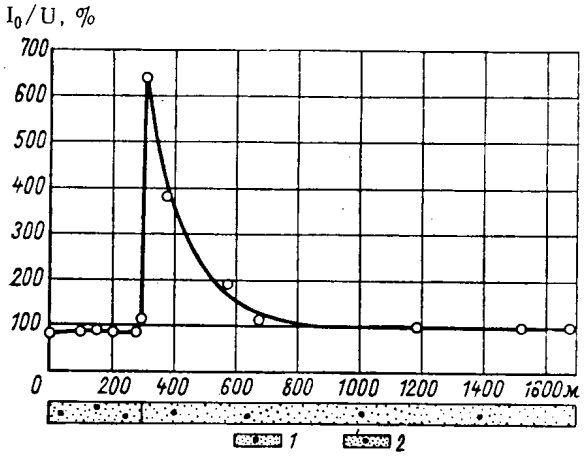

Fig. 6. Change in the ionium/uranium ratio I_0/U for a dip in the bed. Sandstone: 1) stable; 2) oxidized.

of movement of the water; the number of rolls in the third zone increased with time.

The formation of series of rolls may presumably be explained by the non-uniform hydrostatic head during feed of the solutions to the bed in the course of the experiment. But such non-uniformity is usual under natural conditions. Replenishing of water-bearing horizons is intensified during periods of rainfall and decreases during the dry season.

After completion of the experiment the following uranium distribution was observed (see Fig. 2): in the unoxidized sand at the contact with the clay the uranium content at the beginning of the bed was 0.009-0.021% and 0.007% in the rolls; in the oxidation zone, in the initial section of the bed, where uranium was sorbed by limonite, it was 0.009%. In the unchanged sand, at a considerable distance from the rolls, and in the frontal part of the oxidation zone the uranium content was 0.0001-0.0002%.

During the experiments it was found that the boundary between the oxidized and unoxidized rocks has a simple oval shape only if the bed permeability is uniform. But if a lens of argillaceous rock is placed in the path of the oxidation zone, the frontal part of the oxidation zone boundary splits into two tongues which circumvent the lens, as shown in Fig. 3. As a result of the low permeability, oxidation in the clay is slower than in the sand; this leads to formation of an "inverted" roll with its convex side facing the direction of movement of the water. A series of rolls with different orientations and "capricious" shapes, like those described in [3], may evidently be formed in the case of a variegated alternation of areas with different water permeability in rocks.

According to [4], a relation between the distribution of uranium deposits and the filtration capacity* of rocks is observed in the Colorado Plateau. These deposits are most frequently found in rocks with a non-uniform filtration capacity: Morrison sandstones, Shainar conglomerates and Chenelle sandstones. It may be assumed that this law is due to the non-uniform rate of oxidation of the rocks as a result of their different permeabilities, which establishes conditions for the formation of numerous ore rolls, as was shown above.

To determine the geochemical nature of the reduction and concentration of uranium by iron sulfides, we investigated the relation between the redox potential (Eh) and the pH of the medium during oxidation of pyrites. Pyrite from sedimentary rocks, crushed to 100-200 mesh, was placed in distilled water (2 g per 100 ml of H_2O) and oxidized for ten days by atmospheric oxygen. Solutions obtained in this way had a pH of 3.0-4.1, Eh +450 to +550 mv, and contained ferrous and ferric iron (more than 10 mg/liter Fe^{2+}), SO_4 (up to 120 mg/liter) and evidently sulfur ions of lower valence numbers (these were not determined chemically). To obtain the relation between Eh and pH, the solution was titrated in absence of oxygen (in a CO_2 current) with a soda solution (0.5-2%) in a glass beaker with a rubber stopper in which the electrodes and CO_2 inlet and outlet tubes were fixed. pH and Eh measurements were made with an LP-5 potentiometer until the last three measurements were identical. The results obtained are given in Fig. 4,

Uranium/Ionium Ratio in Bed Waters Associated with Sandstones

No.	Characteristics of the adjoining rocks	Depth, m	U cont. g/liter	Io/U, %
1	Alternation of limonitized sandstones and clays	11.0	$3.25 \cdot 10^{-4}$	< 1.0
2	Same	11.0	$7.5 \cdot 10^{-3}$	< 1.0
3	Gray argillaceous sandstone with uranium oxides	17.5	$5.6 \cdot 10^{-3}$	6.5
4	Brown sandstone, markedly limonitized	60.0	$1.1 \cdot 10^{-4}$	7.0
5	Brown-yellow sandstone, weakly cemented with ferruginous carbonate cement	60.0	$2.4 \cdot 10^{-4}$	7.5
6	Brown sandstone, markedly limonitized	60.0	$1.4 \cdot 10^{-4}$	5.5
7	Contact between unmodified (dark-gray sandstone with uranium oxides) and oxidized (brown, limonitized sandstone) rocks	60.0	$1.3 \cdot 10^{-4}$	5.5

* The filtration capacity is the product of the permeability of the rocks (in darcies) and the thickness [4].

which, for comparison, also gives the boundary between the UO_2 and $UO_2(OH)_2$ stability fields from calculation data in [5]. The graph shows that at low pH the system has a high oxidation potential and is an oxidizing system for uranium. At pH 5.5-7 the medium becomes reducing for uranium. During the experiments a red-brown precipitate of ferric hydroxide was formed at pH $\simeq$ 4.5. At pH $\simeq$ 6 the precipitate turned green and then with a further increase in pH to 7.5, black. After the precipitate had been filtered and dried (despite precautions, partial oxidation occurred during this process), ferrous and ferric hydroxides and very fine, black segregations (evidently sulfides) were observed under a binocular microscope.

In our opinion, this experiment reproduces one of the processes of secondary enrichment of the cementation zone of sulfide deposits, in which regenerated metal sulfides are formed as a result of neutralization of acid sulfate precipitated together with regenerated sulfides. This process also leads to formation of economic uranium ores in rocks enriched with iron sulfides.

RESULTS OF RADIOCHEMICAL INVESTIGATIONS

Concentration of uranium in rolls takes place gradually by continuous increase in their uranium content as the oxidation zone moves deeper into the bed. In deposits with an open catchment for the underground water, redistribution of uranium and an increase in the size of the ore beds (and their uranium content) may still be proceeding. This is indicated by the data of a radiochemical investigation of ore beds in a Cretaceous and Paleogene formation of arenaceous-argillaceous rocks.

The rocks of the formation form the gently dipping side of an anticline with Paleozoic granites and slates exposed in the core (Fig. 5). The Paleozoic massif is the catchment for the underground water contained in the sandstone beds. At distances up to several kilometers from the outcrops and up to a depth of 150-200 m the sandstones are markedly limonitized. Uranium minerals (mainly black) are localized in the unmodified sandstones along the lower boundary of the limonitization zone.

Investigations showed that in the ore-bearing horizons uranium and its decomposition products are often found in ratios which do not correspond to the radioactive equilibrium state. The most marked shift in equilibrium is generally observed between uranium and ionium (Th^{230}). In some cases the length of the zones relatively enriched with uranium or ionium reaches several hundred meters. The boundary between the zones is transverse to the direction of descensional movement of the bed water and coincides with the boundary of the bed oxidation zones.

A shift in radioactive equilibrium towards an ionium deficiency is observed in the unoxidized ores. Within the limits of an individual ore bed the ionium/uranium ratio is practically constant and, as one approaches the equilibrium state, increases only in areas where the bed tapers out. In the lower part of the limonitization zone, radioactive equilibrium is displaced towards an excess of ionium with respect to uranium. The decrease in uranium concentration as one passes from unoxidized ores to limonitized sandstones is generally very abrupt, whereas the ionium content decreases smoothly with the rise of the bed and from the floor and roof to the center of the oxidized part of the bed. Near the oxidation zone the ionium concentration in the limonitized sandstones is five to seven times greater than the concentration corresponding to a state of equilibrium with uranium. With increasing distance from this boundary to the rise of the bed, the ionium/uranium ratio in the central part of the sandstone bed gradually approaches the equilibrium value. A rock band characterized by mottled limonitization, within whose limits the ionium/uranium ratio varies by more than 100% from the values observed in unoxidized ores, is usually distinguished at the boundary between the oxidized and unmodified rocks. Fig. 6 shows the character of the change in the ionium/uranium ratio for the central part of the sandstone bed in one of the investigated areas*.

This ionium and uranium distribution in the ore-bearing beds is due to the different mobilities of these elements in oxidizing conditions. Whereas uranium has been removed by water during oxidation of the ore bed and redeposited under reducing conditions, ionium has remained in the limonitized sandstones. The hypothesis of the very limited migration of ionium in the oxidation zone is confirmed by observations on the change in the uranium and ionium concentration in the waters of this zone (table). The waters have a sodium-calcium chloride-sulfate composition and pH 7.3-7.9.

---

* The ionium/uranium ratio was determined by methods described in [6, 7].

The high ionium content of the oxidized rocks, reaching a value equivalent to ore concentrations of uranium, indicates that the ores were previously located much higher than the present position of the boundary between the oxidized and unmodified rocks. As the oxidation zone advanced deeper into the seams the ore beds disintegrated and the uranium which entered the waters during this process was redeposited at the boundary between the oxidized and unoxidized rocks. As a result, in the course of time the ore beds were gradually displaced in the direction of movement of the bed waters, leaving behind an ionium trail. During this process the uranium concentration in the beds probably increased as a result of entry of fresh amounts of uranium from the source of the bed water and from the sandstones undergoing oxidation.

The ionium trail is therefore a natural indicator of the displacement path of the ore beds. If the rate of displacement of the oxidation zone boundary was fairly high, it would evidently be possible to trace this path up to the exposure of the sandstones on the surface. But, as was shown above, in practice the ionium trail is observed in a limited range of the oxidized bed. An equilibrium uranium/ionium ratio is noted above this range in the sandstones. Nevertheless, even here one may establish that the orientation of the ionium trail, and therefore the direction of displacement of the ore beds, coincide with the direction of circulation of the bed waters.

To understand the conditions of a uranium mineralization in sandstones, it was of great importance to determine the duration of the ore-forming process (equivalent to the time of displacement of the oxidation zone boundary to its present level) and the age of mineralization in present-day ore beds.

If uranium redeposition ceased, radioactive equilibrium would be established between ionium and uranium in the ore beds after a certain time. From the half-life of ionium (83,000 years), this time interval may be roughly assessed as 500,000 years (six half-lives). 98.5% of the equilibrium amount of ionium is accumulated in this period. Absence of radioactive equilibrium in ore beds therefore indicates that uranium redeposition has continued during the past 500,000 years. The marked fall in the uranium content of the bed waters at the boundary of the oxidation zone from $n \cdot 10^{-4}$ g/liter under oxidizing conditions to $1 \cdot 10^{-6}$ g/liter in the area of tapering out of the ore beds under reducing conditions [2] indicates that this process is still continuing.

It was more difficult to determine the time of commencement of formation of present-day ore beds. In this case we could not use known geochronological methods for this purpose because of the fine dispersion of the uranium minerals and their varying age. We therefore tried to solve the problem of the lower age limit of the ore beds indirectly, by determining the mean rate of displacement of the boundary of the bed oxidation zone. Our determination of this rate was based on the laws of the change in the ionium/uranium ratio in the ore-bearing beds and data on the behavior of uranium and ionium under oxidizing conditions.

Oxidation leads to relatively rapid disintegration of uranium blacks and removal of uranium from the oxidation zone. There is little change subsequently in the uranium content remaining in the limonitized rocks. After the dissolution of uranium, ionium is retained in the limonitized sandstones and its decrease is mainly due to natural decay, not to removal by water, as was shown above. After a certain period, as a result of decay, ionium reaches equilibrium with the residual uranium in the limonitized sandstones. The time necessary for ionium decay may also be fixed as six half-lives. Knowing the distance from the area where uranium solution is still continuing (corresponding to the present position of the oxidation zone boundary) to the area where ionium reached equilibrium with the uranium left in the limonitized sandstones, the mean rate of displacement of the oxidation zone boundary between these areas may be readily determined.

As may be seen from Fig. 6, the ionium/uranium equilibrium ratio is observed at a distance of ~500-550 m from the oxidation zone boundary, i.e. this boundary was displaced approximately 500-550 m in a period of about 500,000 years.

By comparing the length of the ionium trail with that of the ore beds to the dip of the rocks, the lower age limit of the ore bed may be assessed. It should be mentioned that in some cases the length of the ionium trail was commensurate with that of the ore bed. Therefore the latter was displaced a distance equal to its own length in a period of not more than 500,000 years.

If it is assumed that the mean rate of displacement of the oxidation zone boundary remained constant during the preceding period as well, the time of its displacement from the sandstone bed outcrops, and therefore the time of commencement of formation of the ore rolls may be approximately determined.

SUMMARY

1. Ore beds of the roll type in arenaceous rocks are formed as a result of epigenetic accumulation of uranium from underground waters at the boundaries of zones characterized by oxidizing and reducing conditions.

2. With uniform permeability of the rocks and uniform distribution of their oxidizable matter, the oxidation zone has the shape of a tongue extending in the direction of movement of the waters. Being localized near the oxidation zone boundary, the ore beds reproduce its outlines, with the result that they acquire a crescentiform or roll-like shape.

3. An increase in the uranium content of the rolls to that of a workable one takes place during the continuous movement of the oxidation zone boundary in the direction of movement of the underground current and redistribution of uranium at the boundary between the oxidized and unmodified rocks.

4. Reduction and precipitation of uranium from waters by iron sulfides at the boundary between zones characterized by oxidizing and reducing conditions takes place as a result of precipitation of regenerated sulfides during secondary enrichment of the cementation zone.

5. An investigation of the laws of uranium and ionium migration and displacement of radioactive equilibrium between these elements in ore-bearing sandstones makes it possible to determine the displacement of ore beds during the advance of the oxidation zone and establish its velocity. The age of the investigated ore beds, determined in this way, is less than 500,000 years, and the distance by which the boundary between the oxidized and unmodified rocks was displaced during this period is about 500 m.

LITERATURE CITED

1. D. Shawe, in: Proceedings of the International Conference on the Peaceful Uses of Atomic Energy (Geneva, 1955), [Russian Translation], Vol. 6, Gosgeoltekhizdat, Moscow (1955), p. 397.
2. A. I. Germanov, Izv. AN SSSR, Ser. geol., 8, 75 (1960).
3. D. Shawe, N. Archbold, and G. Simmons, in: Proceedings of the Second International Conference on the Peaceful Uses of Atomic Energy (Geneva, 1958), Selected Reports of Foreign Scientists [Russian translation], Vol. 8, Atomizdat, Moscow (1959), p. 349.
4. D. A. Jobbins, in: Proceedings of the International Conference on the Peaceful Uses of Atomic Energy (Geneva, 1955) [Russian translation], Vol. 6, Gosgeoltekhizdat, Moscow (1955), p. 376.
5. R. Garrels, Amer. Min., 40, No. 11, 12 (1955).
6. L. A. Kuz'mina, Zh. anal. khim., XIII, No. 1, 100 (1958).
7. A. P. Bocharova and V. I. Malyshev, in the symp.: Methods of Determining Radioactive Elements in Mineral Raw Material [in Russian], Gosgeoltekhizdat, Moscow (1961), p. 76.
8. V. I. Malyshev, Sov. geologiya, 7, p. 138 (1958).
9. J. Rosholt, US Geol. Surv. Bull., 1084-A (1959).

All abbreviations of periodicals in the above bibliography are letter-by-letter transliterations of the abbreviations as given in the original Russian journal. *Some or all of this periodical literature may well be available in English translation.* A complete list of the cover-to-cover English translations appears at the back of this issue.

ELASTIC AND INELASTIC SCATTERING OF α-PARTICLES ON Al^{27}

K. P. Artemov, V. Z. Gol'dberg, and V. P. Rudakov

Translated from Atomnaya Énergiya, Vol. 14, No. 5,
pp. 482-484, May, 1963
Original article submitted September 10, 1962

One characteristic feature of the angular distribution of elastically and inelastically scattered α-particles of energy considerably in excess of the Coulomb potential barrier is the regular succession of maxima and minima — the so-called diffraction pattern. In the available experimental data, our attention is immediately drawn to the pronounced relationship linking the angular distributions of elastically and inelastically scattered α-particles: the fluctuations of the differential cross sections either coincide or oppose each other in phase. For those cases where the characteristics of energy states excited in inelastic scattering are known from other independent measurements, it was found that the angular distributions of inelastically scattered alpha-particles corresponding to excitation of even states are out of phase with the angular distributions of elastically scattered α-particles, and the angular distributions of α-particles corresponding to excitation of odd states are in phase with the distribution of elastically scattered α-particles. Deviations from this "phase rule" have not been found to date, except, of course, for cases of two-photon excitation.

Excellent agreement with experimental evidence has been obtained from calculations of inelastic scattering in the Born approximation by the method of distorted waves [1]. Other authors [2-4] take a different approach to the problem. In the adiabatic approximation, excitation of collective states in diffraction scattering on a "black" ellipsoid is treated. From this theory flows the experimentally observed relationship between angular distributions in the excitation of even and odd states. The absolute value of the inelastic scattering cross section in the excitation of collective states depends on the nuclear deformation parameter or on the amplitude of collective surface oscillations. The differential elastic scattering cross section in those instances, where Coulomb interaction may be neglected, is described by the expression

$$\frac{d\sigma}{d\Omega} = (kR_0^2)^2 \left| \frac{I_1(x)}{x} \right|^2,$$

where $\underline{k}$ is the wave number; R_0 is the interaction radius; $I_1(x)$ is a first-order Bessel function; $x = 2kR_0 \sin \frac{1}{2}\theta$ (θ is the scattering angle in the center-of-mass system).

The inelastic scattering cross section for the $0 \rightarrow 2$ transition is described by the expression

$$\frac{d\sigma}{d\Omega} = (kR_0^2)^2 \frac{\beta_2^2}{4\pi} \left[\frac{1}{4} I_0^2(x) + \frac{3}{4} I_2^2(x) \right],$$

where β_2 is the quadrupole deformation parameter. An analysis of experimental data in this approximation, where the collective nature of the states occasions no substantial doubts, provides reasonable values of the nuclear deformation parameters and of the quadrupole and octupole moments.

On the basis of this theory, the results of our measurements of elastic and inelastic scattering of 40, 38, and 36 MeV α-particles on Al^{27} were analyzed. Measurements were carried out on the 1.5-meter cyclotron of the I. V. Kurchatov Institute of Atomic Energy of the USSR. A high-pressure grid ionization chamber was employed to record the α-particles. The energy resolution of the chamber for 40 MeV α-particles was 1.2%; the angular resolution was 0.8° in the measurements. Angular distributions of one group of elastically scattered α-particles and two groups of inelastically scattered α-particles corresponding to the excitation of the first two levels (Q = -0.84 and -1.01 MeV not resolved) and of the third level (Q = -2.22 MeV) of the Al^{27} nuclide were measured. The alpha spectrum and the angular distributions are displayed in Fig. 1 and 2.

The interaction radius of the α-particle with the Al^{27} nucleus was found to be 5.5 fermi, from the position of the maxima in the angular distribution of elastically scattered α-particles. The phase relationships in the measured angular distributions suggest that the 2.2 MeV energy state of Al^{27} possesses positive parity.

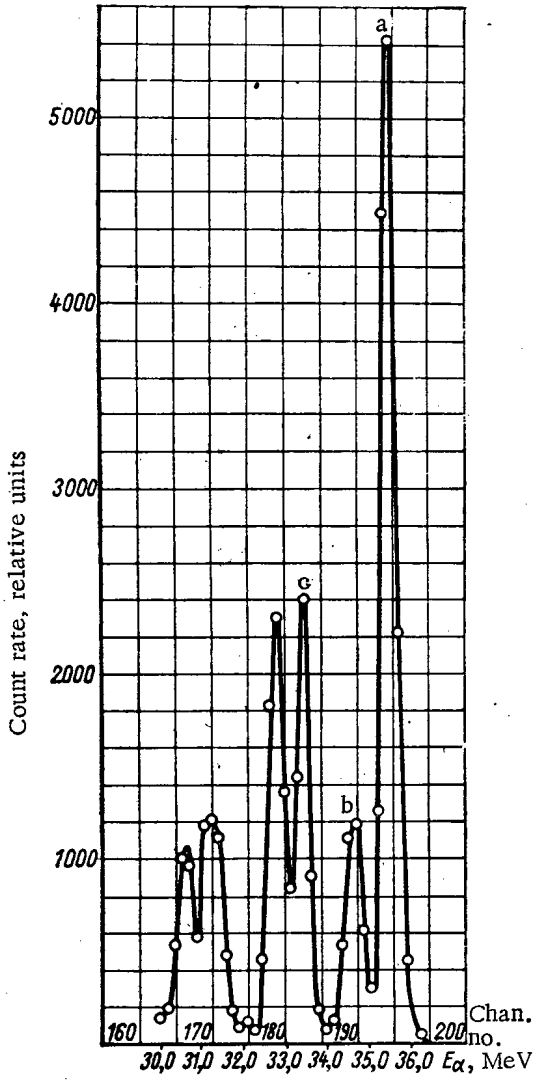

Fig. 1. Spectrum of α-particles scattered on Al^{27} (θ = 50°). Q values: a) 0; b) -0.84 and -1.01 MeV (not resolved); c) -2.2 MeV.

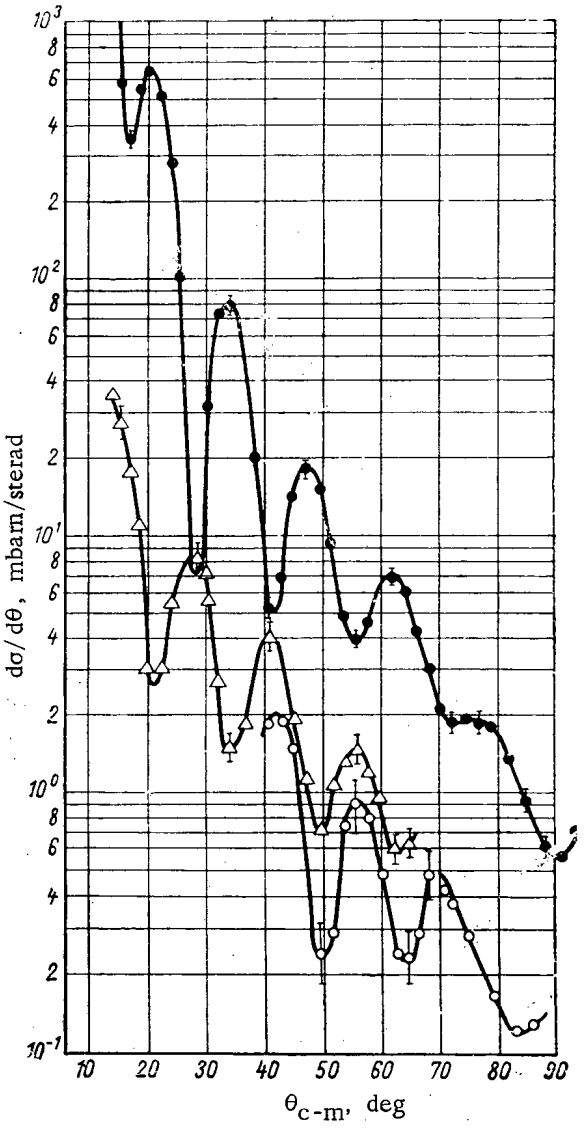

Fig. 2. Differential cross section for elastic and inelastic scattering of 40 MeV alphas on Al^{27}. Q values: ●) 0; ○) -0.84 and -1.01 MeV; △) -2.2 MeV.

It is known that the 0.84, 1.01, and 2.7 MeV excited states of Al^{27} belong to the rotation band $K = \frac{1}{2}$ [5]. There probably exists another rotation band $K = \frac{5}{2}$ in Al^{27}, the precursor of which is the ground state $Al^{27} = D_{5/2+}$ [6]. The first excited level in this band is most likely the 2.2 MeV level. We should then assume the spin and parity of this level to be $^7/_2{}^+$. Calculations for this case, based on diffraction theory, yield the quadrupole deformation parameter and the quadrupole moment of the Al^{27} nuclide, viz. $\beta_2 = 0.2$ and $Q = 0.144$ barn ($R = 1.45\ A^{1/3}$).

As will be readily seen from the above formulas, the energy dependence of the cross section is primarily determined by the factor k^2. Consequently, the value of the cross section divided by k^2 is an energy-independent quantity. These "universal" curves are shown in Fig. 3. The theoretically computed curves were plotted for $R_0 = 5.5$ fermi and $\beta_2 = 0.2$. In line with theoretical predictions, points plotted at 40, 38, and 36 MeV energy of incident α-particles lie on the same curve. As might be expected, given the restrictions introduced into the theory, agreement between theoretically computed and empirical absolute values is attained only over a small range of angles in the forward direction.

The results obtained from scattering of α-particles on Al^{27} are reasonably well accounted for, consequently, within the framework of the rotational model and diffraction scattering theory.

The authors express their indebtedness to S. I. Drozdov for his invaluable discussion of the findings.

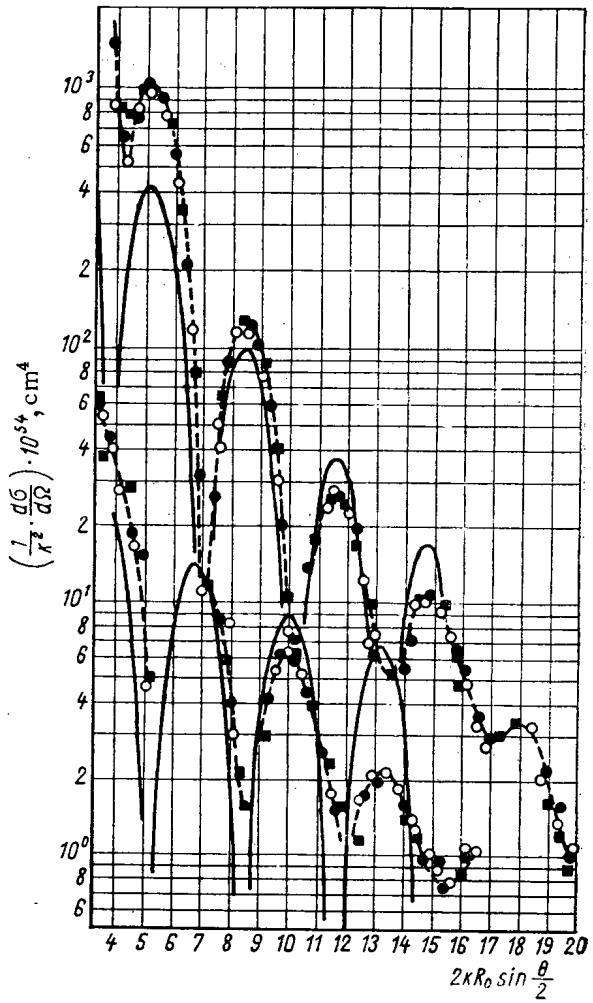

Fig. 3. "Universal" curves for elastic scattering (top curves, Q = 0 MeV) and inelastic scattering (lower curves, Q = -2.2 MeV) of α-particles: ---) experimental curves; ——) theoretical curves. Q values: ●) 40 MeV; ○) 38 MeV; ■) 36 MeV.

LITERATURE CITED

1. N. Austern, Proc. of the Conf. on the Nucl. Structure, Kingston (1960).
2. E. V. Inopin, Zhur. eksptl. i teoret. fiz., 31, 901 (1956).
3. S. I. Drozdov, ibid., 36, 1875 (1959).
4. I. Blair, Proc. of the Conf. on the Nucl. Structure, Kingston (1960).
5. E. Almgwist et al., Nucl. Phys., 19, 1 (1960).
6. H. Gove, Proc. of the Conf. on the Nucl. Structure, Kingston (1960).

FORMATION CROSS SECTIONS OF KRYPTON AND XENON ISOTOPES IN THE FISSION OF URANIUM BY 680 MeV PROTONS

A. N. Dobronravova, L. K. Levskii, A. N. Murin, and N. E. Titov

Translated from Atomnaya Énergiya, Vol. 14, No. 5,
pp. 484-486, May, 1963
Original article submitted July 27, 1962

In an earlier communication [1], we mentioned relative yields of xenon and krypton isotopes as fission products of uranium fissioned by 680 MeV protons. The yields of Xe^{130} and Kr^{86} isotopes were assigned the value of unity.

In what follows, we describe an additional irradiation of two uranium targets using protons of the same energy, in the internal beam of the synchrocyclotron at the Nuclear Problems Laboratory of the Dubna Joint Institute for Nuclear Research. The irradiated targets were placed in tantalum crucibles and were melted using a high-frequency unit. The gases evolved during the melting were collected in an ampule containing activated charcoal, at -183°C temperature, and the nonsorbed gases were evacuated by means of a Toepler pump. The chemically active gases were then removed with CuO and calcium at 600°C temperature. Following the evacuation, a portion of the krypton and xenon was removed for sampling, to determine the isotope composition. The absolute content of the isotopes was determined by the isotope dilution method. The absolute quantity of Xe^{130} and Kr^{86} atoms found by this method was $3.95 \cdot 10^{12}$ and $5.21 \cdot 10^{12}$ per single gram of irradiated uranium.

Use of the MV-23-02 mass spectrometer for isotopic analysis of small quantities of a gas requires rapid and precise adjustments for each isotope. In the standard instrument this is hindered by the stepwise change in the ampere-turns of the electromagnet coil and by the absence of spurious peaks due to hydrocarbon contaminants. The hydrocarbon peaks are particularly harmful when an electron multiplier tube is placed across the mass spectrometer output since, in that case, the hydrocarbon peaks will occasionally be of higher intensity than the peaks of the isotopes of the gases under study. The sweep circuit of the mass-produced instrument is suitable for recording only one isotope (sweep range of 0.2 mass units), and cannot be used efficiently to record five or six or more isotopes.

In the sweep circuit described for recording each isotope, a sweep potentiometer is used in the mass-produced instrument, and the switch from one isotope to another is effected automatically by feeding the potential from the potential divider to the grid of the tube controlling the accelerating voltage.

The accompanying figure depicts the basic sweep circuitry for 11 xenon isotopes (mass numbers 124 to 136). The battery B supplies the divider R_{11}-R_{20}. The resistors R_{11}-R_{20} are made of manganin wire 0.02 mm thick. The

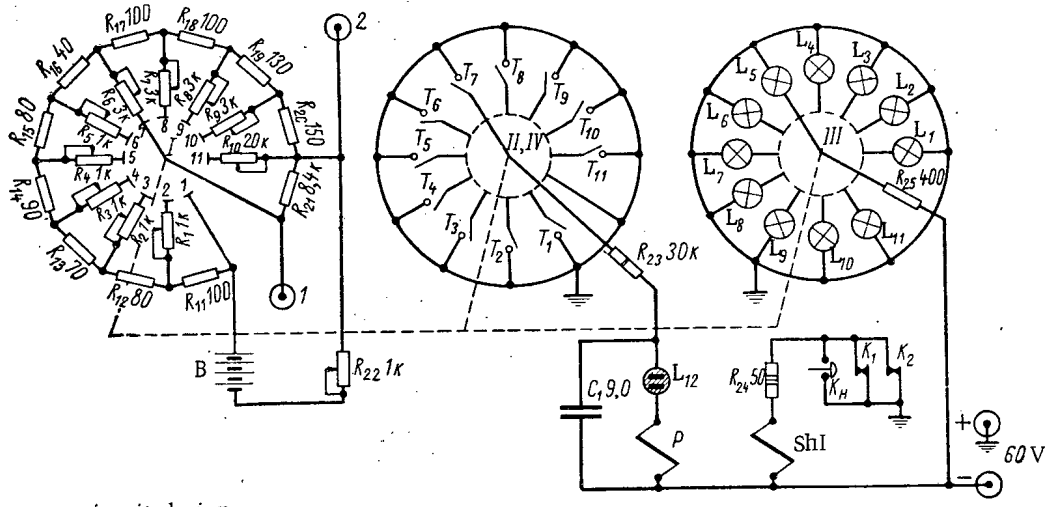

Automatic sweep circuit design.

Relative Yields of Krypton, Xenon, and Rubidium Isotopes

Isotope	Time elapsed after exposure, days		
	56	346	72
Kr^{78}	0,0045±0,002	0,0055±0,005	—
Kr^{80}	0,36±0,03	0,22±0,01	0,208±0,005
Kr^{81}	0,09±0,02	0,12±0,01	0,102±0,005
Kr^{82}	0,56±0,02	0,58±0,02	0,53±0,02
Kr^{83}	1,09±0,02	1,25±0,02*	1,11±0,03
Kr^{84}	1,37±0,01	1,43±0,03†	1,34±0,03
Kr^{85}	0,44±0,01	0,54±0,01	0,54±0,01
Kr^{86}	1	1	1
Xe^{124}	0,09±0,006	0,080±0,005	0,084±0,007
Xe^{126}	0,380±0,01	0,38±0,01	0,40±0,01
Xe^{127}	0,59±0,02‡	—	~0,34‡
Xe^{128}	0,86±0,02	0,87±0,02	0,85±0,02
Xe^{129}	0,66±0,05	0,54±0,02	0,61±0,02
Xe^{130}	1	1	1
Xe^{131}	1,88±0,07	1,90±0,04	1,97±0,03
Xe^{132}	1,72±0,07	1,74±0,05	1,78±0,02
Xe^{134}	1,20±0,03	1,41±0,03	1,41±0,04
Xe^{136}	0,91±0,06	1,07±0,04	1,20±0,04
Rb^{83}**	—	0,28	—
Rb^{84}**	—	0,42	—

• Corrected for yield of $Rb^{83} \simeq 0.98$.
† Corrected for yield of $Rb^{84} \simeq 1.02$.
‡ Corrected for decay of Xe^{127} (T = 36.41).
•• Kr^{86} yield assigned value of unity.

resistors R_1-R_{10} and R_{22} are adjustable wire resistors connected to the first row of blades of the stepping switch Shl (an Shl-11 switch). The voltage change across the reference resistor R_{21} (points 1 and 2) is fed to the grid of the driving tube. The second row of blades is connected to the toggle switches T_1-T_{11}, whose function is to switch on recording of specific isotopes. The recording process proceeds as follows. When all the toggle switches are disengaged (as shown in the diagram), the pulses placed across the electromagnet winding of the switch are fed only through the contact switch K_1 fastened to the axis of the sweep potentiometer. After the sweep potentiometer slider makes one complete revolution, the contact K_1 closes and the stepping switch moves from the first blade to the second. If, for example, the toggle switch attached to the second blade is connected, a voltage will be placed across the relaxation circuit C_1-L_{12} (a neon gas tube). The discharge from the capacitor C_1 actuates the relay P, and via the contact the relay K_2 feeds the pulse to the winding of the stepping switch which immediately connects to the third blade. The time constant of the relaxation circuit is ~0.2 sec. By means of the pushbutton K_H, pulses may be placed manually across the winding of the stepping switch. The third row of blades in the stepping switch is connected to tubes L_1-L_{11}, each of which functions to record a specified isotope. When the selector is positioned on the 12th blade of the fourth row, relay P is activated, and the stepping switch returns to its initial position on the first blade. The unit is adjusted by appropriately varying the values of the resistances R_1-R_{10} and R_{22}. Whenever the voltage supplied by the battery B suffers a sharp decline, the proper level is restored by varying the resistance R_{22}. The functioning of the mass spectrometer with this accessory unit begins by manual tuning for one of the isotopes (by varying the ampere turns of the magnet) with subsequent automatic switching from one isotope to the next.

Similar circuits may be used to record isotopes of the other elements. In our case, the circuit designed to record the isotopes of xenon, krypton, argon, and neon were included in a single unit. Each element required its own sweep circuit. However this is only an apparent disadvantage, for the usual practice is to work with a single element, and less frequently with several elements.

The major advantage of the sweep circuit described here is the rapid transition from one isotope to the next, eliminating any useless expenditure of the experimental material.

A change in the accelerating voltage in passing from one isotope to another occasionally brings about discriminating effects. When working with xenon isotopes, this effect amounts to 10% for the extreme isotopes, so that the mass spectrometer must be first standardized with respect to atmospheric xenon, in order to obtain high-precision results. These discriminating effects are not encountered in work with krypton isotopes.

The results of measurements of relative yields are listed in the accompanying table, which also includes earlier data. The difference in the time intervals between irradiation exposure and measurement for various targets called for the introduction of corrections into the directly measured relative yields of Kr^{83} and Kr^{84}, to take into account decay of Rb^{83} and Rb^{84}. The Rb^{83} and Rb^{84} yields are also listed in the table.

A stream of protons passed through a target was measured in the usual way by the $Al^{27}_{13}(p, 3pn)Na^{24}$ reaction, in order to compute the cross sections of the isotope yields of krypton and xenon. This was attended to in a separate experiment. The Na^{24} yield is determined by the activity of that isotope, using two different methods: counting β-particles on an end-window counter in a specified geometry, and by the absolute intensity of the Na^{24} γ-lines (E_γ = = 1380 keV), measured by scintillation techniques. Both methods yielded findings in agreement within the limits of accuracy of the measurements.

Below, we cite some values, computed from the customary formulas [2], of the effective formation cross sections for isotopes of krypton, xenon, and rubidium:

Isotope	Xe^{124}	Xe^{126}	Xe^{127}	Xe^{128}	Xe^{129}	Xe^{130}	Xe^{131}	Xe^{132}	Xe^{134}	Xe^{136}
σ, millibarns	1,46	7,1	6,1	15,4	10,7	17,9	34,6	31,4	25,2	18,6

Isotope	Kr^{78}	Kr^{80}	Kr^{81}	Kr^{82}	Kr^{83}	Kr^{84}	Kr^{85}	Kr^{86}	Rb^{83}	Rb^{84}
σ, millibarns	0,12	5,0	2,6	13,0	29,6	33,4	12,7	23,6	6,9	9,7

Of the cross sections listed, only the formation cross sections of Kr^{83} and Xe^{131} gave the total yields of isobars having the mass numbers 83 and 131*. In the case of Rb^{83} and Rb^{84}, the cross sections listed correspond to the individual yields of the nuclides in question.

The findings obtained are, generally speaking, inadequate for solving the overall problem of determining independent yields of all fission fragments of given Z and A, without resorting to any additional assumptions or empirical data. Nevertheless, it is possible to attempt to draw some conclusions, albeit on the basis of existing assumptions as to the distribution of fragments with given A and Z. Suppose that this distribution may be represented by a Gaussian curve in the form

$$\sigma_{ind} = \sigma_{max} e^{-R(Z-Z_p)^2}, \tag{1}$$

where R is a parameter determining the half-width of the distribution curve, and Z_p is the most probably charge on the fission fragment. Then the cumulative yield of the isobar such that $Z = Z'$, i.e. the yield of the fragment assembling all of its "precursors" as a result of successive radioactive decay, may be approximated by the formula

$$\sigma(A, Z')_{cum} = \sigma_{max} \int_{Z'-\frac{1}{2} \text{ or } \infty}^{\infty \text{ or } Z'+\frac{1}{2}} e^{R(Z-Z_p)^2} dz. \tag{2}$$

The choice of $(Z' - \frac{1}{2}; \infty)$ or $(-\infty; Z + \frac{1}{2})$ as integration limits depends on whether the group of genetically related isobars is characterized by $Z \geq Z'$ or by $Z \leq Z'$.

It is readily shown that in the first case

$$\frac{\sigma(A, Z')}{\sigma(A)} = 0{,}5 - \Phi\left[\sqrt{R}\left(Z' - Z_p - \frac{1}{2}\right)\right],$$

where σ(A) is the total yield of isobars of given A, and $\Phi(x) = \frac{1}{\sqrt{\pi}} \int_0^x e^{-t^2} dt$ is a function obtainable from available tables. A similar formula is also obtained in the second case. In order to find R and Z_p, we have to know at least three independent yield values (either individual or cumulative yield values)* for a given A.

When uranium is fissioned by 680 MeV protons, the curve of total fission fragment yields apparently displays a broad and flat maximum (possibly even convex at the midpoint) [3]. It is therefore safe to assume that the total cross sections σ(A) = σ(131) = 34.6 mbarn for all the mass numbers in the mass region 124-136 (xenon isotopes) which we measured. Moreover, once we assume $Z_p = B + CA$ and make use of the footnoted remark, we are in a position to determine the coefficients B = 20.4 and C = 0.25, and also to attempt to determine the value of R by a method entirely analogous to that employed earlier [4].

---

* In the particular case where the ratio $\frac{\sigma(A, Z')}{\sigma(A)} = 0{,}5$, $Z_p = Z' \pm \frac{1}{2}$, the minus sign corresponds to $Z \geq Z'$, and the plus sign to $Z \leq Z'$.

The results arrived at indicate that the half-width of the distribution curve (1) in that mass region is of the order of 3.5 mass units. This is in excellent accord with the assumption advanced by Pappas and Alstad [5].

Note that, as should follow from the equation $Z_p = 20.4 + 0.25\ A$, when uranium is fissioned by 680 MeV protons, the probable charge on fragments of mass number 124 to 136 is apparently 0.5 to 1.0 units lower than the charge on the isobar most stable to beta decay. A similar (and essentially just as hypothetical) analysis of the data obtained on the krypton isotopes shows that the half-width of the distribution curve (1) is of the order of two in that case, and that the most probable charge on a fragment of given A is practically the same as the charge on the most beta-stable isobar. Further experiments on determination of yields of isobars of several other elements will be required in order to obtain more accurate yields.

The authors are grateful to V. P. Dzhelepov and to É. K. Gerling for their kindness in allowing us to use the synchrocyclotron and the MV-23-02 mass spectrometer, and to V. I. Baranovskii for his helpful discussion of the findings.

LITERATURE CITED

1. A. N. Dobronravova et al., Geokhimiya, 6, 540 (1962).
2. Radiochemistry and chemistry of nuclear processes, edited by A. N. Murin, V. D. Nefedova, and V. P. Shvedova, Goskhimizdat, Leningrad (1960), p. 645 [in Russian].
3. G. Friedlander et al., Conf. on fission and spallation phenomena and their application to cosmic rays, CERN, September 26-29, No. 13, 1961.
4. V. I. Baranovskii and A. N. Murin, Izv. AN SSSR, seriya fiz., 25, No. 7, 887 (1961).
5. A. Pappas and J. Alstad, J. Inorg. and Nucl. Chem., 17, No. 3/4, 195 (1961).

NOTE ON THE EFFECT OF NEUTRON POLARIZATION ON NEUTRON TRANSMISSION IN MEDIA

P. S. Ot-stavnov

Translated from Atomnaya Énergiya, Vol. 14, No. 5,
pp. 487-488, May, 1963
Original article submitted September 4, 1962

In the case of a spherically symmetric central field, the differential cross section for elastic scattering of unpolarized neutrons is well described by a familiar formula independent of the azimuthal angle φ:

$$\sigma_0(\theta) = \lambda\!\!\!^{-2} \left| \sum_{l=0}^{\infty} (2l+1)\, e^{i\delta_l} \sin\delta_l P_l(\cos\theta) \right|^2, \tag{1}$$

where $\sigma_0(\theta)$ is the scattering cross section over unit solid angle at scattering angle θ; $\lambda\!\!\!^{-}$ is the neutron wavelength divided by 2π; δ_l is the phase of the radial scattered wave function; P_l is a Legendre polynomial of order l; l is the azimuthal quantum number. When fast neutrons are scattered on nuclei, partial neutron polarization is observed; in other words, most of the neutrons are in the same spin state in scattering at angles θ and φ, while the degree of polarization may attain considerable values [1-3]. In partial polarization of incident neutrons, scattering will be described by a formula depending not only on θ, but also on the azimuthal angle φ:

$$\sigma(\theta, \varphi) = \sigma_0(\theta)\,[1 + \mathbf{n_1 n_2} P_1 P_2], \tag{2}$$

where $\sigma_0(\theta)$ is the differential scattering cross section of unpolarized neutrons; $P_1(\varphi)$ is the degree of polarization of the incident neutrons; $P_2(\theta)$ is the degree of polarization of neutrons in response to scattering of the neutrons on a nucleus at angle θ. The unit vectors $\mathbf{n_1}$ and $\mathbf{n_2}$ are determined from the relationships $\mathbf{k_0} \times \mathbf{k_1} = \mathbf{n_1} k^2 \sin\psi$, $\mathbf{k_1} \times \mathbf{k_2} = \mathbf{n_2} k^2 \sin\theta$, where $\mathbf{k_0}$, $\mathbf{k_1}$, $\mathbf{k_2}$ are the unit wave vectors of, respectively, the incident (unpolarized), scattered, and multiply scattered neutrons.

As we see from Eq. (2), the differential cross section $\sigma(\theta, \varphi)$ depends on the scalar product of vectors $\mathbf{n_1}$ and $\mathbf{n_2}$, which is allowed to vary from -1 to +1. P_1 and P_2 in turn depend on the angle of scattering and on the energy of the incident neutrons. The azimuthal angle φ is simply the angle between vectors $\mathbf{n_1}$ and $\mathbf{n_2}$. In the case $\varphi_1 = 0°$ and $\varphi_2 = 180°$, Eq. (2) is simplified to:

$$\sigma(\theta) = \sigma_0(\theta)\,[1 \pm P_1 P_2]. \tag{3}$$

Consider a hypothetical experiment (Fig. 1). Let a beam of unpolarized neutrons impinge on a medium whose dimensions are several mean free path lengths of the neutron. The neutron flux will be N_0 cm^{-2}sec^{-1} incident in a volume element V, and elastically scattered within that volume. Neutrons become polarized on being scattered.

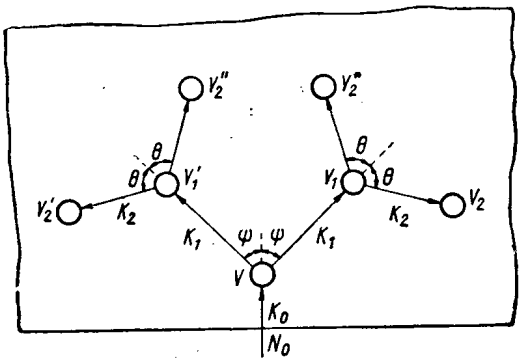

Fig. 1. Neutron scattering in a medium.

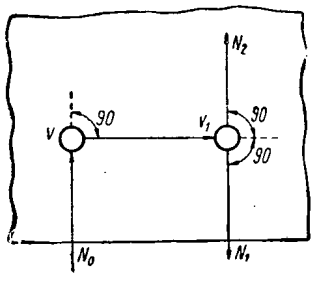

Fig. 2. Illustration for estimating scattering asymmetry.

Since the neutrons impinge in an unpolarized state on the volume element V, scattering will occur axially symmetric to the axis of incidence and the differential cross section will be found from Eq. (1). Impinging on elements V_1 and V_1' will be an equal number of neutrons $N_1 = N_2 = N_0/2$ provided scattering is considered in a single plane and only at angles $\pm\theta$. But these are now partially polarized, and the scattering on elements V_1 and V_1' will be asymmetric, i.e. it will depend on the azimuthal angle φ. More neutrons will be scattered in an element V_2', according to Eq. (2) and (3), than in the element V_2'', i.e. $N_0/m_2' \neq N_0/m_2''$, where

$$m_2'(m_2'') > 2 \text{ and } m_2' < m_2''.$$

Reasoning in a similar manner, we find that more neutrons are scattered in the element V_2 than in the element V_2^*. It is readily seen that the number of neutrons scattered in element V_2' is equal to the number of neutrons scattered in element V_2. The assumption that all the neutrons are scattered in a single plane does not distort the true picture in principle, since the plane passes through all the angles φ when that scattering plane is rotated about the axis of incidence of the neutron beam defined by the vector $\mathbf{k}_0$, and the integral taken from 0 to 2π with respect to φ gives the total number of neutrons impinging on the element V.

It is clear from this simple experiment that the neutrons impinging on the medium are not scattered randomly, but rather evince a tendency to execute curves in response to spin-orbit forces. After a second scattering, the neutrons will have the same probability of escaping from this medium as they have of penetrating it deeper.

We now carry out a rough estimate of this phenomenon for Mg media at neutron energy $E_n = 0.240$ MeV. We neglect energy losses in elastic scattering. Let the neutrons be scattered twice at angle $\psi = \theta = 90°$ and let $P_1(90°) = P_2(90°) = 0.866$ [3]. Then the ratio of the number of twice scattered neutrons (Fig. 2) will be

$$R = \frac{N_1}{N_2} \approx \frac{1 + P_1 P_2}{1 - P_1 P_2} \approx 7.$$

After the second scattering, seven times more neutrons will escape from the medium as there will be remaining within the medium. For a beryllium medium, at angles $\psi = \theta = 110°$ and energy $E_n = 3.1$ MeV [1], this ratio will be ~2. In actuality, this value, when averaged over all angles ψ and θ and over all possible energies, will turn out considerably smaller, but it should not be less than or equal to unity, except in a few rare exceptional cases. However, using the now-existing methods of neutron calculations, we neglect to take this effect into account and do not consider it in our estimates. There are ways of estimating the effect of γ-ray polarization in response to Compton scattering on the transmission [4], which comes to several percent.

It may be assumed that taking the fast-neutron polarization effect into account will yield a perceptible result in some reactor calculations (in particular in albedo calculations). For example, laminated shielding may bring about either an improvement or a deterioration in shielding effectiveness against neutron radiation, depending on the energy of the incident neutrons and on the neutron energy losses in a single scattering event, in given structural materials.

The author expresses his acknowledgments to I. I. Bondarenko, V. V. Orlov, and L. N. Usachev for their kind and helpful discussions.

LITERATURE CITED

1. B. McCormac et al., Phys. Rev., 108, 116 (1957).
2. P. S. Otstavnov and V. I. Popov, Zhur. eksptl. i teoret. fiz., 43, 385 (1962).
3. A. Elwyn and R. Lane, Nucl. Phys., 31, 78 (1962).
4. L. Spencer and C. Wolff, Phys. Rev., 90, No. 4, 510 (1953).

ANGULAR ENERGY DISTRIBUTION OF NEUTRONS AT AN INTERFACE

V. A. Dulin, Yu. A. Kazanskii, and I. V. Shugar

Translated from Atomnaya Énergiya, Vol. 14, No. 5,
pp. 488-90, May, 1963
Original article submitted August 14, 1962

Spectra of scattered neutrons emerging at various angles from a flat slab of graphite in which a source of fast neutrons of mean energy 3.9 MeV is placed 20 cm from the interface were measured in the work described in this note. The results obtained in the angular range 20-70° and energy range 1.3-3.9 MeV are in essence a solution of the kinetic equation at the interface between two media (graphite-water interface) for the given geometry.

The layout of the experimental set-up is seen in Fig. 1. The $H^2(H^2, n)He^3$ reaction at deuteron energy 900 keV provided the neutron source. Neutrons were singled out at a specific angle by means of a conical collimator giving an angular resolution of ~5°. The neutrons emerging from the graphite in the neighborhood of point A at angle θ could not be scattered in the water since an air cavity was established at the interface.

The neutrons were recorded with a single-crystal fast-neutron scintillation spectrometer discriminating against gamma rays [1]. The amplitude distributions of the pulses were measured with an AI-100 analyzer. The energy scale of the spectrometer was checked periodically against measured spectra of unscattered neutrons.

The large size of the tank filled with a solution of 2% boric acid provided a low-level neutron background. The neutron background was measured when the collimator cavity was filled with water. The relationship of the background and the effect for neutrons emerging at various angles are tabulated. This table shows the relationships between neutron flux and gamma emission. The same flux relationships made it possible to set the spectroscopic threshold of the spectrometer at no higher than 1.3 MeV. The γ-emission discrimination at this threshold was $(6-8)\cdot10^{-4}$ at a gamma count rate no higher than $1.3\cdot10^3$ pulses/sec.

It is clear from the table that even at 70° the measured neutron amplitude distributions contain not more than 4% pulses due to gamma emission, since the background is primarily due to gamma emission, and the gamma emission load in the effect and background, and separately in the background, is approximately the same. The amplitude distribution was measured three or four times for each angle. Each amplitude distribution was converted to the neutron energy spectrum by means of a numerical matrix based on [1]. The use of this numerical matrix to convert amplitude distributions to energy spectra is described in detail in [2]. The use of a differentiation technique in processing these amplitude distributions yielded findings which differed by not more than 20%, even in the 1.3-2.0 MeV neutron energy range. Figure 2 gives the angular distributions of neutron energy groups. Root mean square errors are indicated.

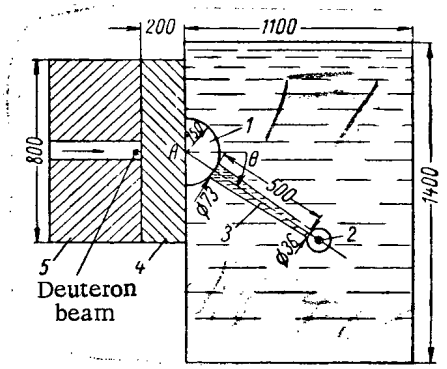

Fig. 1. Design of experimental arrangement. θ) angle of scattering; 1) air cavity; 2) detector; 3) collimator; 4) graphite; 5) target.

Relationship between Neutrons and γ-Emission

Scattering angle, θ	Neutrons		Neutrons and γ-emission		Relation between neutrons and γ-emission
	effect and background	background	effect and background	background alone	effect and background
20°	27	0,2	1000	560	0,03
70°	3	0,5	650	500	0,005

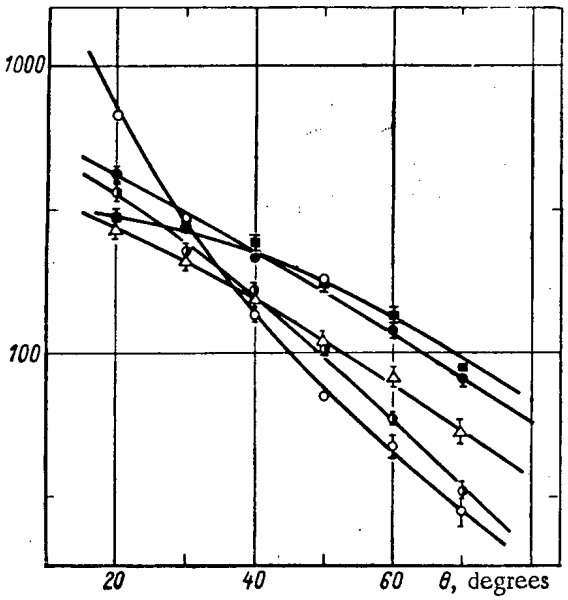

Fig. 2. Angular distributions of neutron energy groups as a function of energy, MeV. ○) 3.5-3.9; ◑) 3.0-3.5; △) 2.5-3.0; ●) 2.0-2.5; ■) 1.3-2.0.

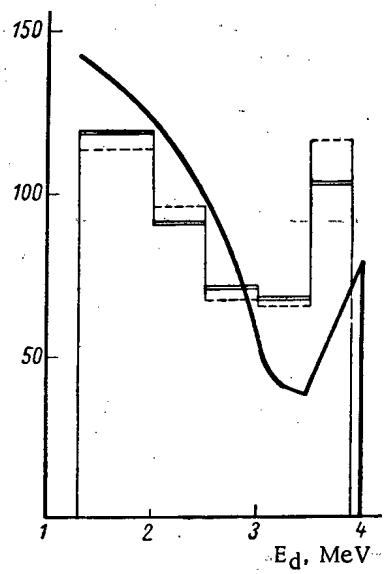

Fig. 3. Energy distribution of neutrons at graphite-water interface: ---) angle range from angular distribution; ═) energy distribution at interface; ——) theoretically predicted spectrum [3].

The energy distribution of the neutrons at the graphite-water interface, obtained by integrating the angular energy distributions over the 0-180° angular interval, appears in Fig. 3. Here the energy distribution of neutrons measured at the graphite-water interface when the spectrometer was placed in the air cavity is plotted (as histograms). All three spectra are area-normalized. The difference in the shape of the measured spectrum and the theoretically computed spectrum is due to the different geometry.

Figure 4 shows the angular distributions of the energy groups 1.3-3.9 and 3.5-3.9 MeV, and the results of calculations in an approximation of single scattering with and without taking energy losses into account. The angular dependence of the 1.3-3.9 MeV group is excellently fitted by the exponential law $\exp[-\theta/\theta_0]$ where $\theta_0 = 28.0 \pm 1.0°$.

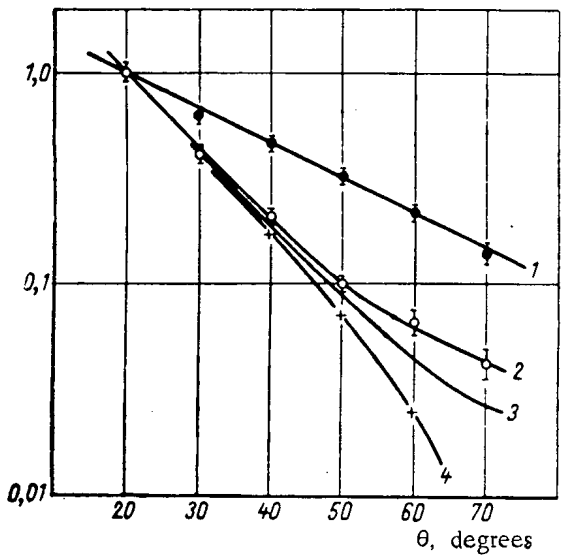

Fig. 4. Comparison of angular distributions of energy groups: 1) 1.3-3.9 MeV; 2) 3.5-3.9 MeV; 3) calculated with energy losses ignored; 4) calculated with energy losses taken into account.

Calculations based on a formula for single scattering with scattering with energy losses taken into account to 3.5 MeV for a given graphite thickness fail to coincide with experimental findings in the case of the 3.5-3.9 MeV group, attesting to an appreciable contribution of multiple scattering, even in the case of such a hard neutron group at large scattering angles. The differential scattering cross section on carbon at 3.65 MeV neutron energy was used in the calculations [4].

Calculations based on the single-scattering formula with energy losses disregarded constituted, in a certain sense, a manner of treating multiple scattering. The theoretically predicted curve was in satisfactory agreement with experimental findings.

The authors express their thanks to S. G. Tsypin for his invaluable remarks, and to N. D. Proskurnina and V. G. Dvukhsherstnov for the part they played in the work.

LITERATURE CITED

1. V. A. Dulin et al., Pribory i tekhnika éksperimenta, No. 2, 35 (1961).
2. Yu. A. Kazanskii, ibid., No. 4, 32 (1959).
3. H. Goldstein, Fundamental Aspects of Reactor Shielding, Addison-Wesley, Cambridge, Mass. (1959).
4. D. Hughes and R. Carter, Neutron Cross Section, Angular Distribution, Washington (1956).

All abbreviations of periodicals in the above bibliography are letter-by-letter transliterations of the abbreviations as given in the original Russian journal. *Some or all of this periodical literature may well be available in English translation.* A complete list of the cover-to-cover English translations appears at the back of this issue.

SLOW-NEUTRON SPECTRUM IN THE HORIZONTAL CHANNEL OF THE VVR-S REACTOR

R. V. Begzhanov, D. A. Gladyshev, S. V. Starodubtsev, and T. Khaidarov

Translated from Atomnaya Énergiya, Vol. 14, No. 5, pp. 490-491, May, 1963
Original article submitted October 25, 1962

In order to determine the neutron energy distribution at the VVR-S reactor of the Institute of Nuclear Physics of the Academy of Sciences of the Uzbek SSR, a mechanical chopper similar to one described by Mostovoi and coworkers [1] was built. The chopper rotor, 150 mm in diameter, had 13 plane-parallel slits 1 mm wide. The distance of neutron flight to reach the detector was 7.6 meters. Most of this distance was traversed through a vacuum duct 300 mm in diameter. A boron counter 35 mm in diameter was employed as detector.

A matrix type multichannel time analyzer was used for the flight velocity analysis and neutron recording. The width of the analyzer time channels could be varied from 1 to 128 microseconds; the dead time due to the use of electromechanical counters as recording components was 10 msec.

The apparatus described above was used to determine the neutron spectrum in the horizontal channel from the core outward. Measurements were performed while rotating the chopper at 1200 rpm and at channel widths 32 and 64 μsec. The selector resolution was 8.5 μsec/meter. Corrections for counting losses in distinct selector channels (as much as 10%), for the chopper transmission function (14% for λ = 1.24 Å), for absorption and scattering in aluminum 30 mm through which the beam passed (as much as 20%) were introduced into the results obtained. The last-mentioned correction was used to successfully remove the irregularity in the shape of the neutron energy distribution curve in the 4.0-4.7 Å wavelength region (Bragg cutoff wavelengths for aluminum). The neutron detector efficiency was 24% at λ_0 = 1.24 Å; the selector background was 3-4% of the effect. Corrections for the geometry of the experiment were determined mainly from the distortion of the spectrum in the beam due to absorption of thermal neutrons by nitrogen in the air traversed by the beam, over a length of 11.7 meters.

As we see from the diagram, which shows the empirically measured energy distribution of neutrons of wavelength less than 4.7 Å, the slow-neutron spectrum is described by a Maxwell distribution only in a small wavelength region, 0.75-1.5 Å, with the distribution peak occurring at λ_0 = 1.24 Å.

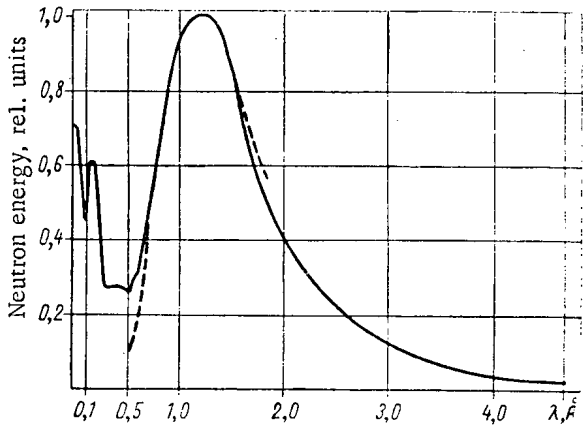

Neutron spectrum at peak reactor power (2000 kW) and at channel width 64 μsec: ——) experimental curve; ---) maximum distribution at temperature 375°K.

The slumps observed in the spectra are accounted for by resonance absorption of neutrons at certain levels of U^{238} (0.062 and 0.11 Å). A remarkable drop in neutron flux is also observed in the resonance region of U^{235} (0.268 and 0.53 Å).

The neutron spectrum in the 0.04-0.50 Å is distorted as a result of the finite selector resolution, and deviates sharply from the Fermi spectrum due to resonance capture of uranium.

The temperature of the energy distribution of neutrons found from the experimental curve at λ_0 = = 1.24 Å is 375°K at moderator temperature 308°K. Calculation of the temperature increment of the neutron gas above the temperature of the moderator medium, using the familiar relation used in [2]:

$$T_n - T_0 = 1{,}4\, T_0 \frac{\Sigma_a}{\xi \Sigma_s},$$

where $\Sigma_a/\xi\Sigma_s$ is the ratio of absorption in the medium to the moderating power of the medium, yields $T_n - T_0 = 90°K$.

LITERATURE CITED

1. V. I. Mostovoi et al., 1958 Geneva conference on peaceful uses of atomic energy.
2. G. Chernik, 1955 Geneva conference on peaceful uses of atomic energy.

All abbreviations of periodicals in the above bibliography are letter-by-letter transliterations of the abbreviations as given in the original Russian journal. *Some or all of this periodical literature may well be available in English translation.* A complete list of the cover-to-cover English translations appears at the back of this issue.

STUDY OF THE SORPTION PROPERTIES OF SILICA GEL IRRADIATED WITH NEUTRONS

V. V. Gromov and Vikt. I. Spitsyn

Translated from Atomnaya Énergiya, Vol. 14, No. 5,
pp. 491-493, May, 1963
Original article submitted June 22, 1962

When nuclear radiation acts on solids, we can observe ionization and excitation of the atoms, ions or molecules, as well as a displacement of the atoms from their places in the crystal lattice. Such phenomena on the surface of irradiated solids are particularly evident in adsorption processes [1-6]. Silica gel was selected for studying the effect of neutron irradiation on sorption processes.

In recently published studies of the sorption properties of silica gel, irradiated chiefly with gamma rays, the sorption capacity was found to increase in some cases and to decrease in others [3-6].

Silica gel dried and heated in a vacuum contains varying amounts of "structural" water, which is found mainly in the form of hydroxyl groups on the surface of the gel particles [7]. The number of these groups determines the degree of hydration of the surface, and therefore the adsorption properties of the silica gel. Dehydration causes the hydroxyl groups to split off; in some cases this increases the adsorption, while in others it decreases the sorption capacity of the silica gel, since adsorption centers of different types are formed on the surface, depending on the manner of dehydration [3, 7, 8].

We studied the variation in the sorption capacity of silica gel in an aqueous medium after it had been irradiated with neutrons and gamma quanta in a nuclear reactor. We used large-pore silica gel with a specific surface area of 370 m^2/g, determined by means of nitrogen. Before the experiments, chemical impurities were removed from the specimen by repeated washing with HCl and HNO_3 and then with water, after which it was dried at 170°C. The amount of structural water was 8.4 μmoles/m^2, and the most probable pore diameter was 80 Å. The silica gel was irradiated with a thermal neutron flux of $2 \cdot 10^{12}$ neutrons/cm^2sec. At the same time, it was subjected to about 10^7 r/h of gamma radiation, under conditions permitting the entry of air at normal atmospheric pressure. The irradiation lasted 2.1 hours in one series of experiments and 20 hours in the other. The silica gel specimens were heated in the reactor channel to about 50°C. After irradiation, Si^{31} atoms were produced, so that the specimens reached radioactivity values of up to 1.5 μCi/g. The color of the gel particles became an intense yellowish-gray and remained so for a long time at room temperautre (no change in color was observed after five months). After three or four days the radioactive isotope Si^{31} disintegrated. We did not observe any residual radioactivity from other atoms, which indicated the high degree of chemical purity of the silica gel used. Adsorption experiments were performed both with radioactive specimens and with non-radioactive specimens obtained after soaking. No differences were observed in the values of adsorption from solution.

The first part of the work was devoted to a comparison of the adsorption of Ca^{2+} by irradiated and unirradiated silica gel. One gram of sorbent in hydrogenous form at a temperature of 24°C was shaken with 25 ml of $CaCl_2$ solution (at a concentration of 0.01-0.8 g-eq/liter), containing the radioactive isotope Ca^{45}. The initial solutions had a pH of 9. Adsorption equilibrium was established after 2-3 h, but the shaking was continued for 70 h.

A number of published studies have shown the feasibility of molecular adsorption of electrolytes by silica gel [9, 10] (equivalent adsorption of anions and cations at the same time), as well as pure ion-exchange adsorption [11-13]. The decrease in the pH of the equilibrium solutions to 4, which we observed during the experiments, is a direct consequence of the ion-exchange sorption mechanism.

The value for the sorption of Ca^{2+}, determined by measuring the concentration of Ca^{2+} in the solution, was always 1.5-3 times the value found by direct determination of the radioactivity of the washed deposit. This suggests that there is "molecular" adsorption of $CaCl_2$ by silica gel. However, since determining the degree of adsorption of

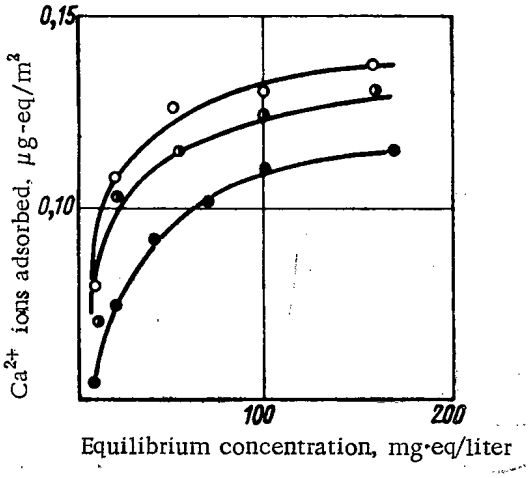

Fig. 1. Adsorption of Ca^{2+} ions by silica gel specimens: ○) not irradiated; ◑) irradiated for 2.1 h; ●) irradiated for 20 h.

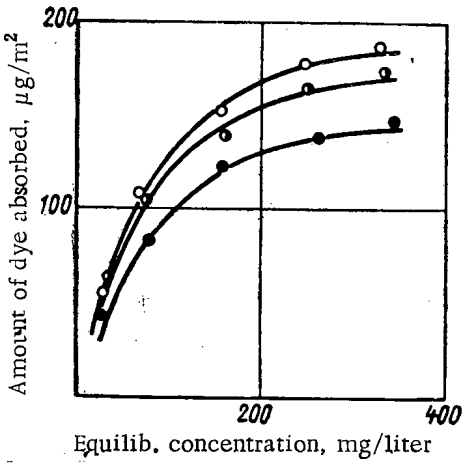

Fig. 2. Adsorption of methylene blue by silica gel specimens: ○) not irradiated; ◑) irradiated for 2.1 hours; ●) irradiated for 20 hours.

Ca^{2+} from the radioactivity of the sorbent involves large errors of up to 10-15% (as a result of the low radioactivity of the solid phase), we shall state below only the results obtained by measuring the concentration of Ca^{2+} in the liquid phase. The experimental error in this case was 4-3%. Figure 1 shows the results for the adsorption of Ca^{2+} by silica gel from aqueous solutions. As can be seen, as the irradiation time increases, there is a decrease in the capacity of the sorbent, from 13.6 to 12.8 μg-eq/m² (2.1 h of exposure) and to 11.4 μg-eq/m² (20 h of exposure).

Since the value of the sorption of Ca^{2+} by silica gel, and the variation in that value, were found to be small, we set up a second series of experiments to investigate the sorption of methylene blue by the same sorbent specimens. We used solutions with initial dye concentrations from 50 to 400 mg/liter at a pH of 6. We added 0.2 g of sorbent to 25 ml of solution. Adsorption equilibrium was reached after vigorous mixing for 18-20 h. The sorption value was calculated from the change in the dye concentration in the solution, as determined spectrophotometrically on the SF-2M apparatus. The experimental error was not more than 2-3%.

As can be seen from Fig. 2, sorption of the dye also decreases after the silica gel is irradiated with neutrons. The pH value of the equilibrium solutions decreases from 6 to 4 in this case. In addition, as can be seen from a comparison of Figs. 1 and 2, the extent to which the adsorption of methylene blue decreases is almost the same as in the case of Ca^{2+}: 0.88 and 0.84, respectively, for irradiation for 2.1 h in a reactor, and 0.77 and 0.77, respectively, after irradiation for 20 h (the sorption value of the unirradiated specimens is taken equal to unity). This indicates that the change in the silica gel surface area after irradiation by neutrons and gamma rays has an equally pronounced effect on the sorption of large organic ions and small inorganic ions. Thus, the mechanism of adorption of these ions may be considered identical.

If we explain the observed adsorption by a purely ion-excahnge type of mechanism (such an assumption is completely justified), then the entire process of the decrease in sorption capacity may be reduced to a radiative dehydration of the surface [3]. In the general case, the process of ion-exchange adsorption of cations on the silica gel surface may be written as follows [13]:

$$-\mathrm{Si}-\mathrm{OH}+\mathrm{Me}^{+} \rightleftarrows -\mathrm{Si}-\mathrm{O}-\mathrm{Me}+\mathrm{H}^{+}.$$

The pH of the equilibrium solutions is reduced because hydrogen ions are forced out into them.

In the irradiation process the $-\mathrm{Si}-\mathrm{O}-\mathrm{H}$ bonds are broken, and free radicals of the type $-\mathrm{Si}-$, $-\mathrm{S}(=\mathrm{O})-$, appear on the surface: the lifetime of these under our experimental conditions is negligibly short. The free bonds are closed, and this naturally leads to a decrease in the number of adsorption centers [7], constituted by the OH groups.

This process is equivalent to a dehydration of the surface, amounting to about 0.02 μmole/m^2 in our calculations based on the sorption of Ca^{2+} and about 0.1 μmole/m^2 in the calculation based on the adsorption of methylene blue. The above-mentioned dehydration values are much lower than those obtained by direct determination of the amount of water released when silica gel is irradiated with gamma rays [3]. This is caused by the difference in experimental conditions: in [3] adsorption from the gaseous phase was studied and a high vacuum was used. On the other hand, in our experiments we could expect to find no influence of the irradiation on the sorption [5], since a re-hydration of the surface should take place in the water. However, as can be seen from the experiments, irradiation (by neutrons, of course) leads partly to an irreversible dehydration of the silica gel. It must also be taken into consideration that the dehydration of the surface is not caused solely by the irradiation of silica gel with neutrons. Other processes, likewise leading to a decrease in adsorption, are also possible [1].

Finally, it must be remarked that within the limitations of purely adsorptive experiments it has been impossible thus far to determine with complete certainty the nature of the adsorption centers appearing as a result of irradiation.

Thus, the following conclusions may be stated:

1) We studied the effect of thermal neutrons and gamma rays from a nuclear reactor on the sorption capacity of silica gel in an aqueous medium;

2) We determined that the sorption capacity of silica gel for Ca^{2+} ions and methylene blue ions is reduced after irradiation of the sorbent in a reactor, and the longer the irradiation, the greater the decrease;

3) The observed phenomena may be explained by a partial irreversible dehydration of the silica gel as a result of neutron irradiation.

LITERATURE CITED

1. V. V. Gromov and Vikt. I. Spitsyn, Dokl. AN SSSR, 141, 891 (1961).
2. Vikt. I. Spitsyn and V. V. Gromov, Radiokhimia, 1, 181 (1959).
3. M. M. Tagieva and V. F. Kiselev, Zh. fiz. khim., 35, 1381 (1961).
4. Sh. A. Ablyaev, O. E. Ermatov, and S. V. Starodubtsev, in the book: "Proceedings of the Tashkent Conference on the Peaceful Uses of Atomic Energy," Vol. 1, Izd-vo AN UzSSR, Tashkent (1961), p. 174.
5. E. K. Vasil'eva and S. V. Starodubtsev, ibid., p. 277.
6. H. Kohn and E. Taylor, Actes du Deuxième Congrès International de Catalyse, II, 1461, Paris (1960).
7. Yu. P. Solonitsyn, Zh. fiz. khim., 32, 1241 (1958).
8. M. M. Egorov et al., ibid, p. 2624.
9. V. A. Kargin, Usp. khim., 8, 998 (1939).
10. F. Umland, Z. anorgan. und allgem. Chem., 280, 211 (1955); Z. Electrochem., 60, 689, 701, 711 (1956).
11. B. P. Nikolskii and O. N. Grigorov, Dokl. AN SSSR, 50, 325 (1945).
12. D. N. Strazhesko and G. F. Yankovskaya, Ukr. khim. zh., 25, 417 (1959).
13. H. Kautsky and H. Saukel, Z. Electrochem., 63, 355 (1959).

All abbreviations of periodicals in the above bibliography are letter-by-letter transliterations of the abbreviations as given in the original Russian journal. *Some or all of this periodical literature may well be available in English translation.* A complete list of the cover-to-cover English translations appears at the back of this issue.

INVESTIGATION OF ION EXCHANGE IN HYDROFLUORIC ACID SOLUTIONS. SEPARATION OF RaD, RaE, AND POLONIUM

M. K. Nikitin and G. S. Katykhin

Translated from Atomnaya Énergiya, Vol. 14, No. 5,
pp. 493-494, May, 1963
Original article submitted June 9, 1962

The prodedure described by Kraus [1] was used to determine under static conditions the separation coefficients K_d of lead (RaD) and bismuth (RaE) using the anionite AV-17×14. The K_d value for polonium was found from the point of peak alpha emission from a chromatographic column filled with AV-17×14 anionite. The distribution functions RaD and RaE are shown in Fig. 1. Under these conditions, $K_d > 100$ for polonium. The resulting data differ from the results obtained by Faris [2], who indicates that the anionite Dowex-1 sorbs lead from HF solutions better than it sorbs bismith.

The chromatographic separation of mixtures of RaD, RaE, and polonium has been described in a number of studies [3-9]. On the basis of the results we obtained concerning the distribution coefficients of these elements in HF (see Fig. 1), as well as in HCl [1] and in a mixture of HCl and HF [9], we suggest the following procedure for the separation of RaD, RaE, and polonium.

A polyethylene column (internal diameter 2.5-3.0 mm) is filled with the anionite AB-17×14 in the Cl^- form, in a layer about 3 cm high (resin grain diameter 20-30 μ). A radon deposit is extracted from ampoules of concentrated HCl which is diluted to 1 M before being added to the column. The final volume of the added solution should not be more than 10-15 free column volumes, since otherwise the RaD peak may be blurred. A mixture of 0.1 M HCl and 1.0 M HF washes out lead in the form of a low peak; bismuth is washed out of the column later than lead with a 20-28 M solution of HF. No alpha activity is observed from polonium in the RaD and RaE fractions, and the entire amount of polonium, firmly held by the anionite, may be washed out from the column quantitatively in the form of a narrow peak by 3 M HNO_3 (Fig. 2). Special experiments showed the complete desorption of polonium from the anionite when polonium was introduced into the column in a solution of HCl or dilute HF, the column was flushed with concentrated HF, and the polonium was washed out with 3 M HNO_3. These results do not agree with the data of I. E. Starik and N. I. Ampelogova [3], who state that polonium adsorbed by the anionite from HCL or HNO_3 cannot be desorbed quantitatively. However, it is known that fluoride complexes of polonium have fairly high

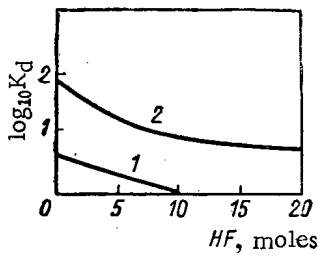

Fig. 1. Distribution coefficients K_d of lead and bismuth as functions of the HF concentration in the solution: 1) bivalent lead; 2) trivalent bismuth.

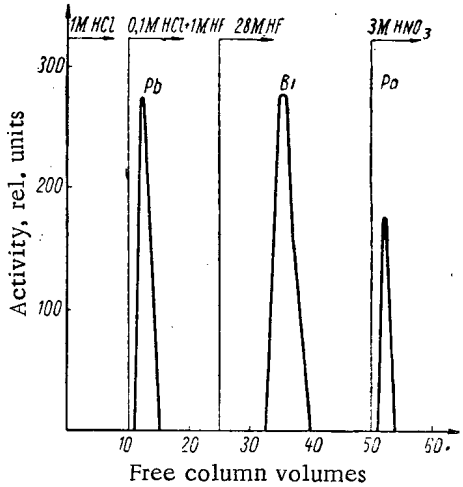

Fig. 2. Separation of Pb(RaD), Bi(RaE), and Po by the anionite AV-17.

stability [10], and if our separation scheme is used, it may be assumed that the polonium is simply dislodged from the anionite by the nitric acid in the form of undissociated fluoropolonic acid.

The beta spectra of the RaD and RaE specimens thus obtained were studied on the magnet-lens beta spectrometer using acceleration.

LITERATURE CITED

1. K. Kraus and F. Nelson, "The Chemistry of Nuclear Fuels" [Russian translation], Goskhimizdat, Moscow (1956), p. 353.
2. J. Faris, Analyt. Chem., 32, 520 (1960).
3. I. E. Starik and N. I. Ampelogova, Radiokhimiya, 3, 37 (1961).
4. P. Radhakrishna, J. Chem. phys., 51, 354 (1954).
5. J. Sasaki, Bull. Chem. Soc. Japan, 28, 89 (1955).
6. W. Dedek, Z. analyt. Chem., 173, 399 (1960).
7. F. Nelson and K. Kraus, J. Amer. Chem. Soc., 76, 5916 (1954).
8. K. Liska and L. Klir, Chem. listy, 51, 1547 (1957).
9. F. Nelson, R. Rush, and K. Kraus, J. Amer. Chem. Soc., 82, 339 (1960).
10. F. Vaigel', Usp. Khim., 29, 686 (1960).

All abbreviations of periodicals in the above bibliography are letter-by-letter transliterations of the abbreviations as given in the original Russian journal. *Some or all of this periodical literature may well be available in English translation.* A complete list of the cover-to-cover English translations appears at the back of this issue.

THE SEPARATION OF OXYGEN ISOTOPES BY THERMAL DIFFUSION

E. P. Ageev and G. M. Panchenkov

Translated from Atomnaya Énergiya, Vol. 14, No. 5,
pp. 494-496, May, 1963
Original article submitted December 25, 1962

In order to separate the isotopes of oxygen, we set up a thermal diffusion cascade consisting of three consecutively connected thermal diffusion columns with a hot wire 9 m long. The internal diameter of the three columns was 12 mm, and the hot filament consisted of a wire 0.4 mm in diameter made of a heat-resistant alloy called Kh25Yu5, having a maximum operating temperature in an air atmosphere of 1473°K. Thermosiphons were used for circulating the gas from the 15-liter reservoir into the upper part of the first column and from the lower part of each column into the upper part of the following one. Provision was made for including the first column as a gas purifier or a separating column.

Reference [1] studied the separation of oxygen isotopes by a single thermal diffusion column. The maximum separation coefficient was found at the following conditions:

Length of column, L	312 cm
Radius of column, R	0.6 cm
Radius of filament, r	0.02 cm
Temperature of cold wall, T_1	293°K
Temperature of hot wall, T_2	1153°K
System pressure, P	625 mm Hg

The basic characteristics of the separation process under the given condition are tabulated below:

Maximum separation coefficient, S_{max}	8.45
Time $t_{S_{max}}$ for which S_{max} was found	168 h
HETP	2.8 cm
Stage separation coefficient, α	1.019
Thermal diffusion factor, α_t	0.0138

To bring about complete or almost complete separation of isotope mixtures in the quickest and economically most advantageous manner, we should not use only one separation method because, as a rule, separation methods with high efficiency are found to have low throughput, while those with high throughput have low efficiency. In all probability it is most advisable to combine a high-throughput separation method with a high-efficiency method. Therefore, in order to obtain a high concentration of the oxygen isotope O^{18} we used water with heavy oxygen, which we had obtained by rectification.

Water containing 40% by weight of H_2O^{18} was electrolyzed, after which the oxygen passed into the three columns of the thermal diffusion cascade. The separation was carried out at a system pressure of 640 mm Hg and a filament temperature of 1103°K. This is somewhat lower than the maximum possible temperature, so that long-term operation is assured. The temperature of the thermosiphons at a length of 70 cm and a diameter of 0.1 cm was 633°K.

After two weeks, when the concentration of O^{18} at the output of the cascade was 94 atomic per cent, we began to withdraw the enriched product. After four months of continuous operation we had obtained more than 2 liters (converted to ordinary conditions) of oxygen containing 85 to 90 atomic per cent of O^{18}.

It is interesting to compare the efficiency of the consecutive separation of oxygen isotopes by combined rectification and thermal diffusion with the case of separation using only one of these methods. The table lists a number of studies designed to obtain by rectification or by thermal diffusion a substantial amount of oxygen with a high per-

Use of the Thermal Diffusion and Rectification Methods to Obtain the Heavy Oxygen Isotope O^{18}

Authors	Method of separation	Characteristics of equip.	Operating time	% of O^{18} obtained	Date	Ref.
Huffman, Urey	Rectification of H_2O in a rotating column	500 theoretical plates	307 h	0.85	1937	[2]
Wells	Thermal diffusion of O_2	Thermal diffusion apparatus consisting of six concentric columns with a total length of 18 m	16 weeks	14	1941	[3]
Clusius, Dickel, Becker	Thermal diffusion of O_2	Two thermal diffusion units with hot filaments having total lengths of 82 and 27 m	1.5 years	99.5	Dec. 1941, May 1943	[4-5]
Wells	Thermal diffusion of O_2	Six-stage apparatus consisting of three concentric columns and three columns with hot filament with a total length of 18 m	20 weeks	17	1946	[6]
Lauder	Thermal diffusion of O_2	Four-stage apparatus with hot filament having a total length of 16 m	24 weeks	20.2	1947	[7]
Whalley, Winter, Briscoe	Thermal diffusion of O_2	Apparatus consisting of two concentric columns with a total length of 10.9 m	—	21.9 (acc. to calc.)	1949	[8]
Dostrovsky, Llewellyn, Vromen, Gillis	Rectification of H_2O in packed column	500 theoretical plates	More than eight weeks	0.6-12(depending on withdrawal)	1952	[9, 10]
Uvarov, Sokol'skii, Zhavoronkov	Rectification of 3% H_2O^{18} in packed column	Height of packed bed 9.5 m, 976 theoretical plates	17 weeks	24.5	1956	[11]
Kuhn	Rectification of 10% H_2O^{18} in multi-tube apparatus	—	—	90	1957	[12]
Dostrovsky, Raviv	Rectification of 1.6% H_2O^{18} in packed column	Two-stage apparatus with 10 columns in first stage; first stage consisting of 450 theoretical plates, second stage of 1000 theoretical plates, HETP about 2 cm	Ten years; as the O^{18} requirement increased, the dimensions of the cascade were increased to the necessary size	95	1957	[13]

(cont'd.)

TABLE, cont'd.

Thürkauf, Narten, Kuhn	Rectification of H_2O	Five-stage cascade of rectification columns with a total length of 574.7 m. HETP value in different stages varied from 1.13 to 1.54 cm. Number of theoretical plates approximately 2500 as the reflux number $R \to \infty$	1.5 years	92	1960	[14]
Ageev, Panchenkov	Thermal diffusion of 40% O_2	Thermal diffusion apparatus with hot filament having a total length of 9 m	2 weeks	94	1960	Present study

centage of the heavy isotope O^{18}. It can be seen from the table that up to the present time an O^{18} concentration of more than 90% has been obtained by thermal diffusion only once and by rectification only three times.*

Unfortunately, the authors have no data for comparing the cost per unit of the product obtained in these experiments. We can compare only the dimensions (length) of the apparatus and the operating time if the problem is to obtain small amounts of O^{18}.

In order to obtain a concentration of 90% or more by rectification using cascades with a total length of several hundred meters (see table) about a year and a half of operating time would be required, and equilibrium would not always be reached in that time. Clusius, Dickel, and Becker [4, 5], using a cascade of thermal diffusion columns 82 m long, obtained a mixture containing 90% O_2^{18} and 10% $O^{17}O^{18}$, and only by repeated concentration in a 27-meter long apparatus for a year and a half of operation were they able to obtain 250 cm^3 of gas containing 99.5% O^{18}. On the other hand, the authors of the present article obtained the above-mentioned product by using an apparatus about 30 m long for 10 months, including the rectification process. The operation was carried out at the Stable Isotopes Laboratory of the Faculty of Chemistry of Moscow University in 1960.

In conclusion, the authors express their thanks to M. S. Antipov and G. N. Vasendo for their help in constructing the cascade.

LITERATURE CITED

1. I. A. Semiokhini et al., Zh. fiz. khim., 1, 124 (1962).
2. J. R. Huffman and H. Urey, Industr. Engng. Chem., 29, 531 (1937).
3. S. Wells, Phys. Rev., 59, 679, 920 (1941).
4. K. Clusius, G. Dickel, and E. Becker, Naturwissenschaften, 31, 210 (1943).
5. K. Clusius and G. Dickel, Z. Phys. Chem., 193, 274 (1944).
6. S. Wells, Phys. Rev., 69, 586 (1946).
7. I. Lauder, Trans. Faraday Soc., 43, 620 (1947).
8. E. Whalley, E. Winter, and H. Briscoe, Trans. Faraday Soc., 45, 1085 (1949).
9. J. Dostrovsky, D. Llewellyn, B. Vromen, and J. Gillis, J. Chem. Soc., 9, 3509 (1952).
10. J. Dostrovsky et al., J. Chem. Soc., 9, 3517 (1952).
11. O. V. Uvarov, V. A. Sokol'skii and N. M. Zhavoronkov, Khim. Prom-st', 7, 20 (1956).
12. W. Kuhn, Chem.-Ingnr-Techn., 29, No. 1, 6 (1957).
13. J. Dostrovsky and A. Raviv, Proceedings of the Symposium on Isotope Separation, Amsterdam (1957), North-Holland Publishing Company, Amsterdam (1958).
14. M. Thürkauf, A. Narten, and W. Kuhn, Helv. chem. acta, 43, 989 (1960).

* No other separation methods have been successfully used to obtain a concentration of 90% or higher of this heavy isotope of oxygen.

GAMMA RADIATION SPECTRA OF RADIOACTIVE ORES IN THEIR NATURAL STRATA, DETERMINED BY PROPORTIONAL COUNTERS

B. M. Kolesov, Yu. P. Lyubavin, and A. K. Ovchinnikov

Translated from Atomnaya Énergiya, Vol. 14, No. 5,
pp. 496-499, May, 1963
Original article submitted May 19, 1962

References [1-5] describe the results of measurements of the scintillation spectra of gamma rays from radioactive ores in their natural strata. Since the energy resolution of scintillation counters for gamma quanta with energies below 100 keV is usually no more than 30-100%, it is of interest to study the soft part of the spectrum by means of a gamma spectrometer using a proportional counter, which has a considerably better energy resolution in this range [6, 7].

The soft part of the gamma-ray spectrum of radioactive ores was measured with a single-channel spectrometer. The gamma-ray detector used was a proportional counter 200 mm long and 34 mm in diameter, filled with xenon at a pressure of two atmospheres. The cathode of the counter was a steel cylinder with walls 1 mm thick. The collecting electrode was a tungsten filament 0.1 mm in diameter. The counter was shielded by an aluminum filter with a thickness of 530 mg/cm^2. The energy resolution of this spectrometer for gamma quanta with energies below 32 keV was 12% when the source was located at the window end of the counter and 28% when the source was at the back. The resolution was evidently poorer in the second case because the small diameter of the counter introduced a considerable wall effect.

The gamma-ray spectra of the radioactive ores were studied on large models of ore deposits which reproduced the conditions of the natural strata. The ore deposit models consisted of hermetically sealed iron tanks 430 mm in diameter and 330 mm high, filled with a mixture of quartz-feldspar sand containing the radioactive elements under study, the concentration of which in each model was 0.1% in units of equivalent uranium. The ore material in the model weighed 80 kg. The central part of each tank contained a coaxial iron tube 100 mm in diameter, simulating a borehole. The tube walls were 0.35 mm in thickness. The gamma-ray spectra were measured at the center of each model. The geometric dimensions of the models and the amount of ore in them are sufficient, under these measuring conditions, for studying the shape of the spectrum of an infinite stratum in the energy range up to 120 keV [8]. In order to allow for the effect of the gamma radiation of the sandy background of the ores, we used a model of similar dimensions, containing quartz-feldspar sand with no admixture of radioactive elements.

Figure 1 shows the gamma-ray spectra of radioactive ores containing elements of the uranium-radium series. An analysis of these data shows that the measured spectrum of the gamma radiation of uranium ores under the conditions of natural strata in the energy range below 100 keV is essentially a continuous distribution with a few blurred maxima between 25 and 30 keV. This continuous spectrum is formed as a result of the processes of multiple scattering of gamma quanta in the ore or the soil [9]. Similar measurements with scintillation counters have shown that for ores of the same essential composition the measured spectrum [1-5] contains a blurred maximum between 80 and 100 keV. This difference may be explained by the special spectral characteristics of the scintillation and proportional counters. It is known that the efficiency of a scintillation counter with a 30×10-mm crystal in the energy range from 100 to 120 keV is almost 100%, while for a proportional counter of the design mentioned the range of 100%

TABLE 1. Fraction of Total Gamma Radiation of Equilibrium Uranium Ore Constituted by the Radiation of Uranium Isotopes and their Short-lived Decay Products (Th^{231}, Th^{234}, Pa^{234}).

Method of measurement	Xe proportional counter		NaI scintillation counter	
	energy range, keV	%	energy range, keV	%
Integral	>3.5	7.7	>20	4.7
Differential	60-100	12.9	80-120	7.1

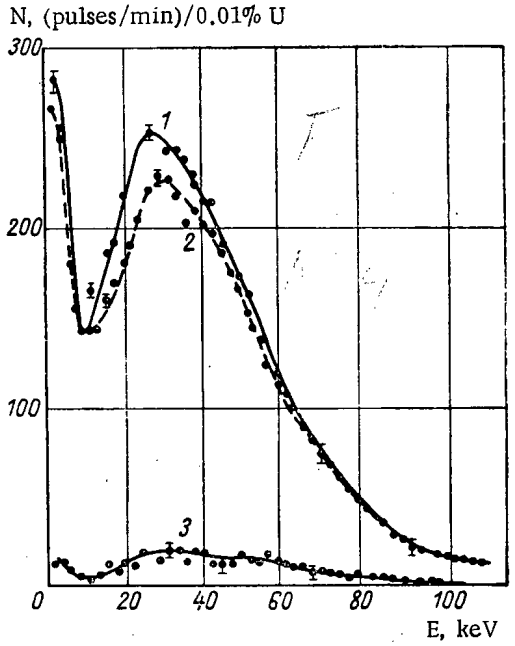

Fig. 1. Measured spectra of gamma radiation of an ore with Z_{eff} = 13: 1) equilibrium uranium ore; 2) radium ore; 3) ore containing a natural mixture of uranium isotopes and their short-lived decay products.

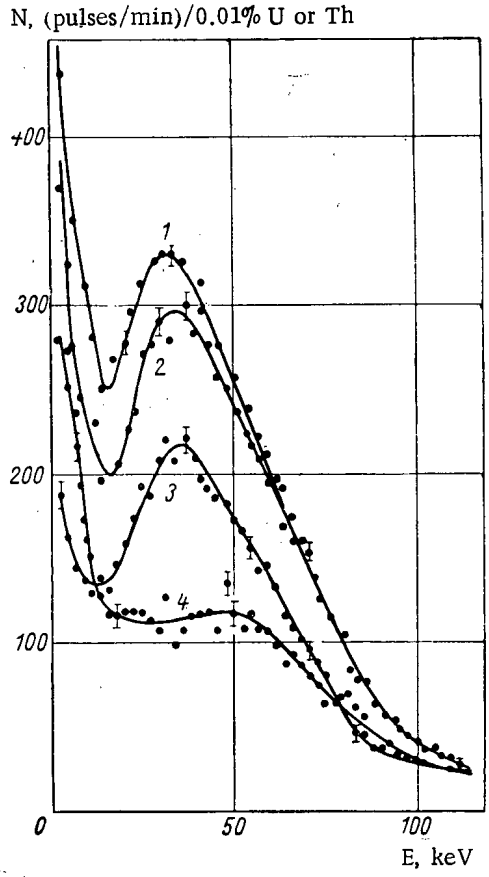

Fig. 2. Measured spectra of the gamma radiation of equilibrium uranium ore models or various essential compositions, with Z_{eff} = = 15, 27, and 17 (graphs 1, 2, and 4, respectively) and thorium ore with Z_{eff} = 15 (graph 3).

efficiency does not extend beyond 20-30 keV. As the energy of the gamma rays increases further, the recording efficiency is sharply reduced, and for gamma quanta with energies of 100 keV it is no more than a few per cent [6, 7]. For that reason, the maxiumum in the spectra shown in Fig. 1 is displaced to about the 25-30 keV range. The steep rise of the spectra in the interval up to 10 keV is apparently explainable by the influence of the wall effect and the scattering of gamma rays on the steel cathode of the counter.

The results of the measurements of the gamma-ray spectra of the ore models and a model containing only a natural mixture of uranium isotopes enabled us to find the energy range in which the part of the gamma radiation caused by uranium and the products of its decay to ionium (Th^{230}) and protactinium (Pa^{231}) constituted the maximum fraction of the total gamma radiation of equilibrium uranium ore (Table 1). In view of the fact that the weight of ore (80 kg) for which the data of Table 1 were obtained does not produce intensity saturation of the gamma rays from radium decay products at the center of the ore deposit model [8], it must be assumed that for saturated ore volumes (weight 2.5 tons) these data should be reduced by 30-40%. For ores with a different essential composition (with a different value of Z_{eff} [10]) the value of the gamma-ray intensity for the uranium isotopes may differ considerably from the data of Table 1. The increase in the relative fraction of uranium isotope gamma radiation when the measurements were made with a proportional counter is caused by the peculiarities of its spectral characteristic and its energy resolution for low gamma quantum energies, which is greater than that of a scintillation counter.

The nature of the variation in gamma-ray spectra as a function of essential composition of the ores was studied in gamma-ray saturated ore deposit models. These consisted of hermetically sealed iron tanks 1100 mm in diameter

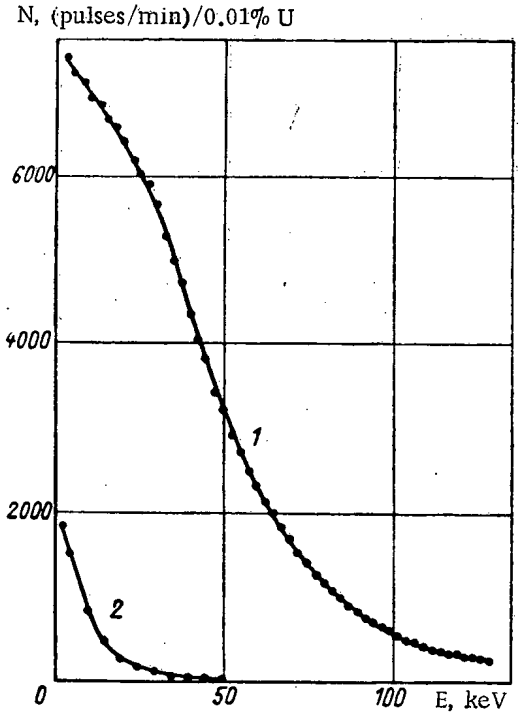

Fig. 3. The effect of a lead shield on the integral spectrum of the gamma radiation from equilibrium uranium ore in a large model: 1) with aluminum filter having a thickness of 530 mg/cm^2; 2) the same, with an additional lead filter having a thickness of 1230 mg/cm^2.

TABLE 2. Relative Values of Gamma Radiation Intensity of Equilibrium Uranium Ores of Various Compositions

Z_{eff}	Xe proportional counter	NaI scintillation counter	
	integral intensity with a threshold of 3.5 keV	integral intensity with a threshold of 20 keV	differential intensity in the 20-50 keV range
15	100	100	100
17	83	97	95
27	48	84	60

and 1000 mm high, filled with ore material. The diameter of the borehole was 100 mm. The measurement results, shown in Fig. 2 and Table 2, indicate that in the energy range below 100 keV the spectral shape and intensity of the gamma radiation of uranium ores depends considerably on the essential composition.

From the above data it follows that the proportional counter apparatus is considerably more sensitive to changes in the Z_{eff} of the ore than scintillation counters. Thus, proportional counters may be used advantageously in the study of essential composition of ores and mining soils by the methods of gamma coring and selective gamma coring of boreholes.

An analysis of the measured spectra of the gamma radiation of uranium and thorium ores with approximately equal values of Z_{eff} indicates (see Fig. 2) that no significant difference is observed in the energy composition of the radiation in the range below 100 keV.

The selective sensitivity of the proportional counters to very-low-energy gamma radiation makes it possible to use it to construct a gamma-ray meter with directional reception. The directionality of reception in this type of gamma meter is ensured by shielding the counter with a slit-type lead filter and selecting the initial threshold of gamma quantum detection. Figure 3 shows the curves of the integral gamma-ray spectra of equilibrium uranium ore at the center of a model an ore deposit model with gamma-ray intensity saturation, constructed from the data obtained by proportional counter measurements. It can be seen from the graphs that the ratio of the pulse counting rate for measurements made with the shield to the rate obtained without the shield decreases as the initial detection threshold is increased, by a factor varying from 5 (threshold 5 keV) to 200 (threshold 45 keV) and more. This absorption of gamma radiation in the lead screen is explainable by the spectral efficiency properties of the proportional counter. For comparison, we may point out that the shielding of an NaI crystal scintillation counter with a lead filter 1-5 mm thick (for any initial detection threshold) reduces the pulse counting rate by a factor of no more than 3 to 7.

Thus, the use of proportional counters with a slit-type shield enables us to obtain a high degree of directionality in the measurement of gamma radiation, combined with high efficiency, amounting to 1000-3000 pulses/min per 0.01% of equilibrium uranium (threshold 60-25 keV) for a solid angle of 2π. A directional-reception radiometer of this type records not only soft gamma rays from the ore layer near the surface, but also the soft scattered gamma radiation caused by the multiple interaction of hard gamma quanta with the atoms of the medium [9]. Because of this, the results are much more easily representable. It should be emphasized that this type of gamma meter may be used for studying the gamma-ray intensity distribution only if the gamma radiation from surrounding objects is low. This restriction is caused by the fact that the gamma meter will detect gamma quanta scattered back from the surface being tested, so that the measurement results will be distorted.

The experimental data obtained indicate that proportional counters, which have hitherto been used chiefly in nuclear physics, may be useful in geological prospecting.

LITERATURE CITED

1. A. G. Grammakov et al., In the collection: "Questions of Ore Geophysics." No. 1, Gostoptekhizdat,
2. A. G. Grammakov et al., Atomnaya Énergiya, 10, No. 6, 624 (1961).
3. Yu. P. Lyubavin and A. M. Sazonov, in the collection: "Questions of Exploratory Geophysics," No. 1, Gostoptekhizdat, Leningrad (1962), p. 85.
4. Yu. P. Lyubavin and A. K. Ovchinnikov, in the collection: "Questions of Ore Geophysics," No. 3, Gosgeoltekhizdat, Moscow (1961), p. 87.
5. S. G. Troitskii, V. L. Shashkin, and K. N. Bykova, Atomnaya Énergiya, 12, No. 1, 67 (1962).
6. B. I. Khazanov, collection: "Nuclear Spectrometry Equipment," No. 1, Atomizdat, Moscow (1960), p. 41.
7. Beta and Gamma Spectroscopy [in Russian], collection edited by K. Zigban, Fizmatgiz, Moscow (1959).
8. A. G. Grammakov et al., Atomnaya Énergiya, 11, No. 1, 69 (1961).
9. G. I. Voskoboinikov, The intensity of gamma radiation in a homogeneous radioactive medium, "Geophysical Symposium" No. 2, Sverdlovsk, Izd-vo Ural'skogo filiala AN SSSR (Publishing House of the Ural Branch of the Academy of Sciences of the USSR), (1957), p. 62.
10. I. V. Poroikov, Roentgenometry [in Russian], Gostekhizdat, Moscow-Leningrad (1950).

All abbreviations of periodicals in the above bibliography are letter-by-letter transliterations of the abbreviations as given in the original Russian journal. *Some or all of this periodical literature may well be available in English translation.* A complete list of the cover-to-cover English translations appears at the back of this issue.

GAMMA RADIATION OF ELEMENTS OF THE URANIUM AND THORIUM SERIES IN THE LOW-ENERGY RANGE

B. I. Khazanov

Translated from Atomnaya Énergiya, Vol. 14, No. 5,
pp. 499-501, May, 1963
Original article submitted August 1, 1962

Gamma-ray spectrometry is coming into increasingly wide use in the radiometric analysis of natural radioactive elements.

Until recently, gamma-ray spectrum measurements were made in the relatively hard energy range, above 200 keV, although the gamma radiation in this range is caused not by uranium and thorium but by elements located in the middle or at the end of the corresponding decay series. The development of spectrometric apparatus for measuring soft gamma rays (and X rays) has made it possible to carry out similar measurements in the 5-200 keV energy range, where the most important contribution should be the one made by just those elements which are situated at the beginning of the natural radioactive series.

The measurements were made with a scintillation spectrometer capable of recording energies up to 120 or 300 keV, and a spectrometer with a side-window proportional counter, which recorded radiation in the 5-40 keV range.

The spectra were recorded on an AI-50 multichannel analyzer. In the scintillation spectrometer, we used an FÉU-13 photomultiplier with a 30×20 mm sodium iodide crystal. The detector and the specimens to be measured were placed inside a lead shield 25 mm thick, with a cadmium-copper covering on the inside walls to attenuate the the characteristic radiation of the lead. The spectrometer had a resolution of 9% at the Cs^{137} line (E = 660 keV).

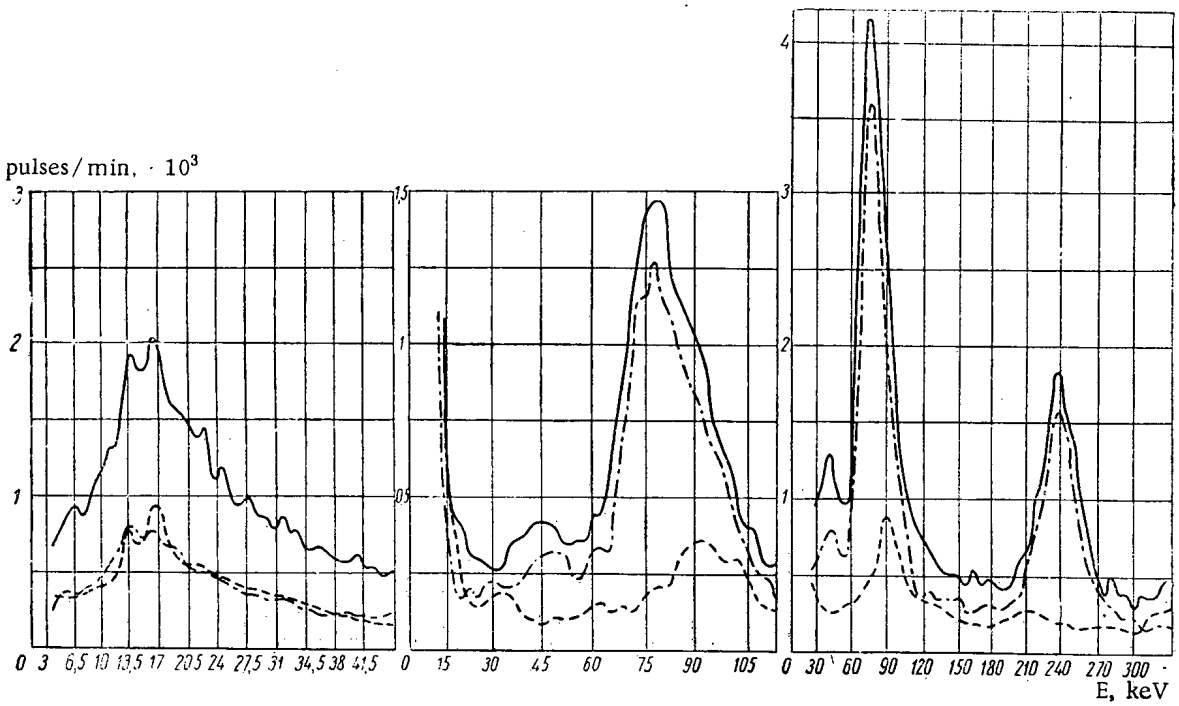

Fig. 1. Gamma-ray spectra of specimens of the thorium series: —— equilibrium thorium; -·- Th + RdTh + ThX + Tn + ThA + ThB + ThC + ThC' + ThC"; --- $MsTh_1$ + $MsTh_2$.

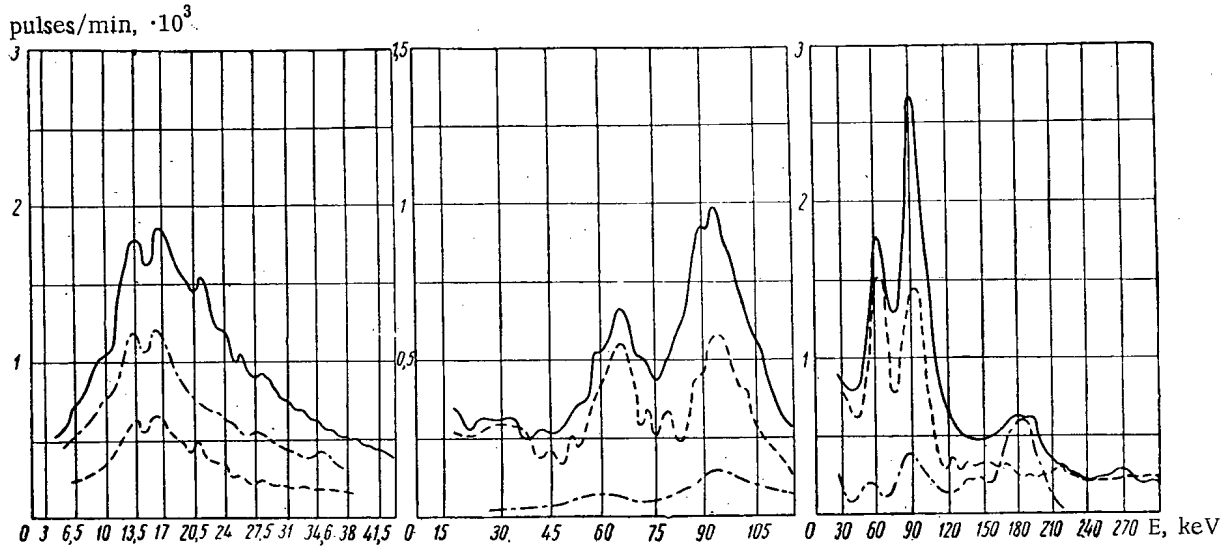

Fig. 2. Gamma-ray spectra of specimens of uranium and UX_1: U + UX_1 + UX_2; --- UX_1 + UX_2; -·- U^{238} + U^{235} + U^{234} (+ UY).

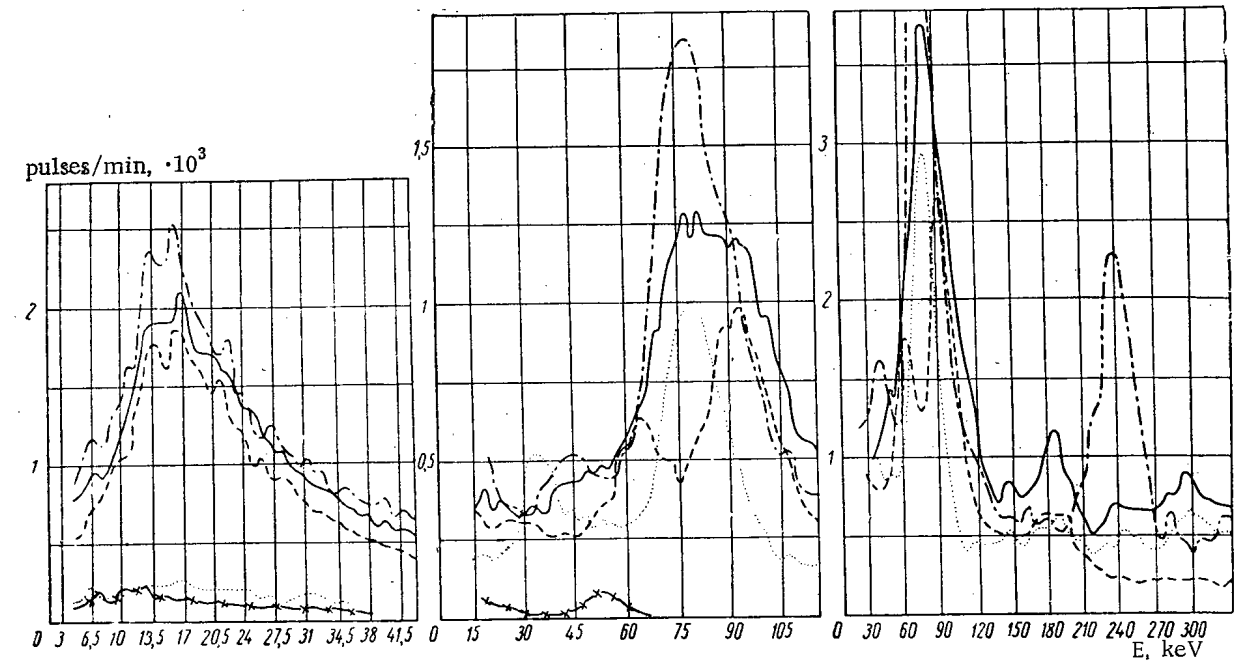

Fig. 3. Comparison of the gamma-ray spectra of equilibrium specimens of uranium, thorium, Ra-RaC", and RaD-Po: —— equilibrium uranium; -·- equilibrium thorium; ··· Ra + Rn + RaA + RaB + RaC + RaC' + RaC"; --- U + UX_1 + UX_2; -×- RaD + RaE + Po.

The low-energy spectrometer used a proportional counter 48 mm in diameter filled with xenon containing 10% isopentane at a pressure of 760 mm Hg. The mica window at the side was 12μ thick, with an area of 3 cm^2. A low-noise amplifier with an amplification factor of 2000 was connected between the counter and the amplitude analyzer. The spectrometer had a resolution of 20% at an energy of 15 keV.

In addition to the spectra of equilibrium ores of thorium and uranium, we also took spectra of individual elements separated by radiochemical means from these ores. All the specimens had approximately the same weight (0.2-0.3 g) and were placed in thin-walled holders with an area of about 1 cm^2; they were placed in the same position with respect to the detector during the measurements. The gamma radiation of specimens containing short-lived isotopes was determined immediately after the specimens were obtained. In a number of cases the gamma-ray spectra were measured repeatedly as one of the elements decayed. The measurement results were reduced to 1 g of equilibrium radium or thorium.

Figure 1 shows the spectra of elements of the thorium series. In addition to the gamma-ray spectrum of an equilibrium ore of thorium, we measured the spectra of radiochemically pure specimens of thorium (Th + RdTh) and radium ($MsTh_1$ + ThX). After 10-15 days the first specimen contained all the elements of the thorium series except for $MsTh_1$ + $MsTh_2$, and the second contained only $MsTh_1$ + $MsTh_2$. The spectrum of equilibrium thorium showed two intense lines at about 80 and 240 keV caused by ThB (quanta with E_γ = 238 keV and internal conversion quanta with E_c = 75 keV). The radiation due to $MsTh_1$ + $MsTh_2$ constitutes a relatively small fraction of the total spectrum of equilibrium thorium. The fairly intense characteristic radiation of radium (E_c = 88.4 keV) is conspicuous in the gamma-ray spectrum of $MsTh_1$ + $MsTh_2$.

Examination of the spectrum in the 10-20 keV range clearly shows the fairly intense lines corresponding to the L_α, L_β, and L_γ characteristic radiation (E = 10.5-13 keV, E = 13-16 keV, and E = 20-23 keV). An approximately equal contribution is made by the MsTh and Th + RdTh groups, together with their decay products. The intense radiation in the soft region of the spectrum, which is the characteristic radiation of the L series, indicates the considerable degree of internal conversion of a number of gamma lines in the spectrum of equilibrium thorium. A high coefficient of internal conversion is indicated, in particular, by the absence of strong lines in the 57-59 keV range.

Figure 2 shows the spectra of elements at the beginning of the uranium series: (U^{238}, U^{235}, U^{234}) + UX_1 + UX_2. We measured the gamma radiation of a specimen of uranous-uranic oxide (about 82% uranium) and of uranium and UX_1 + UX_2 specimens separated from it. In the energy range above 50 keV the gamma radiation of uranium is produced entirely by U^{235} (the 52, 93, 145, and 185 keV lines); the U_{235} lines with energies of 145 and 185 keV make the most important contribution to the total spectrum of U + UX_1 + UX_2. At the same time, for an energy of 60-90 keV the U^{235} contribution is insignificant; in this range we observe intense UX_1 lines (E = 64 keV and E = 93 keV).

In the range of the L characteristic radiation the spectrum of U + UX is similar in form to the thorium spectrum. The intensity is caused almost entirely by direct uranium radiation, which is related to the high internal conversion coefficient of the gamma radiation of U^{238} (E = 48 keV) and the high intensity of the characteristic radiation of U^{235}.

Figure 3 shows, for purposes of comparison, the spectra of equilibrium specimens of thorium, U + UX uranium (uranous-uranic oxide), radium (including the decay series to RaC' and RaC"), and RaD + RaE + Po. The wide peak of the gamma radiation of equilibrium uranium is the sum of the two maxima of the U + UX_1 + UX_2 spectrum, which have different energies, and the maximum of the radium spectrum in the 70-90 keV range. This peak in the radium spectrum is caused by the characteristic radiation of RaB (E = 74.9 keV), Ra (E = 88.4 keV), and RaC (E = 77.1 keV).

In the hardest energy range the spectrum of equilibrium uranium resembles the radium spectrum, with the exception of the 184 keV range. At this energy, as well as at 294 keV, the minimum intensity in the thorium spectrum corresponds to a maximum in the spectrum of equilibrium uranium; the situation is reversed near 240 keV. The results of measurements at these energies have been used earlier in the separation of radium and thorium*.

Finally, in the range of characteristic radiation we must note the relatively small contribution made by specimens of the radium series to the total spectrum of equilibrium uranium.

In conclusion, the author wishes to thank V. L. Shashkin for his attention and interest and A. D. Verevkin for his valuable help in making the measurements.

*P. Hyrley, Bull. Geol. Soc. Amer., 67, 395 (1956).

XIII SESSION OF THE LEARNED COUNCIL OF THE JOINT INSTITUTE FOR NUCLEAR RESEARCH

V. Biryukov and R. Lebedev

Translated from Atomnaya Énergiya, Vol. 14, No. 5, pp. 502-505, May, 1963

The XIII session of the Learned Council of the Dubna Joint Institute for Nuclear Research convened in November 1962, at Dubna.

Prior to the inauguration of the session, the members of the Council observed homage to the memory of the prominent Danish scientist and physicist Niels Bohr.

In opening the session, Director of the Institute and Corresponding Member of the USSR Academy of Sciences D. I. Blokhintsev reported to the Learned Council on the fulfillment of the resolutions adopted by the XI and XII sessions, as well as on the fulfillment of decisions arrived at by the Committee of Authorized Representatives of the Institute's member nations. The report noted that the laboratories of the Institute are conducting, alongside their regular scientific research, extensive work on the design of new large-scale physics equipment: large chambers and pure beam channels.

The Vice-Director of the Institute, Academician S. Titeica (Rumanian Peoples Republic), delivered a report on the 1962 activities and plans for 1963 in reference to collaboration between the Dubna Joint Institute and laboratories in the diverse member nations. During the past year, 12 workshop conferences were held on experimental, theoretical, and methodological investigations, including conferences held in Dresden and Warsaw. About 70 persons paid official visits to the member nations, and the reverse traffic involved some sixty-odd persons. Most of these trips were related to plans for joint work.

Collaboration between teams working with nuclear photoemulsions and films with bubble chambers at Dubna, Sofia, Budapest, Missdorf, Peking, Prague, Ulan-Bator, Alma-Ata, Warsaw, Krakow, and Bucharest, is developing successfully.

Collaboration between Joint Institute laboratories and the institutes of the member nations is carried out in the most varied divisions of science and technology: investigations of weak and strong interactions, the properties of neutron-deficient nuclides, neutron scattering in water, study of the chemical properties of mendelevium, development of multichannel analyzers, fabrication of semiconductor detectors, and many other lines. The theoretical physics laboratory is establishing liaisons with all the theoretical groups working in member nations on allied matters.

The Institute took part in several large international conferences: the Gordon conference on nuclear physics in Seattle, the Geneva conference on the physics of high-energy particles and the Geneva conference on physics experimental equipment, a symposium on semiconductor physics in Great Britain, a conference on direct interactions in Padua, and a symposium on ineleastic scattering of neutrons in solids and liquids. At all of these conferences, Joint Institute scientists delivered well-received papers.

S. Titeica also gave an account of collaboration in progress between the Dubna Joint Institute and CERN, and with the Niels Bohr Institute in Copenhagen.

The Learned Coucil approved the plans for official visits, workshops, and the plan of joint activities of the Joint Institute with research institutes in the member nations. About 16 such workshop conferences will be scheduled during 1963.

Prof. H. Barwich (German Democratic Republic), Vice-Director of the Institute, delivered a paper entitled: "Numerical composition of the scientific personnel of the Joint Institute for Nuclear Research, and staffing plans for 1963."

Administrative director V. N. Sergienko of the Institute delivered an informational report, "Execution of the 1962 budget, and budgetary plans for 1963." The Learned Council approved the report and the proposals of the administrative staff of the Institute for the incoming year.

Academician V. I. Veksler delivered a report on the activities of the High Energies Laboratory.

In the field of strong interactions, the research begun in 1961 on the (π,p)-interaction with generation of strange particles at pion momenta of 7-8 GeV/c were continued. Work was carried out on films with the use of the propane bubble chamber. The presence of two peaks in the pulsed distribution of λ°-hyperons (in the low- and high-momentum ranges) was confirmed. The significant increase in the number of events involving generation of λ°-particles enabled the authors to successfully explain the unusual behavior of the λ°-hyperons. The first peak was due to hyperons having a broad angular distribution in the CM system and in harmony with results computed from statistical theory. The second peak is due to hyperons having a sharply defined angular distribution in the CM system. This peak is explained qualitatively by the methods of diagramming, assuming that there exists a channel in which the escaping pion interacts resonantly with a virtual K-meson belonging to the shell of the nucleon. The speaker noted the fact that this is a qualitative explanation: quantitative calculations to describe such processes are still lacking. In passing, this research also provided an answer to parity conservation in the generation of λ°-particles (the answer was affirmative).

When the firms had been processed, new resonances of various combinations of elementary particles were detected: $\tilde{K}^\circ K^\circ$, $\pi\pi\gamma$, etc. Moreover, a second peak at E_γ = 250-300 MeV was detected in the gamma-ray spectrum. This was identified with radiative decay of η°-mesons.

Investigations based on photographic emulsions on the inelastic interaction of pions (7 GeV/c momentum) with nucleons, while initiated at Dubna, were continued in East Germany, Czechoslovakia, and Hungary. New data were obtained in support of the existence of two modes of inelastic interactions: the two modes are termed peripheral and central.

Proceeding to the study of the structure of nucleons, V. I. Veksler spent some time discussing two research projects: measurement of large-angle pion scattering (180°) at 3.14 and 4.6 GeV/c by means of a complex electronic channel, and measurements of elastic (p,p)- and (π,p)-scattering at very low angles (2° to 9° in the CM system) by means of nuclear emulsions. The electronic channel made it possible to single out backscattered pions. The photographic emulsions recorded recoil protons flying off from an ultrathin hydrogenous target. The recoil protons were then separated according to angle and range in correspondence with low-angle elastic (p,p)-scattering. This method made it possible to obtain statistics competing with electronic computer methods. Measurements were carried out with protons• in the 6-10 GeV energy range; these measurements enabled the investigators to unearth new information on the structure of nucleons.

Several investigative efforts were completed on weak interactions. V. I. Veksler pointed to the work of a team of Joint Institute scientists and scientists of the Physics Institute of the Academy of Sciences of the Georgian SSR. They measured the decay probability of the K_2°-meson into π^+-, π^--, and π°-mesons. They also measured the tentative value of the ratio of the probability of this decay mode and decay into three π°-mesons. This ratio provides information on the possibility of verifying the conservation of selection rules with respect to isotopic spin in weak interactions.

V. I. Veksler also reported on work associated with the design and development of new large-size physics equipment. The principal efforts were directed to the fabrication of large bubble chambers and the devising of channels of pure beams.

An entire range of important and interesting research investigations was completed during the past year in the Nuclear Problems Laboratory. Particular significance was attached to experiments devised to test the universal theory of weak interactions. Prof. V. P. Dzhelepov presented a detailed account of the discovery of beta decay of pions and measurement of the decay probability, on experimental study of a complex of mesoatomic and mesomolecular processes occurring when slow μ^--mesons are stopped in hydrogen and deuterium, and on measurements of the probability of capture of negative μ-mesons by He^3 nuclei. The results of these investigations were reported to the XII session of the Learned Council in May 1962†. During the past year, the statistics of the measurements were aug-

• In the (π,p)-scattering case, the method of perpendicular irradiation of emulsion layers described earlier applies.
† Atomnaya Énergiya, 13, No. 5, 494 (1962).

mented, and more accurate results have been secured: the rate of muon capture by the He^3 is now evaluated as $\lambda = (1.4 \pm 0.14) \cdot 10^3$ sec^{-1}.

The results of the experiments enumerated are compatible with the conclusions of the universal theory. However, because of the meager sensitivity of the total probabilities of the processes to the relationships prevailing between some constants of the theory, it cannot be confirmed at this point that these experiments actually prove the validity of the universal theory. Because of this, much interest focuses in an experiment, conducted at this laboratory, on the study of the angular distribution of neutrons from the capture of polarized μ^--mesons by Ca^{40} nuclei over a broad neutron energy range, from 6.5 to 30 MeV. These angular distributions are more sensitive to the values of the constants in the theory. It was found in the course of experiments that the asymmetry of the angular distribution increases as the neutron energy and becomes equal to unity (with 15% error) at an energy of roughly 25 MeV. Taking into account the theoretical analysis completed earlier, these data point to the nonuniversality of the weak interaction between muons and nucleons. This important conclusion impels us to carry out a more painstaking experimental verification and more detailed theoretical analysis of the phenomenon.

Several theoretical researches were completed in the laboratory. The most important of these were in the field of neutron physics.

V. P. Dzhelepov took note of the importance of experimental and theoretical research on the part of Corresponding Member of the USSR Academy of Sciences B. M. Pontecorvo in the field of weak interactions and neutrino physics, work for which the Institute recommended him for the 1963 Lenin Prize.

In the field of the study of strong interactions, physicists on the laboratory staff made use of a novel technique suggested by theoreticians on the Laboratory of Theoretical Physics staff to carry out for the first time a joint phase analysis of (n,p)- and (p,p)-scattering data, a program for which had already been compiled by the Nuclear Problems Laboratory. The broad scope of the analysis made it possible to secure a comparatively small number of solutions for energies 40, 95, 310 MeV, and, for 150 and 210 MeV, one set of phases was obtained. The value of this analysis also lies in the fact that it renders possible a stipulation of those experiments which will be required to provide a single set of phase data over a wide range of energies below the threshold. A phase analysis was also performed for experimental data on scattering of protons by protons at 660 MeV, obtained on the synchrocyclotron as a result of several years of systematic investigations. A small number of sets of phase shifts resulted.

An interesting phenomenon was discovered in a study of captures of π^--mesons by hydrogen bound chemically to various nuclei. It was found that the rate of meson capture by hydrogen falls in proportion to $z^{-3.5}$ as a result of intensive interception of pions by nuclei. (According to the Fermi-Teller capture mechanism, the capture probability must be of the order $P \sim z^{-1}$.)

Some papers presented dealt with studies of the (π,π)-interaction. The investigation of pion-nucleon collisions at energies 276 and 340 MeV was carried out with a liquid-hydrogen bubble chamber*. The most important result is the detection of an abrupt increase in the cross section of the (π^-,π^+)-interaction in a state of isotopic spin $T = 0$, beginning with energies around 350 MeV. The method of photographic emulsions was used to study the mass spectrum of the (π^+,π^-)-system in the 280-350 MeV energy region. Here, the resonance interaction of the (π,π)-system at high energies was also stressed. No ABC-resonance, of the type found earlier at Berkeley, was detected in these investigations. It has been successfully demonstrated that the American data processed in this manner likewise fail to indicate the presence of this resonance.

Studies of interaction between high-energy nucleons and atomic nuclei have also been developed further, successfully, during the past year. Experimental research is carried out in unison with theoretical physicists at the Theoretical Physics Laboratory. One striking feature in the collaboration between laboratories of the member nations of the Institute in this area is the spadework on developing new radiochemical techniques of isotope separation. Deliveries of radioisotopes produced on the synchrocyclotron have already begun to client institutions in Hungary.

Some interesting work has been completed, on the proton synchrotron, in verifying the hypothesis of the possible, anomalously great interaction between high-energy neutrinos and matter. In experiments using a hodoscopic system of counters, it was shown that no such interaction occurs as far out as cross sections of 10^{-32} cm^2.

An appreciable quantity of experimental work was completed on improving the synchrocyclotron. In early 1962, the proton beam current was successfully increased to 1.2 μA. Longitudinally and transversely polarized proton beams were both produced.

* Atomnaya Énergiya, 13, No. 5, 494 (1962).

In 1962, the laboratory gained the use of new experimental equipment. A meter-wide propane bubble chamber was set up in a magnetic field of up to 17,000 Oe strength, and a path of 5 GeV/c π^--mesons was completed in cooperation with the High Energies Laboratory. New multielectrode spark chambers were devised, and a facility for producing pulsed magnetic fields of up to 150,000 Oe intensity for irradiating emulsion chambers was successfully put into operation. Many other instruments were devised.

Significant advances were scored during 1962 by the Theoretical Physics Laboratory. The results of its activities were recounted in a report by Academician N. N. Bogolyubov.

Work was continued in developing techniques for studying the analytical properties of n-th order Feynman diagrams and perturbation theory. Success was encountered in establishing the analytical properties of partial amplitudes for diverse physical processes.

Interesting results were obtained in a study of the structure of field theory. A quasi-optical approach was developed to the description of bound and resonance states of a two-particle system. This method proved to be very effective in studying the asymptotic behavior of scattering amplitudes in quantum field theory. It has given rise to many research successes in various countries.

Investigations are underway on the theory of quantized space-time. The study of these problems is of intense interest, in that new pathways are being discovered to overcome difficulties encountered in elementary particle theory.

Theoretical physicists, backed by the mathematics section, are engaged in an ambitious program of study of peripheral nucleon-nucleon interactions. The purpose of this effort is to single out those problems an experimental study of which will contribute to improvements in the theory of peripheral interactions. From calculations already carried out, it is apparent that polar theories of peripheral interactions are inadequate to account for the available experimental evidence.

Research on the electromagnetic structure of nucleons is also moving apace.

Investigations of the general properties of the S-matrix and applications of S-matrices to various processes are being conducted in the laboratory. Limiting theorems have been postulated for inelastic processes involving the production of low-energy pions.

Theoretical researches being conducted at the Nuclear Problems Laboratory on the jumping of μ^--mesons from hydrogen to nuclei of other elements are extremely important to experimental physicists at the laboratory.

N. N. Bogolyubov reported on vital research based on the superfluid model to account for the effect of paired correlations on the probability of α-decay and on the properties of strongly deformed nuclei. He told of some interesting work on the application of Regge methods to the discussion of high-energy processes, and of some studies of the theory of vector fields describing particles of spin unity. The basic results of this work had been reported to the Learned Council in May 1962.

Several research projects were devoted to the study of symmetry in interactions and to the physics of weak interactions.

Work is continuing along a new direction in the theory of elastic scattering of heavy particles and on transfer reactions. The major interest here concerns physicists at the Nuclear Problems Laboratory.

A large volume of work has been completed at the computer mathematics section.

At the Nuclear Reactions Laboratory, physical and chemical investigations, experiments on the synthesis of transuranium elements, and advances in technique and experimentation are being carried out. These efforts were discussed by Corresponding Member of the USSR Academy of Sciences G. N. Flerov. Physicists have met with success in observing proton radioactivity of nuclei upon bombardment of nickel or aluminum targets with a beam of neon ions. It was found in the course of such experiments that the reaction may take place either on the target nucleus or on the particle itself. A theoretical analysis has revealed that the process takes the path of the transition $Ne^{17} \xrightarrow{\beta} F^{17}$, with the fluorine being formed in the excited state and emitting delayed protons.

A second run of experiments is aimed at a deeper study of processes associated with exchange of many nucleons. The results of some of these experiments have already been reported. Some new and intriguing phenomena due to exchange of 6.7 and even 8 nucleons have been detected.

Interesting studies of the spontaneously fissioning nucleus of very short half-life, discovered at this laboratory, are in progress. In experiments where various heavy targets are bombarded by beams of neon, oxygen, boron, in all cases a nucleus of half-life 0.015 sec is detected. The assumption is that this nucleus may well be Cm^{245} or Cm^{246} (the lifetime of these nuclides, obtained by conventional methods in reactors, is 10^7 years with respect to spontaneous fission). A series of searches for other spontaneously fissioning isomers is being conducted.

A significant amount of labor is being expended by physicists and chemists on the laboratory staff in the synthesis of transuranium elements. Experiments are being performed both to obtain new elements and to work out novel techniques for isolating already known substances. High intensities of cyclotron beams are making it possible to study the chemical properties of such elements as californium, fermium, and mendelevium.

G. N. Flerov gave an account of improvements in techniques, particularly with reference to the development of high-speed techniques for separating short-lived transuranium elements. A high-level ion source was successfully used to obtain septuply charged argon ions, which were then accelerated by a cyclotron.

Corresponding Member I. M. Frank of the USSR Academy of Sciences discussed work on expanding the experimental facilities and resources of the Neutron Physics Laboratory during 1962. An entire new laboratory division with experimental machine shops became operational. A huge amount of work has been achieved in improving the pulsed reactor. The laboratory boasts a set of new analyzers. Significant advances have been recorded in developing methods for multidimensional analysis of pulses. The electrostatic generator team has completed the remodeling of the generator, with peak voltage successfully raised from 1 to 2 MeV.

The speaker told of experimental investigations now being performed by laboratory staff physicists. Various techniques are being resorted to in the field of neutron spectrometry. On the one hand, measurements of total cross sections for neutron interactions with nuclei, in beam attenuation by experimental samples are involved. On the other hand, a special arrangement is being used to measure the intensity of gamma rays emitted by the samples, and partial neutron radiative capture cross sections are being measured simultaneously. In addition, a specially designed neutron detector is being used to measure partial neutron scattering cross sections. The data so obtained yield valuable information on the states of nuclei. Several of the spectra were demonstrated at the May 1962 session of the Learned Council. I. M. Frank presented the spectrum of fission cross sections for U^{235}.

As an outcome of laborious work, total cross sections for neutron interactions with terbium nuclei, scattering and capture cross sections of neutrons with praseodymium and bromine have been obtained at the laboratory. A lot of work has been completed on investigation of the states of rhodium in the energy range to 1.2 keV. The neutron width of 17 levels has been successfully measured. An interesting anomaly has been detected: instead of the expected continuous distribution of neutron widths, two kinds of levels are observed: narrow and broad levels (of the order of 10^{-5} eV and 10^{-3} eV, respectively). The reporter considered some possible ways of analyzing this phenomenon.

Various projects have been completed on the electrostatic generator as a research tool.

In the course of the session, a panel session was convened by the section of the Council concerned with low-energy physics. A survey report was read by the Chairman of the section, I. M. Frank, discussing the balance of work by conferences and colloquia, and collaborative efforts. The section approved new plans proposed for conducting new conferences and joint research projects. In particular a round of conferences on reactor physics and engineering, on the spectroscopy of neutron-deficient nuclides and the theory of the nucleus, on inelastic scattering of slow neutrons in crystals and fluids, and on other topics was scheduled.

At the concluding session, the Learned Council voiced recommendations for further development of the Institute's scientific activities.

After adopting resolutions, a ceremony was held to hand out diplomas of acknowledgment to authors awarded prizes by the Joint Institute for Nuclear Research, for the most outstanding contributions in research and research techniques.

After the proceedings of the XIII session of the Learned Council were terminated, the Committee of Authorized Representatives of the member nations of the Dubna institute met in session. Authorized representatives of 11 countries sat in on this session. Advisors of these representatives and the directing staff of the Joint Institute also took part in the deliberations.

A report to the Committee of Authorized Representatives was read by D. I. Blokhintsev, on the 1962 activities of the Institute.

V. N. Sergienko reported to the Committee on the fulfillment of the 1962 budget and on the budget, staff, and capital construction plans for 1963.

After the discussion on the plans for scientific research and development of new techniques, as well as organizational measures recommended by the session of the previous year, the Committee adopted a number of resolutions. These resolutions approved the activities of the Institute both in the field of science and development of the Institute, and in the field of the pursuance of international liaisons. The 1963 program of Institute activities was confirmed by this session. The Committee also adopted a decision to extend the term of office of Prof. H. Barwich as head of the Committee for one year.

CONFERENCE ON NUCLEAR REACTIONS ON LIGHT NUCLEI

I. V. Sizov

Translated from Atomnaya Énergiya, Vol. 14, No. 5,
p. 505, May, 1963

A conference on nuclear reactions on light nuclei was held at Dubna in December 1962.

Over 50 scientists from the member nations of the Joint Institute for Nuclear Research were in attendance; 20 papers were read. Studies of elastic and inelastic scattering of protons and deuterons on light nuclei attracted significant attention. These topics were dealt with in reports by V. V. Tokarevskii et al. (USSR), J. Kremenek (Czechoslovakia), and M. Ivascu (Rumania).

The results of experiments on elastic scattering were satisfactorily described by calculations based on the optical model. A theoretical interpretation of elastic scattering of deuterons of 13.6 MeV energy was presented in a report by L. S. Sokolov (USSR). An interesting paper was read on an investigation of proton scattering on tritium and the discovery of an excited state of He^4, by A. V. Kurepin (USSR). Phase analysis of experimental results provided the basis for the inference that experimental data support the existence of a virtual 0^+-state of He^4, with excitation energy ~20 MeV. Investigations of the properties of individual nuclear levels were the subject of papers presented by L. Kesthein and Demetra (Hungary).

E. Habanec (Czechoslovakia) and P. Neamu (Rumania) presented papers on investigations of nucleon polarization. A review of experimental data on radiative capture of protons for a large variety of nuclides, and on the structure of light nuclei, was made by S. P. Tsytko (USSR). Reports by I. B. Teplov (USSR), V. I. Man'ko (USSR), and V. I. Salatskii (USSR) dealt with studies of the mechanisms involved in nuclear reactions.

An information-packed report on the theory of direct processes was presented by I. S. Shapiro (USSR). The reporter drew attention to the possibility of interpreting the mechanism of (t,p) and (He^3,n) type nuclear reactions theoretically. The audience listened with keen interest to the papers "Some experimental problems of interest in the theory of light nuclei" (V. G. Neudachin, USSR), and "Nuclear reactions at high energies and the structure of light nuclei" (V. V. Balashov, USSR).

The conference placed great emphasis on investigations of nuclear reactions at energies ranging to hundreds of millions of electron-volts, in the further study of the structure of atomic nuclei, and pointed to the desirability of conducting suitable experiments in that energy range.

The reports heard at the conference, the ensuing discussion, and the direct exchange of views between participants, contributed to an ample exchange of results of research carried out at the various institutes represented.

CONFERENCE ON HEAVY WATER REACTORS*

Translated from Atomnaya Énergiya, Vol. 14, No. 5,
p. 506, May, 1963

An international conference and exhibit on heavy water reactors, organized by the Canadian Nuclear Association, was held in May 1962 at Ottawa, Canada. The delegates from a variety of nations numbered about 300, and 40 reports were read on engineering, costs, and physical aspects of heavy water reactors. Most of the reports were of a survey nature.

The conference dealt with two trends. Some of the sessions treated the role of nuclear power in various countries, and discussed achievements in the utilization of nuclear energy and development programs.

A second series of papers was devoted to engineering problems in harnessing nuclear energy by means of heavy water reactors. Here, the main interest centered on reports on the Canadian reactors CANDU and OCDR. The CANDU pile, now under construction, 200 MW(e), is a pressurized-tubing reactor in which the fuel elements containing natural uranium are run through the pressurized tubing. The reactor is scheduled for commissioning in 1964. At the present time, the NPD reactor, prototype of the CANDU, is being operated. The NPD rating is 19.3 MW. Unfortunately, no information was made available at the conference on the performance of this reactor.

The OCDR reactor is a variant of the CANDU, and differs from the latter in the use of organic coolant (whereas heavy water coolant is employed in the CANDU pile). Several reports treated the principal problems affecting heavy water reactors with organic coolant. The results of experiments carried out to gain experience on the prototype of the OCDR reactor, the OTR reactor now being built at Whiteshell, Manitoba, attracted particular attention. Chalk River experiments have shown that the mass transfer leading to extremely undesirable encrustations on the surface of the fuel elements depends to a large extent on the presence of traces of water (0.2-0.3%) in the organic coolant. Removal of the water by molecular filters effects something on the order of a factor-of-200 reduction in coolant contamination. It was likewise found that the danger involved in the use of zirconium alloys as fuel element cladding, connected with the hydrogenation of the zirconium immersed in an organic coolant, may be appreciably diminished by reducing the fluorine content in the alloy.

In one of the papers, a new method for controlling reactors using liquid moderator was discussed. The gist of the method is to vary the moderator density by passing a flow of air bubbles through it, thereby increasing the resonance absorption of neutrons. This control technique eliminates unproductive absorption of neutrons and leads to a higher conversion ratio.

An exhibit enjoying the participation of about 25 concerns (mostly Canadian) was open during the conference. Models of various reactors and reloading machines, and stands illustrating applications of radioisotopes in medicine and industry, were demonstrated at the exhibit. We draw attention here to a model of an original reactor, the core of which consisted of overlapping layers of fuel assemblies situated in a cubic moderator vessel. One of the advantages seen in this reactor is the possibility of equalizing energy output in all three directions and using two different coolants.

* Atomwirtschaft, 7, No. 11, 560 (1962).

SYMPOSIUM ON NEUTRON RECORDING, DOSIMETRY, AND STANDARDIZATION

V. I. Ivanov

Translated from Atomnaya Énergiya, Vol. 14, No. 5,
pp. 506-508, May, 1963

A symposium organized by IAEA was held at Harwell (Great Britain) in December 1962, with the participation of roughly 300 scientists from 30 countries and international research bodies. A total of 115 papers were read before the gathering.

The papers presented were divided into four groupings: 1) survey papers; 2) measurement of neutron field characteristics; 3) dose measurements; 4) calibration and standardization.

The first grouping includes papers dealing with organization of neutron measurements and the directions of research now being pursued at various nuclear centers throughout the world.

The second grouping takes up the greatest number of papers read at the symposium. These papers treat of two principal aspects: measurement of neutron flux levels and spectrometric measurements. Experimental techniques attracting the most attention were activation methods of measurement, apparently owing to their general popularity. Reports on activation techniques dealt primarily with problems of approach, refinements on cross sections, and attempts to devise new activation detectors. A paper by W. Zijap (Netherlands) presented data on utilization of the $Ti^{46}(n,p)Sc^{46}$ reaction to measure integrated fast flux in reactors, instead of the widely used reaction $Ni^{58}(n,p)Co^{58}$. A paper by V. Gross (Canada) also pointed to the value of using titanium in combination with other detectors. Information on a practically simple and fairly accurate method of activation of sodium and iodine, included in the composition of the NaI(Tl) scintillator, was given in a paper by B. Griemland et al. (Norway).

Reference to possible use of a "radiation element" to record neutrons was quite interesting (R. Hosemann, West Germany). Conversion of the radiation energy directly into electrical energy in the "radiation element" in response to various conditions of knock-on of charged particles from various electrodes takes place. The potential difference between electrodes, the charge on the electrodes, or the current in the interelectrode space, is measured. For electrodes 50 cm^2 in area, the thermal flux 10^{11} neutrons/cm^2·sec creates a current $\sim 10^{-8}$ A; the current produced by the same flux of fast neutrons is 10^{-9} A.

W. Farinelli (Italy) proposed determining the activity ratios of two sources emitting the same isotope in order to determine integrated neutron flux, one of the sources being activated by neutrons:

$$\int_0^T \Phi(t)\,dt = \frac{1}{\sigma} \ln \frac{r}{r'},$$

where σ is the activation cross section; r is the initial activity ratio of the sources; r' is the activity ratio of the sources after one of the sources has been irradiated for a time T.

The principal advantage in this approach is the elimination of any need for absolute measurement of activity; flux is determined by measuring the activity ratio of the two sources. Suitable isotopes for this technique are Na^{22} and Co^{58}.

Further improvements in the methods for separating neutron and gamma bursts in organic scintillators have been achieved by G. G. Doroshenko and E. L. Stolyarova (USSR). In their method, a photoelectronic multiplier is operated in a special mode of deep space-charge saturation, permitting large pulse amplitudes with small pulse width to be obtained in a simple manner; the method brings the detector load right up to $3 \cdot 10^4$ pulses/sec.

A paper by V. V. Matveev et al. (USSR) discussed the use of single lithium iodide crystals activated by europium for spectrometry of fast neutrons against an intense gamma background. The main features of this method are

the use of the same element (lithium) as detector of gamma photons and of mixed gamma-neutron emission; a different sensitivity to neutrons is gained by the different isotopic composition of the detectors (Li^6 and Li^7).

Several papers discussed the results of applications of semiconductor neutron detectors to flux measurements and to spectrometry.

The efficiency of silicon detectors placed in 3 atmos. He^3 is 10^{-5} for 3 MeV neutrons (M. Lee and M. Avecock, Great Britain); a system of two silicon diodes was used to determine the neutron energy. When measured in the thermal column of a reactor in a flux $5 \cdot 10^5$ neutrons/cm^2·sec, the resolution was found to be 100 keV for the 770 keV peak. A paper by R. Babcock and G. Chan (USA) noted that silicon carbide neutron detectors operate satisfactorily at a temperature upwards of 700°C. A small number of papers dealt with thermal methods for flux measurement and measurement of absorbed pile-neutron energies; attention was directed to the design features of thermopiles and the choice of suitable materials for work in elevated-temperature and high-flux environments.

About 25 reports were devoted to neutron dosimetry specifically. Neutron dosimetry at intermediate energies was the subject of a paper delivered by O. I. Leipunskii (USSR). Tentative calculations showed that the greatest contribution to the intermediate-neutron dose is given by neutrons in the 10^4-$5 \cdot 10^5$ eV range.

R. Hitchie and G. Hurst (USA) made an attempt to present a generalized principle of radiation dosimetry for which the Bragg-Gray rule would constitute a special case*.

The de Panger method using slowing-down of neutrons in the medium surrounding the detector underwent some further refinement. The sensitivity (18 counts/sec for 2.5 millirem/h) of the neutron dosimeter using a BF_3-counter as detector (I. Anderson and I. Braun, Sweden) is constant over the energy interval from 0.025 eV to 10 MeV; the instrument is sensitive to gamma radiation at dose rates to 50 r/h.

Indications of the possible use of semiconductor detectors in neutron dosimetry were welcomed with lively interest. At the Hanford laboratories (USA), the possibility of utilizing silicon diodes as personnel dosimeters is being seriously studied. The resistance of the diode varies linearly with a slope of ~0.2% per rad for neutrons from 0.5 to 4 MeV energy. The lowest dose measured by this dosimeter is 0.5 rad.

Several papers were devoted to the use of ionization chambers. The main achievement registered was an improvement in the familiar technique of differential ionization chambers with tissue-equivalent walls for the dosimetry of mixed neutron-gamma radiation.

B. M. Isaev (USSR) reported on experience in the use of differential ionization chambers to study depth doses of a neutron beam in the biological channel of the IRT-1000 reactor.

A new principle in the use of the ionization method was contained in a paper by N. Zel'chinskii (Dubna Joint Institute). The collection efficiency of ions in a chamber with predominantly column recombination of the ions is determined by the ionization density along the particle tracks. Since the relative biological effectiveness depends on the ionization density, a certain relationship exists between this and the ion collecting efficiency.

A paper by V. I. Ivanov (USSR) discussed a new method for employing a proportional counter of the Hurst type in the dosimetry of mixed gamma-neutron radiation, taking relative biological effectiveness into account. The idea behind this method is that pulses due to gammas will not be discarded entirely, as in the Hurst counter, but rather will be directed in another channel. The totaller at the output of the instrument records pulses due to electrons and protons arriving through different channels. Relative biological effectiveness is handled electronically by varying the signal amplitude in each channel. In papers on calibration and standardization, problems of absolute measurement of neutron flux, spectra, and doses were considered, along with accessories and devices for calibrating instruments, results of comparisons of measurements carried out at various laboratories, etc.

A paper presented by V. D. Vasil'ev, G. A. Dorofeev, et al. (USSR) reported on an interesting possibility for building a thermal neutron source for metrological work.

The results of the discussion of calibration and standardization problems reveal that matters stand at a lower level in the standardization of neutron dosimeters than in the standardization of neutron sources. In essence, problems involving standardization of neutron dosage measurements are only now arriving at the level of recognized vital scientific-engineering problems.

* The main points of this theory will be found in: Health Physics, 8, March-April, 117 (1962).

A special session devoted to discussion of terminology and basic concepts in neutron dosimetry was organized at the symposium. At this session, decisions were arrived at after a free exchange of views.

On termination of the symposium, a panel of experts on standardization of instrumentation for neutron measurements met separately. Of the Soviet delegates, V. I. Ivanov and G. A. Dorofeev participated on this panel. The principal topic of discussion was the proper siting of the projected International Center for checking neutron dosimeters. Following a proposal by J. Axier (USA), the experts agreed to organize such a center at Oak Ridge (USA).

IAEA proposes to publish the proceedings of the symposium during the first half of 1963.

BRIEF COMMUNICATIONS

Translated from Atomnaya Énergiya, Vol. 14, No. 5,
pp. 509-510, May, 1963

USSR. A radiometric technique for determinations of tungsten trioxide in various ore beneficiation products has been developed and put into practice in the A. A. Skochinskii Mining Institute and the Institute of Chemistry of the Academy of Sciences of the Tadjik SSR. It takes 10 min to determine a single dry specimen, while chemical analysis generally takes about 6 h. Measurements of tungsten content by radiometric analysis and comparison of data so obtained with results arrived at by chemical analysis display satisfactory agreement.

USSR. An Atoms for Peace exhibit sponsored by the State Committee on the Uses of Atomic Energy of the USSR has been open to the public for some time during 1963 at the Moscow Polytechnical Museum. The numerous exhibits placed in the various halls of the Museum include placards, models, operating equipment, and instruments demonstrating the development of nuclear power in the Soviet Union and the widespread utilization of atomic energy in the national economy.

The introductory section of the exhibit was devoted to the fundamentals of nuclear reactors. The structure of the atom, chain reactions, and methods for harnessing atomic energy were displayed here. In the section of nuclear power, visitors to the exposition became familiarized with the design of reactors, the layout and operating models of reactor electric power generating stations. In one of the exhibit sections, the avenues and present status of research and development work on controlled fusion were revealed. A special section was devoted to shielding techniques used in handling radiation sources and radioisotopes. Visitors manifested keen interest in those exhibits providing information on the widespread use of radioactive isotopes in industry, agriculture, biology, and medicine.

USSR. The Soviet Union is delivering 10%-enriched U^{235} fuel elements to Finland for use in the critical assemblies of the Institute of Technology at Otaniemi. Deliveries are routed though the offices of IAEA.

Libya. At the traditional fair held in Tripoli, the Soviet pavilion displayed its achievements in the field of the uses of atomic energy. Visitors became acquainted with models of nuclear power stations, experimental and testing reactors, instrumentation for prospecting and exploration of uraniferous ores, etc.

Poland. At the Institute of Nuclear Physics (Krakow), a cyclotron (pole tip diameter 150 cm) has been developed, modeled on the Soviet U-150 accelerator. The use of space modulation of the magnetic field renders this cyclotron suitable, it is hoped, to the task of accelerating protons to relativistic energies, and accelerating heavy ions.

Already in operation at the Institute are a cyclotron (48 cm pole tip diameter) built by the Institute staff itself, and a cyclotron acquired in the USSR (120 cm pole tip diameter), a U-120 machine.

Poland. An electronic counter has been designed at the Institute of Electronics. One of the circuits in this counter is capable of recording pulses at a pulse repetition rate higher than 300,000 pulses/sec, another circuit doing better than 3 million pulses/sec.

Poland. At the Institute of Nuclear Engineering in Krakow, an X-ray technique has been elaborated for industrial analysis of zinc-lead ore using beta emitters. Ore samples are first irradiated in a flux of beta particles. Analysis of the bremsstrahlung spectrum permits technicians to make a foolproof determination of lead and zinc content in the ore. Analysis time is thereby shortened from several h to 10-15 min.

Yugoslavia. At Zagreb, a 16 MW cyclotron, largest in the country, has been commissioned. The magnet weighs 70 tons. The machine was installed in an underground room shielded by thick concrete walls. The cyclotron's function will be primarily that of producing radioactive isotopes.

SYNTHESIS OF A NEW ISOTOPE OF ELEMENT 102

Translated from Atomnaya Énergiya, Vol. 14, No. 5,
p. 510, May, 1963

At the Nuclear Reactions Laboratory of the Joint Institute for Nuclear Research, a new isotope of the element 102, having mass number 256, has been successfully synthesized. It was found that 102^{256} is α-active and has a half-life of ~8 sec.

Synthesis was accomplished in the $U^{238}(Ne^{22},4n)102^{256}$ reaction, and 102^{256} was identified by its daughter Fm^{252}. The procedure followed in the experiment was to make a reliable separation of Fm^{252} nuclei, as α-decay products of element 102, from all other products of the nuclear reactions involved. This was achieved by using a special separator with collection of recoil nuclei after the α-decay by an electric field established in a gas, and following through with ion exchange and a high-resolution α-spectrometer. Ample control experiments confirmed the reliability of this approach.

Experiments were conducted on the internal beam of multiply charged ions in a cyclotron. The high intensity of the beam of Ne^{22} ions made it possible to record hundreds of 102^{256} nuclei in each experiment, despite the exceedingly small cross section of the reaction in question, $4.5 \cdot 10^{-32}$ cm^2 at its very maximum. The large number of 102^{256} nuclei obtained provided for a reliable investigation of the element's properties and of the nature of the synthesis. In particular, we found the half-life of 102^{256} by spontaneous fission to be many tens of times longer than that expected from experimental and theoretical investigations into the properties of the element 102 carried out at the Lawrence Radiation Laboratory of the University of California.

This work was carried out by E. D. Donets, V. A. Shchegolev, and V. A. Ermakov under the supervision of Corresponding Member of the USSR Academy of Sciences G. N. Flerov.

BIBLIOGRAPHY

NEW LITERATURE

Recent Atomizdat Publications

B. N. Tarusov. Pervichnye protsessy luchevogo porazheniya [Primary radiation injury processes]. 1962. 96 pages, 30 kopeks.

This book takes up the primary radiochemical reactions occurring in response to exposure of the organism to ionizing radiations. The first chapter deals with the theory of targets, the second and third chapters describe radiochemical processes occurring in biosubstrates, and investigate means for inhibiting radiation injury reactions, e.g., the oxygen effect and chemical protection. The last two chapters are devoted to primary reactions of sequela and the effect of primary radiochemical reactions on the radiosensitivity of the organism.

Lists of pertinent literature follow each separate chapter.

Mekhanizmy radiobiologicheskogo effekta (Mnogokletochnye organizmy). [Radiobiological effects mechanisms (multicellular organisms)]. Edited by M. Arrer and A. Forsberg. Translated from the English. 1962. 316 pages, 2 rubles, 13 kopeks.

This item is a five-chapter book written by a panel of authors. It discusses radiation effects on embryos and on adult organisms, principally mammals. Special chapters deal with immunological processes in the exposed organism, the mechanism of the effect of protectant and sensitizing media, and recovery processes. Therapy of radiation injury in biological experiments is discussed.

Each chapter ends with a bibliography.

Publications from Elsewhere

D. D. Kalafati. Termodinamicheskie tsikly atomnykh élektrostantsii [Thermodynamical cycles of reactor power stations]. Moscow-Leningrad, State Power Press (Gosénergoizdat), 1963, 280 pages.

This monograph subjects to theoretical analysis many of the aspects of the thermodynamical cycles of reactor power stations incorporating various reactor types. Thermodynamics problems related to the practical design of nuclear electric power stations are broached: power cycles, criteria for evaluating their degree of perfection, reaching peak power, etc.

The first chapter takes up the operating conditions of reactor electric power stations; the second determines the conditions for optimizing thermodynamical cycles when reactor thermal power is varied; the third estimates the effect of the reactor temperature characteristics on the choice of optimum cycle parameters; the fourth chapter deals with heat transfer; the fifth takes up an analysis of the effect of regenerative water heating; the sixth to the ninth chapters consider the thermodynamical cycles of nuclear electric power stations using water (steam), organic, liquid-metal, and gas coolants, respectively. An analysis is carried out with due attention to the conditions governing cost economy in the operation of nuclear power stations.

Plutonii-239 [Plutonium-239], raspredelenie, biologicheskoe deistvie, uskorenie vyvedeniya [distribution, biological effects, and rapid isolation of]. Edited by A. V. Lebedinskii and Yu. I. Moskalev. Moscow, Medgiz, 1962, 168 pages.

This symposium contains papers by Soviet scientists on various aspects of the biological effects of one of the most radiation-hazardous α-active isotopes, Pu^{239}.

The basic problems of plutonium toxicology, distribution patterns and the isolation of this element in various types of animals, in particular the course run by radiation sickness in affected animals, the effects of α-exposure by incorporated plutonium on blood circulation, liver function, bone tissue metabolism, are among the topics discussed in detail.

In addition to an analysis of standard compounds, the distribution pattern and the biological effects of new plutonium compounds are cited. Worthy of special interest are some experimental data on the relationship between Pu^{239} distribution and the type of animal.

ARTICLES FROM THE PERIODICAL LITERATURE

I. NUCLEAR PHYSICS

Neutron Physics and Reactor Physics. Physics of Hot Plasma and Controlled Fusion. Physics of Charged-Particle Acceleration.

Vestnik akad. nauk SSSR, No. 1 (1963)

S. M. Ryvkin, 56-58. Semiconductor particle counters.

Doklady akad. nauk SSSR, 146, No. 6 (1962)

L. A. Artsimovich and K. B. Kartashev, 1305-1308. Effect of a transverse magnetic field on a toroidal discharge.

Zhur. tekhn. fiz., 33, No. 1 (1963)

V. E. Golant, 3-18. Diffusion of charged plasma particles in a strong magnetic field affecting particle collisions.

V. A. Ankudinov et al., 19-27. Acceleration of charged particles by periodically time-varied magnetic fields.

A. N. Didenko and E. S. Kovalenko, 28-33. Note on the choice of frequency for high-energy cyclic accelerators.

V. I. Pakhomov and K. N. Stepanov, 43-50. On emission by an electron moving on a spiral in a magnetoactive plasma. II.

É. A. Pashitskii, 51-57. On an electron beam-plasma interaction in a magnetic field. I. "Longitudinal" oscillations.

É. A. Pashitskii, 58-64. On an electron beam-plasma interaction in a magnetic field. II. "Transverse" oscillations.

E. A. Bamberg and S. V. Dresvin, 65-72. Determination of various parameters of a high-frequency annular discharge.

V. S. Erofeev and Yu. V. Sanochkin, 73-79. Some aspects of the magnetogasdynamics of a quasi-one-dimensional plasma flow. II.

E. S. Borovik et al., 100-104. Investigation of the possible application of a helium condensation pump to pump out magnetic traps.

S. V. Iordanskii, 105-114. On resonance excitation of waves in an infinitely conducting fluid.

Zhur. éksptl. i teoret. fiz., 44, No. 1 (1963)

L. É. Gurevich and V. I. Vladimirov, 166-176. Kinetic properties of a rarefied plasma with high radiation pressure, and effects of mutual attraction of electrons and photons.

A. A. Kolomenskii and A. N. Lebedev, 261-269. Resonance phenomena in the motion of particles in a plane electromagnetic wave.

Izvestiya vyssh. ucheb. zaved. Radiofizika, 5, No. 5 (1962)

V. N. Lugovoi, 901-907. Propagation of plane electromagnetic waves in a periodically nonstationary magnetoactive plasma.

Trudy inst. metallurgii im. Baikova, No. 10 (1962)

L. N. Bystrov et al., 209-214. Spray-on of radioactive coats.

Energia Nucleare, 9, No. 12 (1962)

M. Corazza et al., 690-693. Sensitivity of ion chambers to pulsed gamma radiation.

U. Facchini, 699-708. Latest results in nuclear reaction studies.

J. Appl. Phys., 33, No. 12 (1962)

C. Sanathanan, 3491-3498. Optimization of efficiency of a cesium direct converter.

M. Dunn and A. Maitland, 3598-3599. Extracting energy from a Carnot engine using a gas ionized by thermal neutrons as working fluid.

Kernenergie, 5, No. 10/11 (1962)

L. Funke et al., 734-746. Iron-free double-lens magnetic beta spectrometer measures beta, gamma-coincidences.

E. Johannes, 747-752. Logarithmic reading count rate meter.

Kerntechnik, 4, No. 10 (1962)

W. Schwertführer, 447-448. Method for determining the energy spectrum of ion emission from accelerators.

Kerntechnik, 4, No. 12 (1962)

Experiments on controlled fusion.

Nucl. Instrum. and Methods, 17, No. 3 (1962)

J. Monahan et al., 225-230. Measurement of lifetimes of radioactive sources.

S. Svennerstedt et al., 231-247. Magnetic field and temperature measurements in a toroidal pinch.

Nucleonics, 20, No. 12 (1962)

M. Okada, 61-62. 14 gamma spectra of short-lived nuclides.

Nucleonics, 21, No. 1 (1963)

S. Gorbics et al., 63-67. New values for half-lives of Cs^{137} and Co^{60} nuclides.

Nuovo Cimento, 26, No. 6 (1962)

A. Caruso and A. Cavaliere, 1389-1404. Structure of a transitional collision-free plasma layer.

Physics of Fluids, 5, No. 10 (1962)

F. Fishman and H. Petschek, 1188-1195. Departure of performance of an annular magnetic shock tube from the one-dimensional model.

W. Powers and R. Patrick, 1196-1206. Magnetic annular arc.

R. Jain and K. Metha, 1207-1211. Laminar magnetohydrodynamic flow in an annular porous-walled region.

B. Tanenbaum and D. Mintzer, 1226-1236. Propagation of waves in a partially ionized gas.

R. Lewis and J. Keller, 1248-1263. Conductivity tensor and dispersion equation for a plasma.

S. Ichimaru, 1264-1271. Wave properties of a plasma with a two-humped velocity distribution.

S. Yoshikawa, 1272-1276. Electrical conductivity of a turbulent plasma.

A. Futch et al., 1277-1287. Formation of a plasma in the injection of neutral ions.

T. Falk and D. Turcotte, 1288-1292. Diffusion of a current sheath in a one-dimensional pinch.

K. Uo et al., 1293-1300. Experiments on confinement of a plasma in the magnetic field of the Helitron B machine.

P. Ramamoorthy, 1302-1304. Equations of a laminar boundary layer at small magnetic Reynolds numbers.

T. Sakurai, 1304-1305. Gravity waves of a conducting field in a horizontal magnetic field.

W. Bostick et al., 1305-1307. Interaction between a plasma and a two-dimensional magnetic field.

O. Eldridge and M. Feix, 1307-1308. Fokker-Planck coefficient for a one-dimensional plasma.

F. Robben, 1308-1309. Nonequilibrium ionization in a magnetohydrodynamic generator.

Plasma Phys., 4, No. 5 (1962)

T. Fowler and M. Rankin, 311-320. Plasma potential and energy distribution in high-energy particle injection facilities.

J. Wesson, 321-324. Ohmic heating of a multicomponent plasma.

B. Liley, 325-328. Generalization of the sufficient condition for magnetohydrodynamic stability.

P. Weissglas, 329-336. Longitudinal plasma oscillations.

J. Wilcox, 337-340. Structures for producing a highly ionized hydrogen plasma.

R. Medford et al., 341-346. Longitudinal shock waves in inverse pinch geometry.

D. Ben Daniel and H. Hurwitz, 347-352. Conditions for matching solutions at gradual plasma boundaries.

D. Wort, 353-358. Emission of microwave noise by a plasma.

Rev. Sci. I., 33, No. 11 (1962)

R. Lowder and F. Hoh, 1236-1238. Rapid-action valve for supplying gas in plasma research.

The 7 GeV proton synchrotron

The fourth issue of Pribory i tekhnika éksperimenta, 1962, is entirely devoted to papers relating to the construction of the 7 GeV proton synchrotron. The issue contains 48 articles. These provide information on the design of the proton synchrotron, its basic parameters, the programmed frequency control system, the design of the electromagnet and the electrical supplies system, the electronic systems, the vacuum chamber, and the proton injection system. Several papers concern the tuning-up of the machine.

Conference on AVF cyclotrons

The proceedings of the international conference on azimuthally varied field cyclotrons (Los Angeles, April 17-20, 1962) were published in the November issue of Nuclear Instruments and Methods, vols. 18, 19 for 1962.

77 papers presented at the conference are grouped under ten headings: I. Performance and design of AVF cyclotrons; II. Magnetic fields; III. Radio-frequency systems; IV. Theory of orbits; V. Computer programs; VI. Central region of various cyclotron types; VII. Pion-energy accelerators; VIII. Beam extraction techniques; IX. Mechanical components and parts; X. Miscellaneous topics.

II. NUCLEAR POWER ENGINEERING

Nuclear Reactor Theory and Calculations. Reactor Design. Performance of Reactors and Reactor Power Stations.

Zhur. tekhn. fiz., 33, No. 1 (1963)

A. G. Ryabinin and A. I. Khozhainov, 80-89. Turbulent flow of an electrically conducting fluid in tubes of rectangular cross section in response to electrodynamic motive forces.

Zhur. éksptl. i teoret. fiz., 44, No. 1 (1963)

A. T. Bakov et al., 3-9. Comparison of gamma-ray spectra of radiative capture of thermal and fast neutrons.

Inzhener.-fiz. zhur., 6, No. 1 (1963)

I. G. Morozov et al., 72-78. Kinetics of a reactor with linearly varying reactivity.

Teploénergetika, No. 12 (1962)

S. L. Rivkin and B. N. Egorov, 60-63. Experimental investigation of specific heat of heavy water in the supercritical region of parameters of state.

N. B. Vargaftik and O. N. Oleshchuk, 64-66. Thermal conductivity of heavy water vapor.

Trudy inst. énergetiki akad. nauk Gruz. SSR, 16 (1962)

V. I. Gomelauri et al., 101-112. Experimental study of heat transfer in the fuel assembly of the IRT research reactor.

Atomic Energy, 5, No. 4 (1962)

A. Marks, 9-22. The MOATA reactor of the Australian AEC.

Chem. and Process Engng., 43, No. 12 (1962)

P. Blacker and D. Melain, 630-633. Heat transfer coefficient and temperature gradients in fluidized beds.

Énergie nucléaire, 4, No. 6 (1962)

P. Huet, 389-395. Costs outlook for exploitation of nuclear power.

B. Goldschmidt, 411-419. French nuclear energy development program.

G. Combet, 420-423. Role of French industry in the development of nuclear power.

W. Cartellieri, 424-427. West Germany nuclear power development program.

E. Reuter, 428-436. Reactor design in West Germany.

R. Stahl, 437-441. Nuclear power in Austria.

L. Heem, 442-444. Nuclear power in Belgium.

M. Koch, 445-448. The Danish Atomic Energy Commission.

O. Navascués, 449-451. The Spanish nuclear power development program.

F. Ippolito, 452-469. Experience in nuclear power in Italy.

G. Randers, 470-473. Nuclear power practice in Norway.

R. Dee, 474-479. Nuclear power in the Netherlands.

R. Makins, 484-500. Nuclear power in Great Britain.

H. Brynielsson, 500-504. Nuclear power in Sweden.

E. Choisy, 505-509. Switzerland and nuclear power.

Y. Sousselier, 510-516. Review of the activities of the Eurochemik consortium.

P. Marien, 517-534. Design of the DRAGON reactor.

ibid., 445-462. Tables of research reactors, reactor electric power stations, and atomic industry plants.

Énergie nucléaire, 4, No. 7 (1962)

M. Dardare and M. Lyon, 582-588. Control and operation of the Chinon reactor power station.

Engineer, 215, No. 5580 (1963)

R. Strickland, 14-15. Review of nuclear power development in 1962.

Engineer, 215, No. 5582 (1963)

ibid., 154-58. Review of nuclear power development over the past two decades.

Engineer, 215, No. 5583 (1963)

ibid., 213-214. Experimental plutonium-fueled breeder reactor.

Kernenergie, 5, No. 12 (1962)

H. Röllig, 809-824. Compatibility of ceramic fuel with cladding materials and metallic matrix elements.

H. Kiesewetter and H. Marbach, 824-829. Burnup in a continuously loaded cylindrical reactor.

C. Polze, 829-831. On the direct solution of some difference equations in diffusion theory.

G. Ruickoldt, 831-839. Spectrum of fast collimated neutrons from the Rossendorf reactor, and variation of spectrum in passage through a layer of water.

P. Morzek, 839-845. Activation analysis errors due to self-absorption and deformation of flux.

Kerntechnik, 4, No. 10 (1962)

R. Gain, 449-452. Design of graphite in-pile irradiation capsules.

Kerntechnik, 4, No. 12 (1962)

W. Hanle, 537-540. Nuclear engineering in Western Europe.

M. Pollermann, 541-552. Research reactors in Western Europe.

R. Boedege, 553-562. Power reactors in Western Europe.

H. Adam, 587-592. Training personnel for nuclear engineering functions in Western Europe.

K. Diebner, 596-600. Nuclear engineering in Western Europe.

Nucl. Energy, January (1963)

W. Curtis, 4-11, 14-16. Development of master-slave manipulators.

J. Baxter, 22-23. The Australian AEC research center.

Nucl. Engng., 8, No. 81 (1963)

H. Coles, 58-63. Plans for a steam-cooled water-moderated maritime reactor.

H. Young, 64-69. Fuel reloading in action at the EGCR reactor.

Nucl. Sci. and Engng., 14, No. 3 (1962)

E. Starr and J. Koppel, 224-229. Determination of the diffusional increment in the hardness of neutron spectra in water.

W. Rothenstein and J. Helholtz, 239-43. Dancoff correction in void geometry.

J. Ferziger, 244-248. Resonance absorption of neutrons in slugs of uneven temperature distribution.

J. Beeler, 254-265. Diffusion anisotropy in periodic lattices.

H. Garabedian and D. Thomas, 266-271. Analytical method for solving two-group diffusion equations.

A. Nahvandi, 272-286. Computer-based study of damage to a nuclear power installation as a result of blockage of coolant flow.

C. Griffin, 304-311. Study of the power coefficient of reactivity for a sodium reactor.

A. Kirchenmayer, 312-314. Dependence of effective resonance integral on the properties of the moderator.

A. Claesson, 314-316. Theory of neutron transport, accounting for high-energy sources.

B. Arcipiani et al., 316-317. Measurement of cadmium ratio for U^{238}.

Nucleonics, 21, No. 1 (1963)

V. Ajdacic et al., 60-62. Measuring in-core neutron fluxes with semiconductors.

H. Schlein, 70-71. Digital monitor checks reactor-flow ratios.

Nucleonics, 21, No. 2 (1963)

D. McLaughlin, 36-41. Effect of neutron fluxes on embrittlement of carbon steel reactor pressure vessels.

M. Hunter, 42-45. Nuclear-powered spaceships.

B. Raab, 46-47. Use of spaceship reactor shield as energy source.

D. Thompson, 60. Experience with the Brookhaven graphite reactor.

Nukleonik, 4, No. 8 (1962)

E. Hellstrand and G. Lundgren, 323-326. The niobium resonance integral.

W. Eichelberger, 326-331. Effect of the chemical bond on slowing-down of neutrons in heavy water.

P. Schmid, 331-347. Simplified treatment of reactor kinetics in safety evaluations.

T. Gozani, 348-349. Modified approach to evaluation of experiments using a pulsed source in a subcritical reactor.

Nukleonika, 7, No. 11 (1962)

Z. Szoda, 681-691. Numerical-graphical technique determines reactor critical mass when diffusion coefficient is anisotropic.

Reactor Sci. and Technol., 16, No. 10 (1963)

J. Barry, 467-472. Cross section of $Ni^{58}(n,p)Co^{58}$ reaction for 1.6-14.7 MeV neutrons.

Rev. Sci. I., 33, No. 11 (1962)

J. Gray and F. Hagemann, 1258-1264. Thermal neutron counter for nuclear and analytical measurements.

Technical Digest, 5, No. 11 (1962)

J. Becvár, 3-7. Gas turbines in nuclear power practice.

Technical Digest, 5, No. 1 (1963)

F. Vozenilek, 41-45. Continuous pH and conductivity measurements of distilled water in the primary loop of the Czechoslovak nuclear reactor.

III. NUCLEAR FUELS AND MATERIALS

Nuclear Geology and Primary Ore Technology. Nuclear Metallurgy and Secondary Ore Technology. Chemistry of Nuclear Materials.

Azerbaidzh. neft. khoz., No. 11 (1962)

I. A. Mamedov and A. A. Émirdzhanova, 40-42. Arsenato-iodometric determination of uranium.

Vestnik Mosk. univ., seriya 2, Khimiya, No. 5 (1962)

I. P. Alimarin et al., 50-54. Study of the uranium (IV)-uranium(III) system.

Vikt. I. Spitsyn et al., 60-62. Study of mixed sodium and potassium uranates.

Wang Shih-hua and L. M. Kovba, 63-65. Hydrogen reduction of uranyl vanadates.

Voprosy razved. geofiziki, No. 2 (1962)

V. A. Zolotnitskii et al., 24-28. Mass absorption coefficient of gamma emission of radioactive ores.

N. A. Voroshilov, 87-92. Note on analysis of uranium in geochemical prospecting.

I. M. Khaikovich and V. M. Bondarev, 105-117. On geometry in the measurements of gamma-sampled uranium ores in place by the difference effect.

O. D. Gorbunov, 166-168. Example of the development of secondary scattering halos of lead, molybdenum, and uranium in rocky or meadow terrain.

Zhur. anal. khim., 17, No. 6 (1962)

V. D. Ponomarev and I. V. Tananaev, 718-720. Composition of uranyl ferrocyanides forming in the presence of organic solvents.

Zhur. neorg. khim., 7, No. 11 (1962)

N. N. Elovskikh and K. T. Rumyantseva, 2639-2640. Mixed ammonium-sodium uranyl and uranium(IV) oxalate complexes.

Zhur. strukturn. khim., 3, No. 5 (1962)

R. T. Golovatenko and O. Ya. Samoilov, 529-535. Temperature dependence of partition coefficients in solvent extraction of uranyl nitrate from aqueous solutions.

Zavod. lab., No. 11 (1962)

K. B. Zaborenko and Atif Alian, 1380-1382. New device automatically records activity for continuous extraction of radioactive isotopes.

Izvestiya vyssh. ucheb. zaved. Tsvet. metallurgiya, No. 5 (1962)

E. I. Kazantsev, 106-112. Study of the rate of equilibration in the sorption of uranium(VI) on cation exchange resins.

V. G. Vlasov and A. F. Bessonov, 113-122. Oxidation of uranium dioxide.

Uch. zap. Sredneaz. nauchno-issled. inst. geolog. i mineral. syr'ya, No. 7 (1962)

V. S. Morgunov and V. F. Mazanov, 171-174. On the possible use of the SRP-2 radiometer for recording integrated and "hard" components of the spectrum of scattered gamma radiation.

Chem. and Process Engng., 44, No. 1 (1963)

C. Hanson and D. Kaye, 27-30. High-capacity mixer-settlers.

Econ. Geology, 57, No. 7 (1962)

F. Habashi, 1081-1084. Relation between content of uranium and content of other elements in rocks.

Energia Nucleare, 9, No. 12 (1962)

A. Scaroni and R. Sesini, 709-712. Conference on corrosion of nuclear materials (Salzburg, 1962).

Énergie nucléaire, 4, No. 6 (1962)

ibid., 480-483. Activity of prospecting and ore development service of the Portugal AEC.

Énergie nucléaire, 4, No. 7 (1962)

J. Nadal, 589-599. Fabrication of fuel elements for graphite-moderated, carbon dioxide-cooled reactors.

R. Gautier, 600-606. Chemical composition of uraniferous ores.

J. Appl. Phys., 33, No. 12 (1962)

P. Price and R. Walker, 3400-3406. Observation of tracks of charged particles in solids.

P. Price and R. Walker, 3407-3412. Etching charged-particle tracks in solids.

R. Coltman et al., 3509-3522. Radiation damage to pure metals in a reactor.

J. Appl. Radiation and Isotopes, 13, September (1962)

M. Debeauvais-Wack, 483-486. Micrometering of radium in solution by means of nuclear emulsions.

J. Inorg. and Nucl. Chem., 24, December (1962)

G. Mason et al., 967-977. Synergetic effects in the extraction of metal cations by mono-(2-ethylhexyl)phosphoric acid.

W. Marshall et al., 995-1000. Aqueous systems at elevated temperatures. VII. Liquid immiscibility and critical phenomena in UO_3-SO_3-H_2O, UO_3-SO_3-D_2O, and CuO-SO_3-D_2O systems at 270-430°C.

L. Lynds, 1007-1009. Preparation of stoichiometric UO_2 by thermal decomposition of UO_2I_2.

L. Wittenberg and R. Steinmeyer, 1015-1017. Solubility of plutonium (VI) carbonate in lithium carbonate.

Kernenergie, 5, No. 12 (1962)

H. Rommel, 859-860. Activation analysis determination of boron using the nuclear reaction $B^{11}(p,n)C^{11}$.

ibid., 861-868. Leipzig Institute of Applied Radioactivity.

Kerntechnik, 4, No. 10 (1962)

K. Zander, 444-445. Electronic control of evaporation with automatic sample changing.

Kerntechnik, 4, No. 12 (1962)

G. Böhme and W. Köhler, 580-582. Laboratories for research on high-level materials.

W. Wimmenauer, 583-585. Status of the uranium industry in the countries of Western Europe.

D. Thiele, 586-587. Fuel reprocessing plants in Western Europe.

Nucleonics, 21, No. 1 (1963)

V. Storhok, 38-42. Fabricating plutonium for better performance.

H. Hummel et al., 43-47. Using plutonium in fast reactors.

E. Eschbach and S. Goldsmith, 48-52. Using plutonium in thermal reactors.

P. Holz et al., 72-73. Cutting up the HRE core vessel.

Nucleonics, 21, No. 2 (1963)

N. Michael et al., 62, 64. Inorganic ion exchange resins purify reactor water.

Nukleonika, 7, No. 11 (1962)

T. Urbanski and S. Minc, 703-713. Solvent extraction of cations from sulfate solutions by alkylphosphoric acids. II. Extraction of U^{VI} and Fe^{III} by di-(2-ethylhexyl)phosphoric acid in the presence of various cations.

W. Korpak, 715-723. Solvent extraction of mineral acids and uranyl ions by alkylsulfo oxides.

Reactor Sci. and Technol., 16, No. 10 (1962)

G. Greenwood and R. Johnson, 473-476. Investigation of stress-induced constant variations in the dimensions of uranyl slugs with β-phase fuel nuclei.

B. Pawelski and J. Stobo, 477-481. Prediction of rate of radiation-induced growth of uranium by measuring specific resistivity and expansion.

IV. NUCLEAR RADIATION SHIELDING

Radiation Safety. Shielding against Penetrating Radiations.

Chem. and Engng. News, 40, No. 49 (1962)

—, 54. Furnace for ashing radioactive wastes.

J. Appl. Radiation and Isotopes, 13, September (1962)

A. Gandy, 501-513. Measurements of absolute activity by beta and gamma coincidences.

Kernenergie, 5, No. 12 (1962)

C. Hamann, 845-853. Measurement of dose fields of high-level gamma sources with a scintillation microdetector.

Nucleonics, 21, No. 2 (1963)

I. Draganić, 33-35. In-pile radiations measured by oxalic acid.

H. Faissner, et al., 50 ff. New liquid scintillators.

T. Blosser and R. Freestone, 56. ORNL mobile radiation measurements lab.

—, 58. Solidification of hot wastes.

Nukleonika, 7, No. 11 (1962)

A. Jagielski et al., 725-728. Sr^{90} content in Polish soils.

Nukleonika, 7, No. 12 (1962)

I. Zlotowski and M. Wróblewska, 776-787. Simplified method for determining deuterium concentration in water by droplet techniques.

Vestnik Leningrad. univ., No. 16 (1962). Seriya fiziki i khimii, No. 3

M. S. Zakhar'evskii and Li Sung-ki, 131-134. Tracer measurements of diffusion coefficient in strontium chloride solutions.

Zhur. Vsesoyuz. khim. obshchestva im. Mendeleeva, 7, No. 5 (1962)

A. V. Sokolov and F. V. Turchin, 489-494. Pa^{32} and N^{15} applied in agronomic chemistry.

Zavod. lab., 28, No. 11 (1962)

B. P. Pakhomov, 1385-1388. Count rate meter probes wear on machine parts in tracer tests.

Konserv. i ovoshchesush. prom., No. 11 (1962)

M. L. Frumkin et al., 23-26. Gamma rays disinfect foodstuffs.

Lakokrasochnye materialy i ikh primenenie, No. 5 (1962)

E. I. Chuikinet al., 64-70. Tracer studies of flow patterns of process solutions in titanium dioxide production.

Khim. prom., No. 9 (1962)

B. I. Vainshtein et al., 27-28. Spent fuel elements as sources of gamma radiation in radiation-chemical equipment.

Jaderna energie, No. 4 (1963)

M. Zaduban. Tracer determination of adsorbed quantities.

M. Holinka, V. Masaryk, and E. Karnikovâ. Note on the compatibility of the uranium-titanium system.

M. Mrkous. Effect of ionizing radiations on rubber.

B. Kourim. Composition of heteropolyacid salts and esters.

I. Eder and B. Kourim. Precipitation of uranium fission products and isolation of cesium.

B. Kourim and K. Vacek. Electron paramagnetic resonance spectrum in the methylene group of deuterated methyl polymethacrylate after gamma irradiation.

J. Kucera. Chromatography of some aliphatic alcohols, glycols, and diketones on a thin layer of aluminum oxide.

J. Bina and T. Ertl. Radiation vulcanization of rubber silicones.

T. Fukatko and F. Bilek. Pulsed generator with statistical or linear time distribution of pulses.

Soviet Journals Available in Cover-to-Cover Translation

ABBREVIATION	RUSSIAN TITLE		TITLE OF TRANSLATION	PUBLISHER	TRANSLATION Vol.	Issue	BEGAN Year
AÉ	Atomnaya énergiya		Soviet Journal of Atomic Energy	Consultants Bureau	1	1	1956
Akust. zh.	Akusticheskii zhurnal		Soviet Physics – Acoustics	American Institute of Physics	1	1	1955
	Astronomicheskii zhurnal		Soviet Astronomy – AJ	American Institute of Physics	34	1	1957
Astr(on). zh(urn).	Avtomaticheskaya svarka		Automatic Welding	Br. Welding Research Assn. (London)	12	1	1959
Avto(mat). svarka	Avtomatika i Telemekhanika		Automation and Remote Control	Instrument Society of America	27	1	1956
	Biofizika		Biophysics	National Institutes of Health**	6	1	1961
	Biokhimiya		Biochemistry	Consultants Bureau	21	1	1956
Byull. éksp(erim). biol. (i med.)	Byulleten' éksperimental'noi biologii i meditsiny		Bulletin of Experimental Biology and Medicine	Consultants Bureau	41	1	1959
		Life Sciences	Doklady Biological Sciences Sections (includes: Anatomy, biochemistry, biophysics, cytology, ecology, embryology, endocrinology, evolutionary morphology, genetics, histology, hydrobiology, microbiology, morphology, parasitology, physiology, zoology)	National Science Foundation*	112	1	1957
		Life Sciences	Doklady Botanical Sciences Sections (includes: Botany, phytopathology, plant anatomy, plant ecology, plant embryology, plant physiology, plant morphology)	National Science Foundation*	112	1	1957
		Chemical Sciences	Proceedings of the Academy of Sciences of the USSR, Section: Chemical Technology	Consultants Bureau	106	1	1956
		Chemical Sciences	Proceedings of the Academy of Sciences of the USSR, Section: Chemistry	Consultants Bureau	106	1	1956
DAN (SSSR)	Doklady Akademii	Chemical Sciences	Proceedings of the Academy of Sciences of the USSR, Section: Physical Chemistry	Consultants Bureau	112	1	1957
Dokl(ady) AN SSSR	Nauk SSSR	Earth Sciences	Doklady Earth Sciences Sections (includes: Geochemistry, geology, geophysics, hydrogeology, lithology, mineralogy, oceanology, paleontology, permafrost, petrography)	American Geological Institute	124	1	1959
		Earth Sciences	Proceedings of the Academy of Sciences of the USSR, Section: Geochemistry	Consultants Bureau	106-123	1-6	1956-1958
		Earth Sciences	Proceedings of the Academy of Sciences of the USSR, Section: Geology	Consultants Bureau	112-123	1-6	1957-1958
		Mathematics	Soviet Mathematics – Doklady	American Mathematical Society	130	1	1960
		Physics	Soviet Physics – Doklady (includes: Aerodynamics, astronomy, crystallography, cybernetics and control theory, electrical engineering, energetics, fluid mechanics, heat engineering, hydraulics, mathematical physics, mechanics, physics, technical physics, theory of elasticity sections)	American Institute of Physics	106	1	1956
	Elektrosvyaz'		Telecommunications	Am. Inst. of Electrical Engineers		1	1957
Entom(ol). oboz(r).	Entomologicheskoe obozrenie		Entomological Review	National Science Foundation**	37	1	1958
FMM	Fizika metallov i metallovedenie		Physics of Metals and Metallography	Acta Metallurgica	5	1	1957
FTT, Fiz. tv(erd). tela	Fizika tverdogo tela		Soviet Physics – Solid State	American Institute of Physics	1	1	1959
Fiziol. Zh(urn). SSSR	Fiziologicheskii zhurnal imeni I.M. Sechenov		Sechenov Physiological Journal USSR	National Institutes of Health**	47	1	1961
Fiziol(ogiya) rast.	Fiziologiya rastenii		Plant Physiology	National Science Foundation*	4	1	1957
	Geodeziya i aerofotosyemka		Geodesy and Aerophotography	American Geophysical Union			1962
	Geokhimiya		Geochemistry	The Geochemical Society	1	1	1956
Geol. nefti i gaza	Geologiya nefti i gaza		Petroleum Geology	Petroleum Geology	2	1	1958
	Geomagnetizm i aeronomiya		Geomagnetism and Aeronomy	American Geophysical Union	1	1	1961
	Iskusstvennye sputniki zemli		Artificial Earth Satellites	Consultants Bureau	1	1	1958
Izmerit. tekhn(ika)	Izmeritel'naya tekhnika		Measurement Techniques	Instrument Society of America	7	1	1958

The translation of this journal is published in sections

Izv. AN SSSR O(td). Kh(im). N(auk)	Izvestiya Akademii Nauk SSSR: Otdelenie khimicheskikh nauk	Bulletin of the Academy of Sciences of the USSR: Division of Chemical Science	Consultants Bureau	16	1	1952
Izv. AN SSSR O(td). T(ekhn). N(auk): Metall). i top.	(see Met. i top)					
Izv. AN SSSR Ser. fiz(ich).	Izvestiya Akademii Nauk SSSR: Seriya fizicheskaya	Bulletin of the Academy of Sciences of the USSR: Physical Series	Columbia Technical Translations	18	3	1954
Izv. AN SSSR Ser. geofiz.	Izvestiya Akademii Nauk SSSR: Seriya geofizicheskaya	Bulletin of the Academy of Sciences of the USSR: Geophysics Series	American Geophysical Union	7	1	1957
Izv. AN SSSR Ser. geol.	Izvestiya Akademii Nauk SSSR: Seriya geologicheskaya	Bulletin of the Academy of Sciences of the USSR: Geologic Series	American Geological Institute	23	1	1958
Iz. Vyssh. Uch. Zav., Tekh. Teks. Prom.	Izvestiya Vysshikh Uchebnykh Zavedenii Tekhnologiya Tekstil'noi Promyshlennosti	Technology of the Textile Industry, USSR	The Textile Institute (Manchester)	4	1	1960
Kauch. i rez.	Kauchuk i rezina	Soviet Rubber Technology	Palmerton Publishing Company, Inc.	18	3	1959
	Kinetika i kataliz	Kinetics and Catalysis	Consultants Bureau	1	1	1960
	Koks i khimiya	Coke and Chemistry, USSR	Coal Tar Research Assn. (Leeds, England)		8	1959
Kolloidn. zh(urn).	Kolloidnyi zhurnal	Colloid Journal	Consultants Bureau	14	1	1952
	Kristallografiya	Soviet Physics – Crystallography	American Institute of Physics	2	1	1957
Metallov. i term.	Metallovedenie i termicheskaya obrabotka metallov	Metals Science and Heat Treatment of Metals		6	1	1958
	Metallurg	Metallurgist	Acta Metallurgica		1	1957
Met. i top.(gorn.)	Metallurgiya i toplivo (gornoye delo)	Russian Metallurgy and Fuels (mining)	Scientific Information Consultants, Ltd.		1	1960
Mikrobiol.	Mikrobiologiya	Microbiology	National Science Foundation*	26	1	1957
	Ogneupory	Refractories	Acta Metallurgica	25	1	1960
OS, Opt. i spektr.	Optika i spektroskopiya	Optics and Spectroscopy	American Institute of Physics	6	1	1959
Paleontol. Zh(urn)	Paleontologicheskii Zhurnal	Journal of Paleontology	American Geological Institute		1	1962
	Pochvovedenie	Soviet Soil Science	National Science Foundation**	53	1	1958
	Poroshkovaya Metallurgiya	Soviet Powder Metallury and Metal Ceramics	Consultants Bureau	2	1	1962
	Priborostroenie	Instrument Construction	Taylor and Francis, Ltd. (London)	4	1	1959
Pribory i tekhn. éks(perimenta)	Pribory i tekhnika éksperimenta	Instruments and Experimental Techniques	Instrument Society of America	3	1	1958
Prikl. matem. i mekh(an).	Prikladnaya matematika i mekhanika	Applied Mathematics and Mechanics	Am. Society of Mechanical Engineers	22	1	1958
PTE	(see Pribory i tekhn. éks.)					
	Problemy Severa	Problems of the North	National Research Council of Canada		1	1958
	Radiokhimiya	Radiochemistry	Consultants Bureau	4	1	1962
Radiotekh.	Radioteknika	Radio Engineering	Am. Institute of Electrical Engineers	16	1	1961
Radiotekhn. i élektron(ika)	Radiotekhnika i électronika	Radio Engineering and Electronic Physics	Am. Institute of Electrical Engineers	6	1	1961
	Stal'	Stal (in English)	Iron and Steel Institute	19	1	1959
	Stanki i instrument	Machines and Tooling	Production Engineering Research Assoc.	30	1	1959
Stek. i keram.	Steklo i keramika	Glass and Ceramics	Consultants Bureau	13	1	1956
Svaroch. proiz-vo	Svarochnoe proizvodstvo	Welding Production	Br. Welding Research Assn. (London)	5	4	1959
Teor. veroyat. i prim.	Teoriya veroyatnostei i ee primenenie	Theory of Probability and Its Application	Soc. for Industrial and Applied Math.	1	1	1956
Tsvet. metally	Tsvetnye metally	The Soviet Journal of Nonferrous Metals	Primary Sources	33	1	1960
UFN	Uspekhi fizicheskikh nauk	Soviet Physics – Uspekhi (partial translation)	American Institute of Physics	66	1	1958
UKh, Usp. khimi	Uspekhi khimii	Russian Chemical Reviews	Chemical Society (London)	29	1	1960
UMN	Uspekhi matematicheskaya nauk	Russian Mathematical Surveys	Cleaver-Hume Press, Ltd. (London)	15	1	1960
Vest. mashinostroeniya	Vestnik mashinostroeniya	Russian Engineering Journal	Production Engineering Research Assoc.	39	4	1959
Vop. onk(ol).	Voprosy onkologii	Problems of Oncology	National Institutes of Health**	7	1	1961
Zav(odsk). lab(oratoriya)	Zavodskaya laboratoriya	Industrial Laboratory	Instrument Society of America	24	1	1958
ZhAKh, Zh. anal(it). Khim(ii)	Zhurnal analiticheskoi khimii	Journal of Analytical Chemistry	Consultants Bureau	7	1	1952
ZhETF Zh. éksperim. i teor. fiz.	Zhurnal eksperimental'noi i teoreticheskoi fiziki	Soviet Physics – JETP	American Institute of Physics	28	1	1955
ZhFKh Zh. fiz. khimii	Zhurnal fizicheskoi khimii	Russian Journal of Physical Chemistry	Chemical Society (London)	33	7	1959
ZhNKh Zh. neorg(an). khim.	Zhurnal neorganicheskoi khimii	Journal of Inorganic Chemistry	Chemical Society (London)	4	1	1959
ZhOKh Zh. obshch. khim.	Zhurnal obshchei khimii	Journal of General Chemistry USSR	Consultants Bureau	19	1	1949
ZhPKh Zh. prikl. khim.	Zhurnal prikladnoi khimii	Journal of Applied Chemistry USSR	Consultants Bureau	23	1	1950
ZhSKh Zh. strukt(urnoi) khim.	Zhurnal strukturnoi khimii	Journal of Structural Chemistry	Consultants Bureau	1	1	1960
ZhTF	Zhurnal tekhnicheskoi fiziki	Soviet Physics – Technical Physics	American Institute of Physics	26	1	1956
Zh. tekhn. fiz.	Zhurnal vychislitel'noi matematika i matematicheskoi fiziki	U.S.S.R. Computational Mathematics and Mathematical Physics	Pergamon Press, Inc.	1	1	1962
Zh. vyssh. nervn. deyat. (im. Pavlova)	Zhurnal vysshei nervnoi deyatel'nosti (im I. P. Pavlova)	Pavlov Journal of Higher Nervous Activity	National Institutes of Health**	11	1	1961

*Sponsoring organization. Translation published by Consultants Bureau.
**Sponsoring organization. Translation published by Scripta Technica.

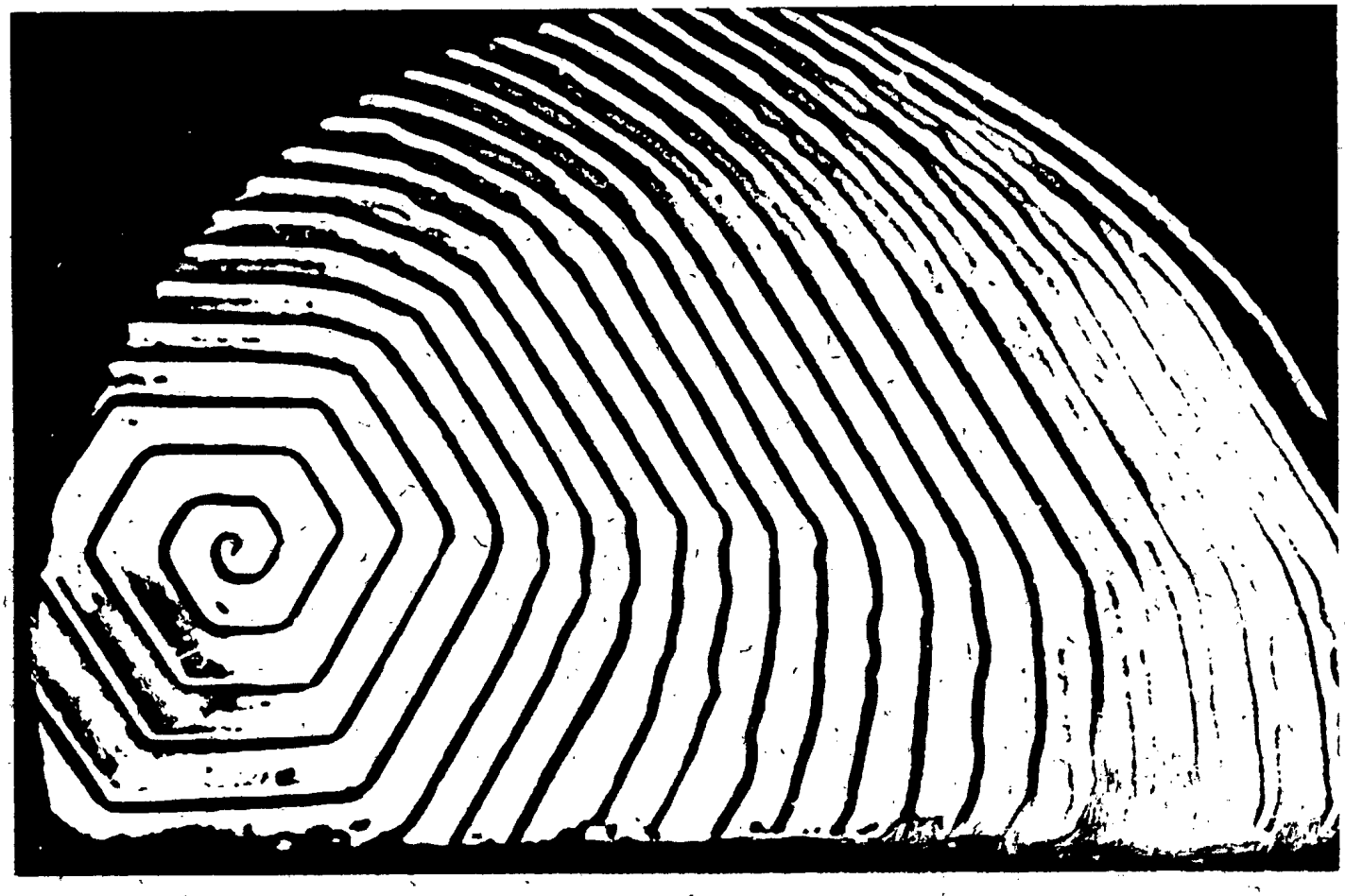

SURFACE PROPERTIES OF SEMICONDUCTORS

Edited by
A. N Frumkin,
A. V. Rzhvanov,
and R. Kh. Burshtein

This volume consists of the papers read at a Conference on the Surface Properties of Semiconductors, held at the Institute of Electrochemistry of the USSR Academy of Sciences. The work is devoted mainly to studies of the effect of the surface states of semiconductors, principally germanium and silicon, on their electrical properties.

Distinctively, this new work presents the fundamental studies of the surface state, keeping firmly in view the applications to stabilization and reproducibility of the electrical properties of semiconductors and semiconducting devices. Both "clean" and real oxide covered surfaces are discussed, the adsorption of various gases on semiconductors, local surface states, surface electron processes, and effects of various surface treatments are covered.

Practical applications include surface treatments suitable for production of semiconducting devices with stable and reproducible properties. A considerable part of the volume deals with studies of the electrical properties of semiconductors governed by the existence of local electron states on the semiconductor surface, reflecting recent detailed investigations of surface electron processes.

The book will prove of substantial value to research physicists and chemists, and will also be of interest to development engineers concerned with semiconducting devices.

170 pages **Translated from Russian** **$22.50**

CONSULTANTS BUREAU 227 West 17 St., New York 11, N. Y.

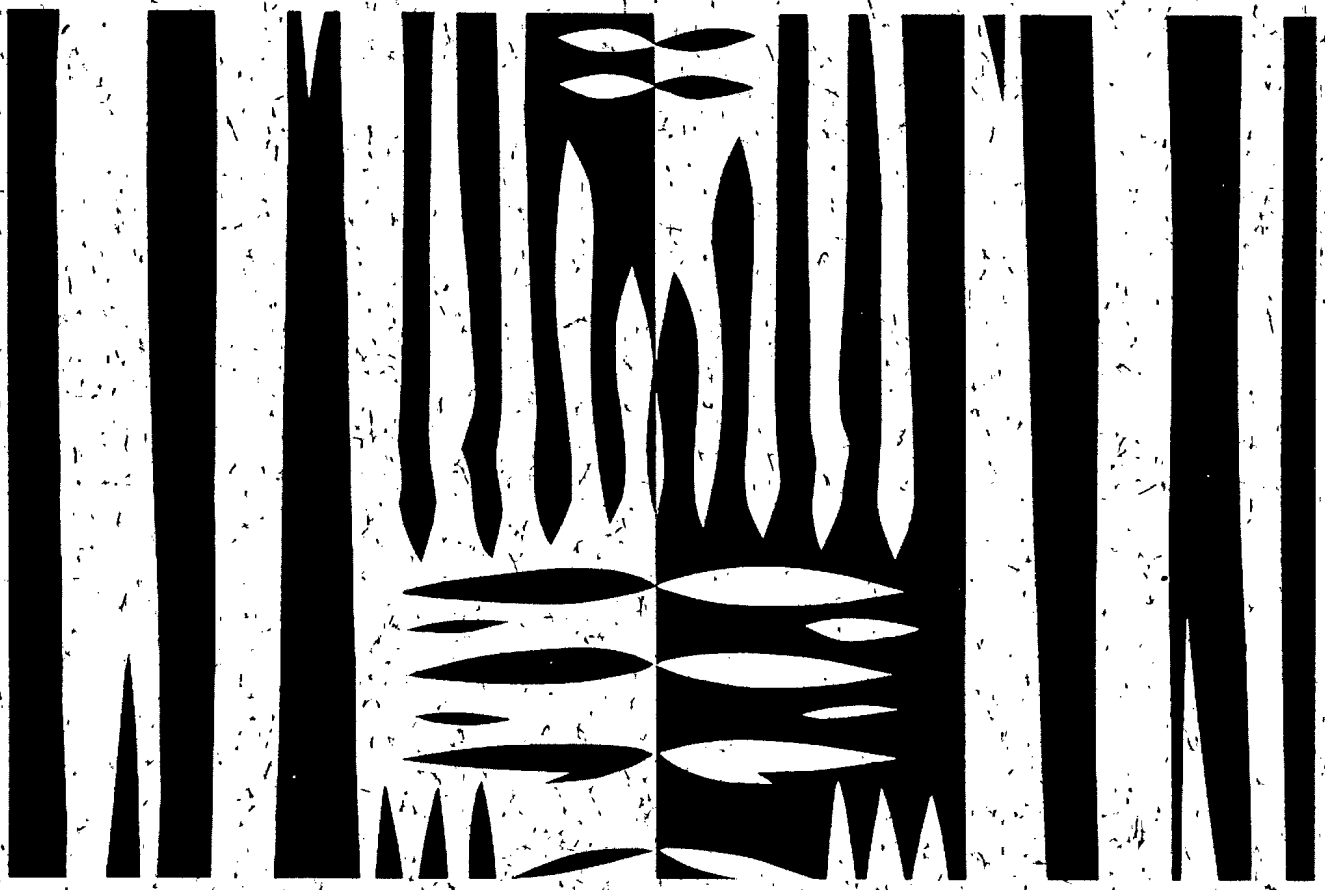

MECHANICAL TWINNING OF CRYSTALS

by M.V. Klassen-Neklyudova

This work by M.V. Klassen-Neklyudova broadens the scope of the literature on mechanical twinning from the usual specialist study of reorientation in response to mechanical stress, to include many effects related to mechanical twinning, such as formation of reoriented regions in response to high temperatures, and to electric and magnetic fields.

Before the physical nature of deformation and rupture processes can be properly elucidated for metals, minerals, rocks or other crystalline bodies, a thorough grounding in the basic laws of twinning is essential. In addition, this understanding can also contribute to a better appreciation of the properties of ferroelectrics and piezoelectrics.

The material in the volume is so arranged as to provide information on each of the major aspects of twinning while not omitting possible fruitful links existing between related fields. The book is divided into three sections beginning with a discussion of the experimental evidence on twinning with and without change of shape. The subject is continued with an examination of the lattice reconstruction in martensite-type (diffusionless) transformations, formation of twins by recrystallization, and formation of reoriented regions (irrational twins, kinks, deformation bands, etc.) in inhomogeneous deformation. The book concludes with an elucidation of the macroscopic and microscopic theories of twinning. The entire work has thus been conceived in such a way that the book can function not only as a reference tool, but also as a spur toward inspiring new work in the field.

225 pages **Translated from Russian** **$19.50**

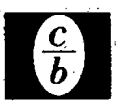

CONSULTANTS BUREAU 227 West 17 St., New York 11, N.Y.